doi : 10.17596/0003217

R/V Mirai Cruise Report
MR09-04

November 4, 2009 – December 12, 2009
Tropical Ocean Climate Study (TOCS)

Japan Agency for Marine-Earth Science and Technology
(JAMSTEC)

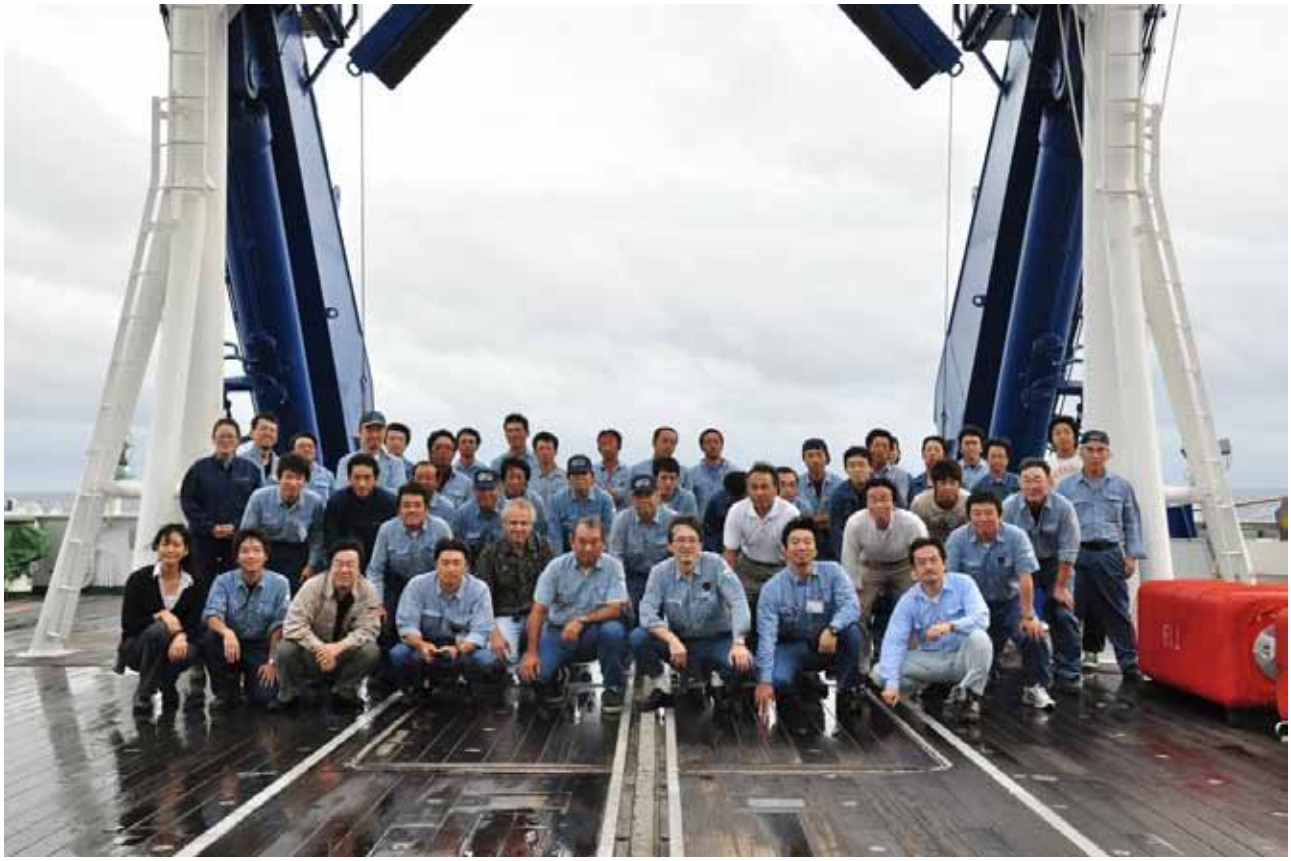

Cruise Report ERRATA of the Nutrients part

page	Error	Correction
6-40	potassium nitrate CAS No. 7757-91-1	potassium nitrate CAS No. 7757-79-1

Table of contents

Note:

This cruise report is a preliminary documentation as of the end of the cruise. It may not be revised even if new findings and others are derived from observation results after publication. It may also be changed without notice. Data on the cruise report may be raw or not processed. Please ask the chief scientist for the latest information before using this report. Users of data or results of this cruise are requested to submit their results to Data Integration and Analysis Group (DIAG), JAMSTEC (e-mail: diag-dmd@jamstec.go.jp).

1. Cruise name and code

Tropical Ocean Climatology Study

MR09-04

Ship: R/V Mirai

Captain: Yasushi Ishioka

2. Introduction and observation summary

2.1 Introduction

The purpose of this cruise is to observe ocean and atmosphere in the western tropical Pacific Ocean for better understanding of climate variability involving the ENSO (El Nino/Southern Oscillation) phenomena. Particularly, warm water pool (WWP) in the western tropical Pacific is characterized by the highest sea surface temperature in the world, and plays a major role in driving global atmospheric circulation. Zonal migration of the WWP is associated with El Nino and La Nina which cause drastic climate changes in the world such as 1997-98 El Nino and 1999 La Nina. However, this atmospheric and oceanic system is so complicated that we still do not have enough knowledge about it.

In order to understand the mechanism of the atmospheric and oceanic system, its high quality data for long period is needed. Considering this background, we developed the TRITON (TRIangle Trans-Ocean buoy Network) buoys and have deployed them in the western equatorial Pacific and Indian Ocean since 1998 cooperating with USA, Indonesia, and India. The major mission of this cruise is to maintain the network of TRITON buoys along 147E and 156E lines in the western equatorial Pacific. Additionally, subsurface Acoustic Doppler Current Profiler (ADCP) buoys at the equator are maintained to obtain time-series data of equatorial ocean current.

We have been observed ocean fine structure in order to understand ocean mixing effect on tropical ocean climate since MR07-07 leg 1. For this purpose, we conducted CTD observations with a LADCP until 500m depth every 30nm along 147E and 156E lines. Additionally, ocean turbulence observation was newly conducted using a turbulence microstructure profiler, Turbo-Map during this cruise.

We also observed profiles of temperature, salinity, and chemical parameters using CTD system to check performance of pCO2 sensors which was developed by Central Research Institute of Electric Power Industry (CRIEPI, Japan) and to sample bacteria in the deep ocean near the TRITON buoys. Sampled water was analyzed for salinity, dissolved oxygen, nutrients, and microflora.

During this cruise, halobates (sea skaters) were sampled using a net in order to research their distribution and ecology in the western equatorial Pacific.

Before we arrived at TRITON buoy area, we conducted CTD/XCTD observations in the region of the Kuroshio Extension on the way to the tropical region and check J-KEO and KEO buoys which were deployed at 38-05N, 145-25E and 32-19N, 144-32E. We also deployed three Argo floats were launched.

Except for above, automatic continuous oceanic, meteorological and geophysical observations are also conducted along ship track during this cruise as usual. In particular, a cesium magnetometer was towed east of Mariana Islands in order to get more accurate geomagnetic data in this region.

2.2 Overview

1) Ship

R/V Mirai

Captain Yasushi Ishioka

2) Cruise code

MR09-04

3) Project name

Tropical Ocean Climate Study (TOCS)

4) Undertaking institution

Japan Agency for Marine-Earth Science and Technology (JAMSTEC)

2-15, Natsushima-cho, Yokosuka, 237-0061, Japan

5) Chief scientist

Yuji Kashino (JAMSTEC)

6) Period

November 4, 2009 (Sekinehama, Japan) – December 11, 2009 (Hachinohe, Japan) – December 12, 2009 (Sekinehama, Japan)

7) Research participants

Nine scientists and sixteen technical staffs from seven Japanese institutions and companies

One scientists from USA

2.3 Observation summary

TRITON mooring recovery and re-installation: 9 moorings were deployed and recovered

Subsurface ADCP mooring recovery and re-installation: 2 moorings were deployed and recovered

CTD (Conductivity, Temperature and Depth) and water sampling: 43 casts

Deep cast to the ocean bottom 7 casts

XCTD: 35 casts

Ocean turbulence observation 35 casts

Launch of Argo floats 3 floats

Halobates sampling 8 casts

Rain, water vapor and surface water sampling for isotope analysis

31 casts for rain, 76 casts for water vapor, and 37 cast for surface water

Current measurements by shipboard ADCP:	continuous
Sea surface temperature, salinity, dissolved oxygen, and CO2 measurements by intake method:	continuous
Surface meteorology:	continuous
Doppler radar observation:	continuous
Water vapor observation:	continuous
Underway geophysics observations	continuous
Towing a cesium magnetometer	continuous, two times

We successfully recovered and re-installed nine TRITON buoys at 147E and 156E lines during this cruise. Only when we deployed the buoy at 2S156E, data communication from meteorological sensors was stopped after deployment, but they were repaired next day.

It is notable that there were few damages and distortions in the recovered buoys due to vandalism except for small damage (e.g., lost of vane of wind gage) at 5S156E.

Some optional sensors were recovered and re-installed in the TRITON buoys. At first, optional sensors for CO2 measurement by Mutsu Institute of Oceanography (MIO) of JAMSTEC and Central Research Institute of Electric Power Industry (CRIEPI, Japan) were recovered and re-installed in the TRITON buoys at 2N156E (#3). The former was attached to the float at the sea surface, and the latter was underwater sensors installed at the depth of 25m. There is no damage in both sensors attached to the recovered buoy. Next, we recovered two ADCPs in the buoy at 0N156E (#4) which was deployed in MR08-03 cruise, however, the transducer of upper one installed at 175m depth was off its body when we recovered it because bolts of transducer were lost.

We have been maintaining the subsurface ADCP buoys in the western equatorial region since 1996. Two ADCP buoys at 0N147E and 0N156E were recovered and re-installed during this cruise with no trouble. Unfortunately, data from a CTD (SBE-16) in the buoy at 0N156E was not acquired.

During this cruise, we conducted shallow CTD casts with a LADCP until 500m or 800m depth and ocean turbulence observation using Turbo-Map every 30nm along 156E and 147E lines. Although it is first time to use the Turbo-Map in the TOCS cruises, we got good and interesting data combined with LADCP data for discussing ocean fine structure in the western equatorial region. Seven deep CTD casts until the ocean bottom were conducted at the TRITON buoy sites for check of pCO2 sensors and sampling bacteria. For these purpose, water was sampled using Niskin bottles and analyzed for salinity, dissolved oxygen, nutrients, and microflora. Furthermore, we also CTD observation to 2000m depth near the J-KEO and KEO buoys, and before launch of Argo floats. These observations were successfully conducted and good quality data was obtained.

XCTD observations were conducted in the Kuroshio Extension region. Because large air-sea interaction seems to occur in the Kuroshio Extension region as same as the tropics, JAMSTEC and PMEL/NOAA(USA) deployed surface moorings, J-KEO and KEO buoys, in this region. These XCTD observations were conducted in order to obtain supplement data for these buoys on the way

to equatorial region.

XCTD observations were also conducted after deployment work of TRITON buoys. Because we found large negative salinity bias (0.05-0.1 PSU) in the data during MR06-05 leg3, MR07-07 leg 1 and other TOCS cruises, we compared XCTD data with data from CTD observations which were conducted before recovery of the TRITON buoy. Then, we found that large negative bias largely improved. We will discuss this result with XCTD maker, Tsurumi Seiki, Co. Ltd.

With regard to automatic continuous meteorological, oceanographic and geophysical observations, all observations except for shipboard ADCP were carried out well. Although the shipboard ADCP of R/V Mirai was installed last year, it has not been working well since MR09-02. Particularly, data was not good when ship speed exceeded 12knot. We strongly hope that this instrument will be improved because data from the shipboard ADCP is very important for tropical climate research.

During this cruise, we newly towed a cesium magnetometer east Mariana Islands on the way to and from the equatorial region. Data was successfully acquired.

Thus, we conducted all planed observations on schedule in this cruise.

2.4 Observed oceanic and atmospheric conditions

In 2009 boreal summer, atmosphere and ocean in the tropical Pacific was changed to El Nino condition. Japan Meteorological Agency forecasted this El Nino will continue until 2008/09 boreal winter. In fact, high sea surface temperature (SST) anomaly exceeding 2℃ appeared in the central Pacific (Figure. 2-1). SST along the equator between 150E and dateline exceeded 30℃, and westerly wind anomaly was seen in the observation area.

Weather during observations along 156E line was good and suitable for buoy maintenance work. However, when R/V Mirai arrived at 147E line, Maddan Julian Oscillation arrived at the observation area (Figure 2-2) and weather after then was almost rainy.

Temperature, salinity and potential density sections along 156E are shown in Figure 2-3. Sea surface temperature exceeded 30℃ between 4S and 4N, i.e., SST during this cruise was higher than that during MR08-03 in this region. Sea surface salinity (SSS) was largely lower than MR08-03; fresh water lens, which was only seen north of 3N during MR08-03, occupied along this line. This result suggests large precipitation in this region.

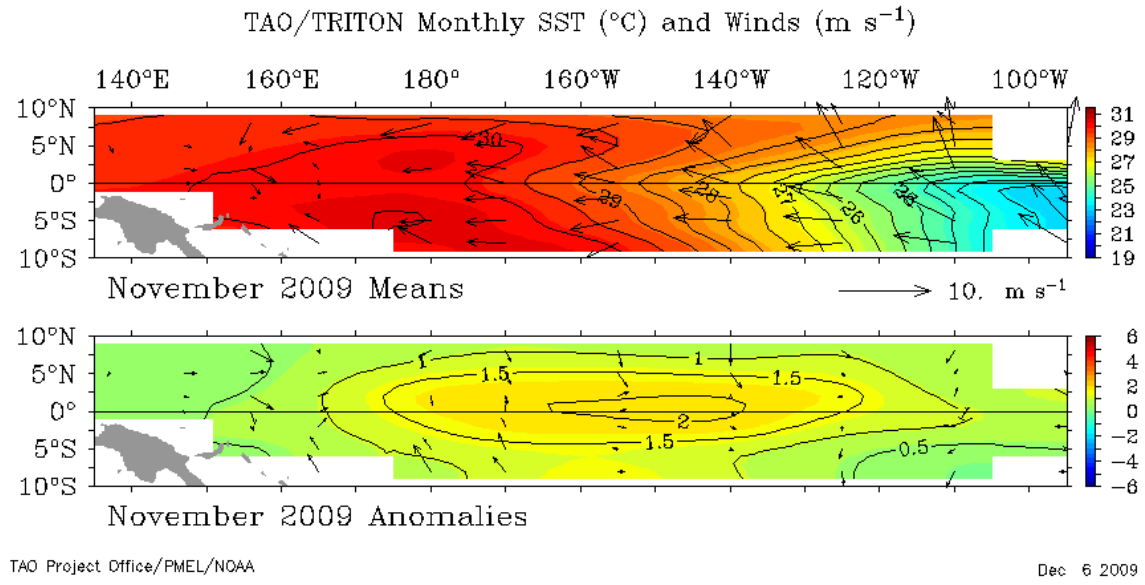

Figure 2-1. Maps of monthly sea surface temperature and winds (upper panel), and their anomaly (lower panel) obtained from TAO/TRITON buoy array in November 2009. (http://www.pmel.noaa.gov/tao/jsdisplay/)

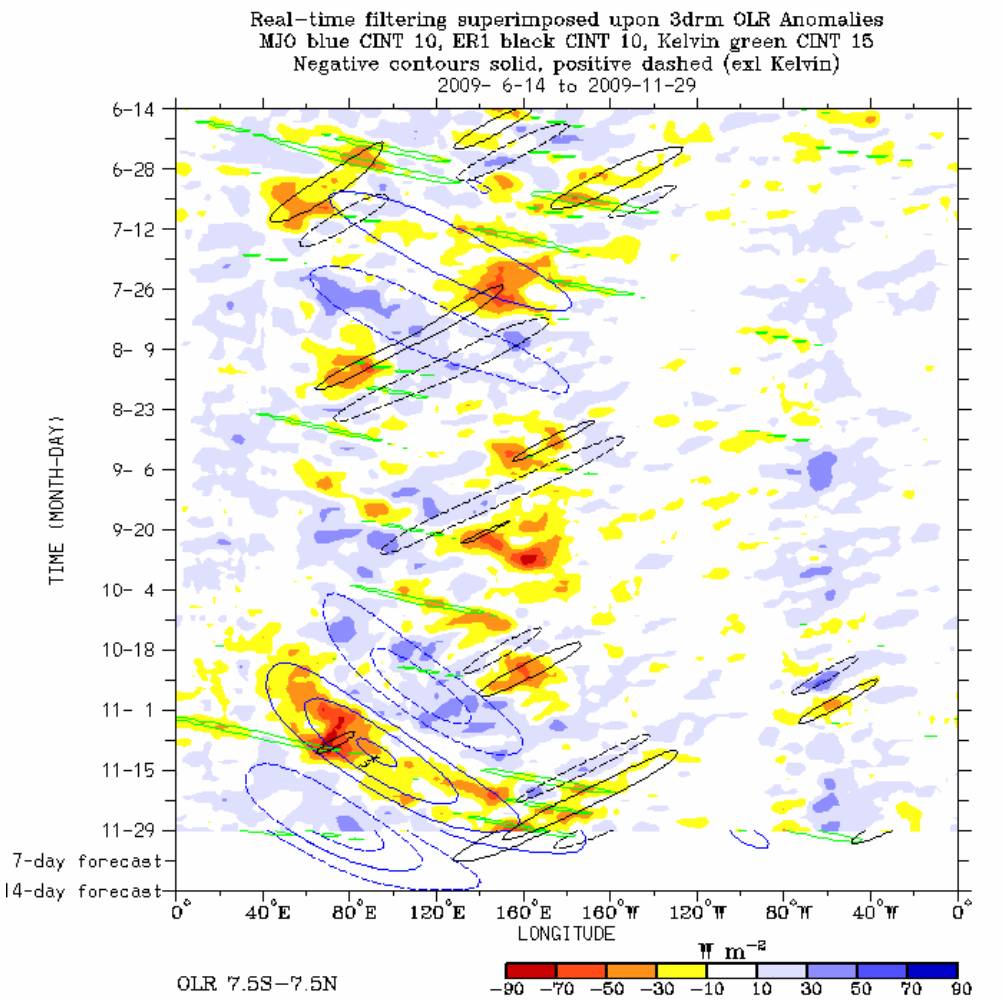

Figure 2-2. Outgoing radiation anomaly averaged over 7.5S-7.5N from the web page of the Climate Diagnostic Center (CDC), National Oceanic and Atmospheric Association (NOAA) (http://www.cdc.noaa.gov/map/clim/olr_modes/).

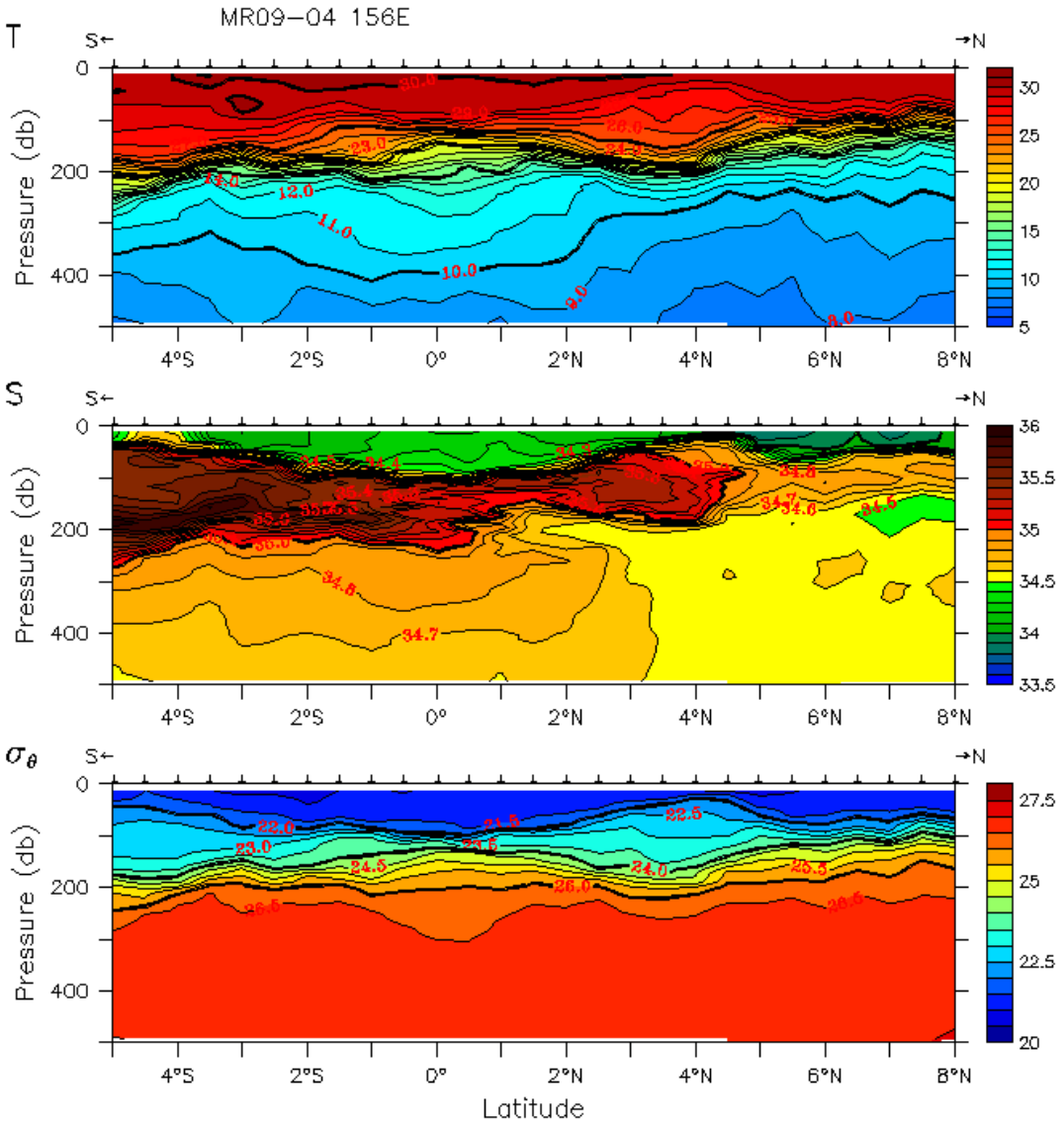

Figure 2-3. Temperature, salinity and potential density sections along 156E line.

3. Period, ports of call, cruise log and cruise track

3.1 Period

03th November, 2009 – 12th December, 2009

3.2 Ports of call

Sekinehama, Japan (Departure: 03 November, 2009)

Hachinohe, Japan (Arrival and Departure: 11 December, 2009)

Sekinehama, Japan (Arrival: 12 December, 2009)

3.3 Cruise Log

SMT	UTC	Event
Nov. 04th (Wed.) 2009		
07:00	22:00 (-1day)	Departure of Sekinehama
		[Ship Mean Time (SMT)=UTC+9h]
08:30	23:30	Surface sea water sampling start
09:00	00:00	Safety guidance
10:00	01:00	Meeting for MR09-04 observation
16:45	07:45	Konpira ceremony
18:33 – 23:30	09:33 – 13:30	Free fall for CTD cable
Nov. 05th (Thu.) 2009		
09:14	00:14	XCTD observation E-01 (#01)
11:31	02:31	XCTD observation E-02 (#02)
14:06	05:06	XCTD observation E-03 (#03)
05:00	19:00	Arrival at St.1 (38-05N, 146-25E)
06:01 – 06:23	20:01 – 20:23	CTD/pH/pCO_2 C01M01 (2000m)
05:00	19:00	Departure of St.1
20:40	11:40	XCTD observation E-04 (#04)
23:23	14:23	XCTD observation E-05 (#05)
Nov. 06th (Fri.) 2009		
00:46	15:46	XCTD observation E-06 (#06)
02:08	17:08	XCTD observation E-07 (#07)
03:30	18:30	XCTD observation E-08 (#08)
04:50	19:50	XCTD observation E-09 (#09)
06:12	21:12	XCTD observation E-10 (#10)
07:33	22:33	XCTD observation E-11 (#11)
08:58	23:58	XCTD observation E-12 (#12)
10:23	01:23	XCTD observation E-13 (#13)
11:48	02:48	XCTD observation E-14 (#14)

SMT	UTC	Event
13:11	04:11	XCTD observation E-15 (#15)
14:34	05:34	XCTD observation E-16 (#16)
15:56	06:56	XCTD observation E-17 (#17)
21:48	12:48	XCTD observation E-19 (#19)
22:00	13:00	Time adjustment +1h (SMT=UTC+10h)
Nov. 07th (Sat.) 2009		
02:49	16:49	XCTD observation E-20 (#20)
05:00	19:00	Arrival at St.2 (38-05N, 146-25E)
05:25 – 06:40	19:25 – 19:40	CTD/pH/pCO_2 C02M01 (2000m)
07:18	20:18	Departure of St.2
08:54	22:54	XCTD observation E-21 (#21)
14:13	04:13	XCTD observation E-22 (#22)
19:35	09:35	XCTD observation E-23 (#23)
Nov. 08th (Sun.) 2009		
Nov. 09th (Mon.) 2009		
05:50 – 06:16	19:50 – 20:16	Figure-8 turn for Three-component magnetometer calibration
06:31	20:31	Start of Cesium magnetometer observation (#1)
Nov. 10th (Tue.) 2009		
22:43	12:43	End of Cesium magnetometer observation (#1)
Nov. 11th (Wed.) 2009		
22:00	12:00	Time adjustment +1h (SMT=UTC+11h)
Nov. 12th (Thu.) 2009		
13:18	02:18	Arrival at St.3 (10-00N, 154-51E)
13:21 – 14:42	02:21 – 03:40	CTD/pH/pCO_2 C03M01 (2000m)
14:48	03:48	Launch of Argo float (#1)
15:36 – 16:09	04:36 – 05:09	MSP test observation (#01, 500m)
19:04 – 19:24	08:04 – 08:24	Net sampling (#01-1)
19:29 – 19:47	08:29 – 08:47	Net sampling (#01-2)
19:53 – 20:12	08:53 – 09:12	Net sampling (#01-3)
20:18	09:18	Departure of St.3
Nov. 13th (Fri.) 2009		
05:48	18:48	Arrival at St.4 (08-00N, 156-00E)
06:08 – 06:55	19:08 – 19:55	CTD C04M01 (800m)
08:07 – 11:50	21:07 – 00:50	Recovery of TRITON buoy #01 (8N, 156E)
13:05 – 16:25	02:05 – 05:25	CTD/pH/pCO_2 C04M02 (bottom)
16:31	05:31	Launch of Argo float (#2)
18:51 – 19:10	07:51 – 08:10	Net sampling (#02-1)
19:12 – 19:30	08:12 – 08:30	Net sampling (#02-2)
19:33 – 19:51	08:33 – 08:51	Net sampling (#02-3)

SMT	UTC	Event
Nov. 14th (Sat.) 2009		
08:19 – 11:24	21:19 – 00:24	Deployment of TRITON buoy #01 (8N, 156E)
		(Fixed Position: 08-00.9993N, 155-57.1699E)
13:50	02:50	Departure of St.4
13:53	02:53	XCTD observation (#24)
16:11	05:11	XCTD observation (#25)
18:24	07:24	XCTD observation (#26)
20:34	09:34	XCTD observation (#27)
22:48	11:48	XCTD observation (#28)
Nov. 15th (Sun.) 2009		
01:06	14:06	XCTD observation (#29)
05:24	18:24	Arrival at St.5 (05-00N, 156-00E)
05:36 – 06:24	18:36 – 19:24	CTD C05M01 (800m)
06:30 – 07:08	19:30 – 20:08	MSP observation (#02, 500m)
08:01 – 11:27	21:01 – 00:27	Recovery of TRITON buoy #02 (5N, 156E)
13:06 – 15:43	02:06 – 04:43	CTD/pH/pCO_2 C05M02 (bottom)
15:48	04:48	Launch of Argo float (#2)
18:36 – 18:58	07:36 – 07:58	Net sampling (#03-1)
19:00 – 19:18	08:00 – 08:18	Net sampling (#03-2)
19:20 – 19:41	08:20 – 08:41	Net sampling (#03-3)
Nov. 16th (Mon.) 2009		
08:17 – 10:54	21:17 – 23:54	Deployment of TRITON buoy #02 (5N, 156E)
		(Fixed Position: 04-58.3910N, 156-02.0351E)
11:30	00:30	Departure of St.5
11:34	00:34	XCTD observation (#30)
13:36	02:36	Arrival at St.6 (04-30N, 156-00E)
13:43 – 14:13	02:43 – 03:13	CTD/LADCP C06M01 (500m)
14:21 – 14:59	03:21 – 03:59	MSP observation (#03, 500m)
15:00	04:00	Departure of St.6
17:30	06:30	Arrival at St.7 (04-00N, 156-00E)
17:34 – 18:05	06:34 – 07:05	CTD/LADCP C07M01 (500m)
18:12 – 18:43	07:12 – 07:43	MSP observation (#04, 500m)
18:48	07:48	Departure of St.7
20:54	09:54	Arrival at St.8 (03-30N, 156-00E)
21:02 – 21:30	10:02 – 10:30	CTD/LADCP C08M01 (500m)
21:36 – 22:12	10:36 – 11:12	MSP observation (#05, 500m)
22:12	11:12	Departure of St.8
Nov. 17th (Tue.) 2009		
04:48	17:48	Arrival at St.9 (03-00N, 156-00E)

SMT	UTC	Event
05:02 – 05:36	18:02 – 18:36	CTD/LADCP C09M01 (500m)
05:43 – 06:16	18:43 – 19:16	MSP observation (#06, 500m)
06:18	19:18	Departure of St.9
08:36	21:36	Arrival at St.10 (02-30N, 156-00E)
08:44 – 09:14	21:44 – 22:14	CTD/LADCP C10M01 (500m)
09:20 – 09:54	22:20 – 22:54	MSP observation (#07, 500m)
09:54	22:54	Departure of St.10
12:00	01:00	Arrival at St.11 (02-00N, 156-00E)
13:16 – 15:20	02:16 – 04:20	Deployment of TRITON buoy #03 (2N, 156E)
		(Fixed Position: 02-02.2610N, 156-01.2920E)
16:05	05:05	XCTD observation (#31)
17:28 – 17:56	06:28 – 06:56	CTD/LADCP C11M01 (500m)
18:00 – 18:30	07:00 – 07:30	MSP observation (#08, 500m)
18:40 – 18:58	07:40 – 07:58	Net sampling (#04-1)
19:00 – 19:19	08:00 – 08:19	Net sampling (#04-2)
19:20 – 19:39	08:20 – 08:39	Net sampling (#04-3)
Nov. 18th (Wed.) 2009		
05:01 – 07:10	18:01 – 20:10	CTD/pH/pCO_2 C11M02 (bottom)
08:03 – 11:15	21:03 – 00:15	Recovery of TRITON buoy #03 (2N, 156E)
11:18	00:18	Departure of St.11
13:24	02:24	Arrival at St.12 (01-30N, 156-00E)
13:27 – 13:56	02:27 – 02:56	CTD/LADCP C12M01 (500m)
14:02 – 14:33	03:02 – 03:33	MSP observation (#09, 500m)
14:36	03:36	Departure of St.12
17:24	06:24	Arrival at St.13 (01-00N, 156-00E)
17:32 – 18:03	06:32 – 07:03	CTD/LADCP C13M01 (500m)
18:11 – 18:45	07:11 – 07:45	MSP observation (#10, 500m)
18:48	07:48	Departure of St.13
20:54	09:54	Arrival at St.14 (00-30N, 156-00E)
20:58 – 21:27	09:58 – 10:27	CTD/LADCP C14M01 (500m)
21:34 – 22:02	10:34 – 11:02	MSP observation (#11, 500m)
22:06	11:06	Departure of St.14
Nov. 19th (Thu.) 2009		
01:36	14:36	Arrival at St.15 (EQ, 156-00E)
05:14 – 05:41	18:14 – 18:41	CTD/LADCP C15M01 (500m)
05:48 – 06:19	18:48 – 19:19	MSP observation (#12, 500m)
08:15 – 10:08	21:15 – 23:08	Deployment of TRITON buoy #04 (EQ, 156E)
		(Fixed Position: 00-00.9705N, 156-02.4404E)
10:37	23:37	XCTD observation (#32)

SMT	UTC	Event
12:58 – 14:34	01:58 – 03:34	Recovery of ADCP buoy #01 (EQ, 156E)
15:32 – 17:20	04:32 – 06:20	CTD/pH/pCO_2 C15M02 (bottom)
18:46 – 19:04	07:46 – 08:04	Net sampling (#05-1)
19:06 – 19:25	08:06 – 08:25	Net sampling (#05-2)
19:26 – 19:45	08:26 – 08:45	Net sampling (#05-3)
Nov. 20th (Fri.) 2009		
08:01 – 11:25	21:01 – 00:25	Recovery of TRITON buoy #04 (EQ, 156E)
13:33 – 14:25	02:33 – 03:25	Deployment of ADCP buoy #01 (EQ, 156E)
		(Fixed Position: 00-02.2231S, 156-08.0188E)
14:42	03:42	Departure of St.15
17:18	06:18	Arrival at St.16 (00-30S, 156-00E)
17:28 – 17:56	06:28 – 06:56	CTD/LADCP C16M01 (500m)
18:02 – 18:28	07:02 – 07:28	MSP observation (#13, 500m)
18:30	07:30	Departure of St.16
20:42	09:42	Arrival at St.17 (01-00S, 156-00E)
20:45 – 21:16	09:45 – 10:16	CTD/LADCP C17M01 (500m)
21:23 – 21:51	10:23 – 10:51	MSP observation (#14, 500m)
21:54	10:54	Departure of St.17
Nov. 21th (Sat.) 2009		
02:42	15:42	Arrival at St.18 (01-30S, 156-00E)
08:01 – 08:30	21:01 – 21:30	CTD/LADCP C18M01 (500m)
08:38 – 09:06	21:38 – 22:06	MSP observation (#15, 500m)
09:06	22:06	Departure of St.18
11:18	00:18	Arrival at St.19 (02-00S, 156-00E)
13:12 – 15:01	02:12 – 04:01	Deployment of TRITON buoy #05 (2S, 156E)
		(Fixed Position: 02-01.0030N, 155-57.5011E)
15:31	04:31	XCTD observation (#33)
16:00 – 16:41	05:00 – 05:41	CTD/LADCP/pH/pCO_2 C19M01 (800m)
16:47 – 17:17	05:47 – 06:17	MSP observation (#16, 500m)
Nov. 22th (Sun.) 2009		
08:00 – 10:53	21:00 – 23:53	Recovery of TRITON buoy #05 (2S, 156E)
13:05 – 15:01	02:05 – 04:01	Repair of TRITON buoy #05 (2S, 156E)
15:06	04:06	Departure of St.19
17:18	06:18	Arrival at St.20 (02-30S, 156-00E)
17:32 – 18:01	06:32 – 07:01	CTD/LADCP C20M01 (500m)
18:07 – 18:40	07:32 – 07:40	MSP observation (#17, 500m)
18:42	07:42	Departure of St.20
20:48	09:48	Arrival at St.21 (03-00S, 156-00E)
20:53 – 21:21	09:53 – 10:21	CTD/LADCP C21M01 (500m)

SMT	UTC	Event
21:26 – 21:56	10:26 – 10:56	MSP observation (#18, 500m)
22:00	11:00	Departure of St.21
Nov. 23th (Mon.) 2009		
06:30	19:30	Arrival at St.25 (05-00S, 156-00E)
08:12 – 09:59	21:12 – 22:59	Deployment of TRITON buoy #06 (5S, 156E)
		(Fixed Position: 05-01.7337N, 156-01.4370E)
10:20	23:20	XCTD observation (#34)
12:27 – 13:07	01:27 – 02:07	CTD/LADCP C25M01 (800m)
13:13 – 13:41	02:13 – 02:41	MSP observation (#19, 500m)
13:42	02:42	Departure of St.25
15:36	04:36	Arrival at St.24 (04-30S, 156-00E)
15:41 – 16:11	04:41 – 05:11	CTD/LADCP C24M01 (500m)
16:16 – 16:46	05:16 – 06:46	MSP observation (#20, 500m)
16:48	05:48	Departure of St.24
18:54	07:54	Arrival at St.23 (04-00S, 156-00E)
18:57 – 19:24	07:57 – 08:24	CTD/LADCP C23M01 (500m)
19:30 – 20:00	08:30 – 09:00	MSP observation (#21, 500m)
20:11 – 20:38	09:11 – 09:38	Figure-8 turn for Three-component magnetometer calibration
20:42	09:42	Departure of St.23
Nov. 24th (Tue.) 2009		
03:42	16:42	Arrival at St.25 (05-00S, 156-00E)
08:01 – 10:41	21:01 – 23:41	Recovery of TRITON buoy #06 (5S, 156E)
10:42	23:42	Departure of St.25
16:24	05:24	Arrival at St.22 (03-30S, 156-00E)
16:28 – 16:57	05:28 – 05:57	CTD/LADCP C22M01 (500m)
17:05 – 17:33	06:05 – 06:33	MSP observation (#22, 500m)
17:36	06:36	Departure of St.22
Nov. 25th (Wed.) 2009		
22:00	11:00	Time adjustment –1h (SMT=UTC+10h)
Nov. 26th (Thu.) 2009		
06:00	20:00	Arrival at St.26 (EQ, 147-00E)
08:36 – 11:45	22:36 – 01:45	CTD/pH/pCO_2 C26M01 (bottom)
13:12 – 15:49	03:12 – 05:49	Deployment of TRITON buoy #TR09 (EQ, 147-00E)
		(Fixed Position: 00-03.5892N, 147-00.6358E)
17:32 – 18:15	07:32 – 08:15	CTD/LADCP C26M02 (800m)
18:24 – 18:54	08:24 – 08:54	MSP observation (#23, 500m)
Nov. 27th (Fri.) 2009		
08:01 – 11:23	22:01 – 01:23	Recovery of TRITON buoy # TR09 (EQ, 147E)
13:50 – 15:55	03:50 – 05:55	Recovery of ADCP buoy #02 (EQ, 147E)

SMT	UTC	Event
Nov. 28th (Sat.) 2009		
08:03 – 09:42	22:03 – 23:42	Deployment of ADCP buoy #02 (EQ, 147E)
		(Fixed Position: 00-02.2231S, 156-08.0188E)
10:12	00:12	Departure of St.26
12:42	02:42	Arrival at St.27 (00-30N, 147-00E)
12:48 – 13:16	02:48 – 03:16	CTD/LADCP C27M01 (500m)
13:21 – 13:51	03:21 – 03:51	MSP observation (#24, 500m)
13:54	03:54	Departure of St.27
16:00	06:00	Arrival at St.28 (01-00N, 147-00E)
16:10 – 16:38	06:10 – 06:38	CTD/LADCP C28M01 (500m)
16:43 – 17:12	06:43 – 07:12	MSP observation (#25, 500m)
17:12	07:12	Departure of St.28
19:30	09:30	Arrival at St.29 (01-30N, 147-00E)
19:33 – 20:01	09:33 – 10:01	CTD/LADCP C29M01 (500m)
20:06 – 20:35	10:06 – 10:35	MSP observation (#26, 500m)
20:36	10:36	Departure of St.29
Nov. 29th (Sun.) 2009		
01:54	15:54	Arrival at St.30 (02-00N, 147-00E)
05:12 – 05:53	19:12 – 19:53	CTD/LADCP C30M01 (800m)
05:58 – 06:27	19:58 – 20:27	MSP observation (#27, 500m)
08:01 – 11:51	22:01 – 01:51	Recovery of TRITON buoy # TR08 (2N, 147E)
13:03 – 16:17	03:03 – 06:17	CTD/pH/pCO_2 C30M02 (bottom)
Nov. 30th (Mon.) 2009		
08:13 – 10:52	22:13– 00:52	Deployment of TRITON buoy #TR08 (2N, 147E)
		(Fixed Position: 01-59.5103N, 147-01.2417E)
11:48	01:48	XCTD observation (#35)
12:36	02:36	Departure of St.30
14:48	04:48	Arrival at St.31 (02-30N, 147-00E)
14:50 – 15:18	04:50 – 05:18	CTD/LADCP C31M01 (500m)
15:23 – 15:51	05:23 – 05:51	MSP observation (#28, 500m)
15:54	05:54	Departure of St.31
21:12	11:12	Arrival at St.32 (03-00N, 147-00E)
Dec. 01st (Tue.) 2009		
04:31 – 04:51	18:31 – 18:51	Net sampling (#06-1)
04:52 – 05:11	18:52 – 19:11	Net sampling (#06-2)
05:12 – 05:31	19:12 – 19:31	Net sampling (#06-3)
05:41 – 06:10	19:41 – 20:10	CTD/LADCP C32M01 (500m)
06:15 – 06:46	20:15 – 20:46	MSP observation (#29, 500m)
06:48	20:48	Departure of St.32

SMT	UTC	Event
09:12	23:12	Arrival at St.33 (03-30N, 147-00E)
09:17 – 09:44	23:17 – 23:44	CTD/LADCP C33M01 (500m)
09:48 – 10:17	23:48 – 00:17	MSP observation (#30, 500m)
10:18	00:18	Departure of St.33
12:48	02:48	Arrival at St.34 (04-00N, 147-00E)
12:51 – 13:17	02:51 – 03:17	CTD/LADCP C34M01 (500m)
13:22 – 13:52	03:22 – 03:52	MSP observation (#31, 500m)
13:54	03:54	Departure of St.34
16:18	06:18	Arrival at St.35 (04-30N, 147-00E)
16:19 – 16:50	06:19 – 06:50	CTD/LADCP C35M01 (500m)
16:55 – 17:27	06:55 – 07:27	MSP observation (#32, 500m)
17:30	07:30	Departure of St.35
23:00	13:00	Arrival at St.36 (05-00N, 147-00E)
Dec. 02nd (Wed.) 2009		
08:12 – 11:05	22:12 – 01:05	Deployment of TRITON buoy #TR07 (5N, 147-00E)
		(Fixed Position: 04-57.6570N, 147-01.8325E)
13:02 – 16:03	03:02 – 06:03	CTD/pH/pCO_2 C36M01 (bottom)
18:30 – 18:50	08:30 – 08:50	Net sampling (#07-1)
18:51 – 19:08	08:51 – 09:08	Net sampling (#07-2)
19:10 – 19:28	09:10 – 09:28	Net sampling (#07-3)
Dec. 03rd (Thu.) 2009		
08:02 – 11:50	22:02 – 01:50	Recovery of TRITON buoy # TR07 (05N, 147E)
13:02 – 13:45	03:02 – 03:45	CTD/LADCP C36M02 (500m)
13:50 – 14:21	03:50 – 04:21	MSP observation (#33, 500m)
14:26 – 14:51	04:26 – 04:51	MSP observation (#34, 500m)
15:00 – 15:30	05:00 – 05:30	MSP observation (#35, 500m)
15:30	05:30	Departure of St.36
Dec. 04th (Fri.) 2009		
18:12	08:12	Arrival at St.37 (10-00N, 147-00E)
18:21 – 18:39	08:21 – 08:39	Net sampling (#08-1)
18:41 – 18:59	08:41 – 08:59	Net sampling (#08-2)
19:01 – 19:18	09:01 – 09:18	Net sampling (#08-3)
19:24	09:24	Departure of St.37
Dec. 05th (Sat.) 2009		
Dec. 06th (Sun.) 2009		
08:58	22:58	Start of Cesium magnetometer observation (#2)
Dec. 07th (Mon.) 2009		
13:27	03:27	End of Cesium magnetometer observation (#2)
22:00	12:00	Time adjustment -1h (SMT=UTC+9h)

SMT	UTC	Event
Dec. 08th (Tue.) 2009		
Dec. 09th (Wed.) 2009		
Dec. 10th (Thu.) 2009		
10:00 – 10:28	01:00 – 01:28	Figure-8 turn for Three-component magnetometer calibration
16:00	07:00	Surface sea water sampling stop
Dec. 11th (Fri.) 2009		
08:40	23:40	Arrival of Hachinohe
15:30	06:30	Departure of Hachinohe
Dec. 12th (Sat.) 2009		
09:10	00:10	Arrival of Sekinehama

3.4 Cruise track

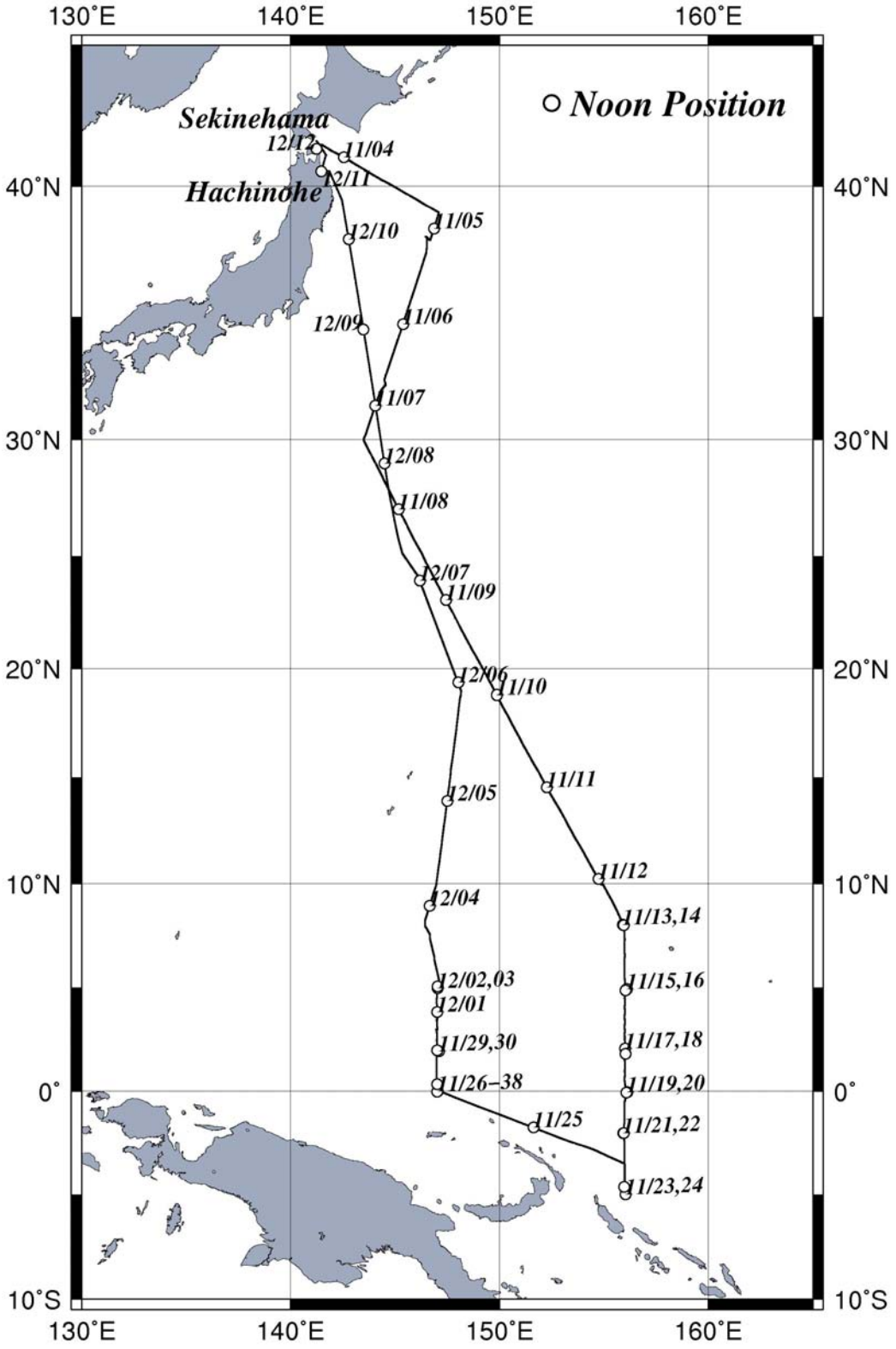

Fig 3.4 MR09-04 Cruise track and noon positions

4. Chief scientist

Chief Scientist

Yuji Kashino

Research Scientist

Research Institute for Global Change (RIGC),

Japan Agency for Marine-Earth Science and Technology (JAMSTEC)

2-15, Natsushima-cho, Yokosuka, 237-0061, Japan

Tel: +81-468-67-9459, FAX: +81-468-67-9835

e-mail: kashinoy@jamstec.go.jp

5. Participants list

5.1 R/V MIRAI scientists and technical staffs

Name	Affiliation	Occupation
Yuji Kashino	JAMSTEC	Chief Scientist
Kelvin Richards	IPRC, University of Hawaii	Scientist
Yasuhiro Arii	Marine Works Japan Ltd	Scientist
Tetsuo Harada	Kochi University	Scientist
Kohki Iyota	Kochi University	Scientist
Takashi Shiraki	Kochi University	Scientist
Chihiro Katagiri	Hokkaido University	Scientist
Yasuroh Kurusu	Ibaraki University	Scientist
Hiroe Hayashi	Ibaraki University	Scientist
Kiminori Shitashima	Central Research Institute of Electric Power Industry	Scientist
Tomoyuki Takamori	Marine Works Japan Ltd	Technical Staff
Tomohide Noguchi	Marine Works Japan Ltd	Technical Staff
Keisuke Matsumoto	Marine Works Japan Ltd	Technical Staff
Tatsuya Tanaka	Marine Works Japan Ltd	Technical Staff
Akira Watanabe	Marine Works Japan Ltd	Technical Staff
Shungo Oshitani	Marine Works Japan Ltd	Technical Staff
Yuichi Sonoyama	Marine Works Japan Ltd	Technical Staff
Masanori Enoki	Marine Works Japan Ltd	Technical Staff
Kimiko Nishijima	Marine Works Japan Ltd	Technical Staff
Junji Matsushita	Marine Works Japan Ltd	Technical Staff
Hironori Sato	Marine Works Japan Ltd	Technical Staff
Masaki Taguchi	Marine Works Japan Ltd	Technical Staff
Masaki Furuhata	Marine Works Japan Ltd	Technical Staff
Masaki Yamada	Marine Works Japan Ltd	Technical Staff
Soichiro Sueyoshi	Global Ocean Development Inc	Technical Staff
Ryo Kimura	Global Ocean Development Inc	Technical Staff

5.2 R/V MIRAI crew members

Name	Rank or rating
Yasushi Ishioka	Master
Takeshi Isohi	Chief Officer
Norihumi Watanabe	First Officer
Takao Nakayama	Jr.First Officer
Hajime Matsuo	Second Officer
Mitsunobu Asanuma	Third Officer
Youichi Hurukawa	Chief Engineer
Koji Masuno	First Engineer
Koji Manako	Second Engineer
Keisuke Nakamura	Third Engineer
Ryo Ohyama	Operator
Hisao Oguni	Boatswain
Yoshiharu Sakai	Able Seaman
Yasuhiro Ito	Able Seaman
Yosuke Kuwahara	Able Seaman
Tsuyoshi Sato	Able Seaman
Takeharu Aisaka	Able Seaman
Tsuyoshi Monzawa	Able Seaman
Masashige Okada	Able Seaman
Hiroki Saito	Able Seaman
Hideaki Tamotsu	Ordinary Seaman
Masaya Tanikawa	Ordinary Seaman
Keita Nishimura	Ordinary Seaman
Sadanori Honda	No.1 Oiler
Toshimi Yoshikawa	Oiler
Yoshihiro Sugimoto	Oiler
Osamu Hamasaki	Oiler
Kazumi Yamashita	Oiler
Keisuke Yoshida	Oiler
Hitoshi Ota	Chief Steward
Tamotsu Uemura	Cook
Sakae Hoshikuma	Cook
Michihiro Mori	Cook
Kozo Uemura	Cook
Hiroyuki Yoshizawa	Cook

6. General Observations

6.1 Meteorological Measurements

6.1.1 Surface Meteorological Observations

(1) Personnel

Kunio Yoneyama	(JAMSTEC) : Principal Investigator (not on-board)
Souichiro Sueyoshi	(Global Ocean Development Inc., GODI)
Ryo Kimura	(GODI)
Ryo Ohyama	(Mirai Crew)

(2) Objectives

Surface meteorological parameters are observed as a basic dataset of the meteorology. These parameters bring us the information about the temporal variation of the meteorological condition surrounding the ship.

(3) Methods

Surface meteorological parameters were observed throughout the MR09-04 cruise. During this cruise, we used three systems for the observation.

i. MIRAI Surface Meteorological observation (SMet) system
ii. Shipboard Oceanographic and Atmospheric Radiation (SOAR) system

i. MIRAI Surface Meteorological observation (SMet) system

Instruments of SMet system are listed in Table.6.1.1-1 and measured parameters are listed in Table.6.1.1-2. Data were collected and processed by KOAC-7800 weather data processor made by Koshin-Denki, Japan. The data set consists of 6-second averaged data.

ii. Shipboard Oceanographic and Atmospheric Radiation (SOAR) measurement system

SOAR system designed by BNL (Brookhaven National Laboratory, USA) consists of major three parts.

a) Portable Radiation Package (PRP) designed by BNL – short and long wave downward radiation.
b) Zeno Meteorological (Zeno/Met) system designed by BNL – wind, air temperature, relative humidity, pressure, and rainfall measurement.
c) Scientific Computer System (SCS) developed by NOAA (National Oceanic and Atmospheric Administration, USA) – centralized data acquisition and logging of all data sets.

SCS recorded PRP data every 6 seconds, while Zeno/Met data every 10 seconds. Instruments and their locations are listed in Table.6.1.1-3 and measured parameters are listed in Table.6.1.1-4.

For the quality control as post processing, we checked the following sensors, before and after the cruise.

i. Young Rain gauge (SMet and SOAR)

Inspect of the linearity of output value from the rain gauge sensor to change Input value

by adding fixed quantity of test water.

ii. Barometer (SMet and SOAR)

Comparison with the portable barometer value, PTB220CASE, VAISALA.

iii. Thermometer (air temperature and relative humidity) (SMet and SOAR)

Comparison with the portable thermometer value, HMP41/45, VAISALA.

(4) Preliminary results

Figure 6.1.1-1 shows the time series of the following parameters;

Wind (SOAR)
Air temperature (SOAR)
Sea surface temperature (SMet)
Relative humidity (SOAR)
Precipitation (SMet, Optical rain gauge)
Short/long wave radiation (SOAR)
Pressure (SOAR)
Significant wave height (SMet)

(5) Data archives

These meteorological data will be submitted to the Data Integration and Analysis Group (DIAG) of JAMSTEC just after the cruise.

(6) Remarks

i. SST (Sea Surface Temperature) data was available in the following periods.
23:30UTC 3 Nov. 2009 – 07:00UTC 10 Dec. 2009

Table.6.1.1-1 Instruments and installation locations of MIRAI Surface Meteorological observation system

Sensors	Type	Manufacturer	Location (altitude from surface)
Anemometer	KE-500	Koshin Denki, Japan	foremast (24 m)
Tair/RH	HMP45A	Vaisala, Finland	
with 43408 Gill aspirated radiation shield		R.M. Young, USA	compass deck (21 m) starboard side and port side
Thermometer: SST	RFN1-0	Koshin Denki, Japan	4th deck (-1m, inlet -5m)
Barometer	Model-370	Setra System, USA	captain deck (13 m) weather observation room
Rain gauge	50202	R. M. Young, USA	compass deck (19 m)
Optical rain gauge	ORG-815DR	Osi, USA	compass deck (19 m)
Radiometer (short wave)	MS-801	Eiko Seiki, Japan	radar mast (28 m)
Radiometer (long wave)	MS-200	Eiko Seiki, Japan	radar mast (28 m)
Wave height meter	MW-2	Tsurumi-seiki, Japan	bow (10 m)

Table.6.1.1-2 Parameters of MIRAI Surface Meteorological observation system

Parameter	Units	Remarks
1 Latitude	degree	
2 Longitude	degree	
3 Ship's speed	knot	Mirai log, DS-30 Furuno
4 Ship's heading	degree	Mirai gyro, TG-6000, Tokimec
5 Relative wind speed	m/s	6sec./10min. averaged
6 Relative wind direction	degree	6sec./10min. averaged
7 True wind speed	m/s	6sec./10min. averaged
8 True wind direction	degree	6sec./10min. averaged
9 Barometric pressure	hPa	adjusted to sea surface level
		6sec. averaged
10 Air temperature (starboard side)	degC	6sec. averaged
11 Air temperature (port side)	degC	6sec. averaged
12 Dewpoint temperature (starboard side)	degC	6sec. averaged
13 Dewpoint temperature (port side)	degC	6sec. averaged
14 Relative humidity (starboard side)	%	6sec. averaged
15 Relative humidity (port side)	%	6sec. averaged
16 Sea surface temperature	degC	6sec. averaged
17 Rain rate (optical rain gauge)	mm/hr	hourly accumulation
18 Rain rate (capacitive rain gauge)	mm/hr	hourly accumulation
19 Down welling shortwave radiation	W/m2	6sec. averaged
20 Down welling infra-red radiation	W/m2	6sec. averaged
21 Significant wave height (bow)	m	hourly
22 Significant wave height (aft)	m	hourly
23 Significant wave period (bow)	second	hourly
24 Significant wave period (aft)	second	hourly

Table.6.1.1-3 Instruments and installation locations of SOAR system

Sensors (Zeno/Met)	Type	Manufacturer	Location (altitude from surface)
Anemometer	05106	R.M. Young, USA	foremast (25 m)
Tair/RH	HMP45A	Vaisala, Finland	
with 43408 Gill aspirated radiation shield		R.M. Young, USA	foremast (23 m)
Barometer	61202V	R.M. Young, USA	
with 61002 Gill pressure port		R.M. Young, USA	foremast (23 m)
Rain gauge	50202	R.M. Young, USA	foremast (24 m)
Optical rain gauge	ORG-815DA	Osi, USA	foremast (24 m)

Sensors (PRP)	Type	Manufacturer	Location (altitude from surface)
Radiometer (short wave)	PSP	Epply Labs, USA	foremast (25 m)
Radiometer (long wave)	PIR	Epply Labs, USA	foremast (25 m)
Fast rotating shadowband radiometer		Yankee, USA	foremast (25 m)

Table.6.1.1-4 Parameters of SOAR system

Parameter	Units	Remarks
1 Latitude	degree	
2 Longitude	degree	
3 SOG	knot	
4 COG	degree	
5 Relative wind speed	m/s	
6 Relative wind direction	degree	
7 Barometric pressure	hPa	
8 Air temperature	degC	
9 Relative humidity	%	
10 Rain rate (optical rain gauge)	mm/hr	
11 Precipitation (capacitive rain gauge)	mm	reset at 50 mm
12 Down welling shortwave radiation	W/m2	
13 Down welling infra-red radiation	W/m2	
14 Defuse irradiance	W/m2	

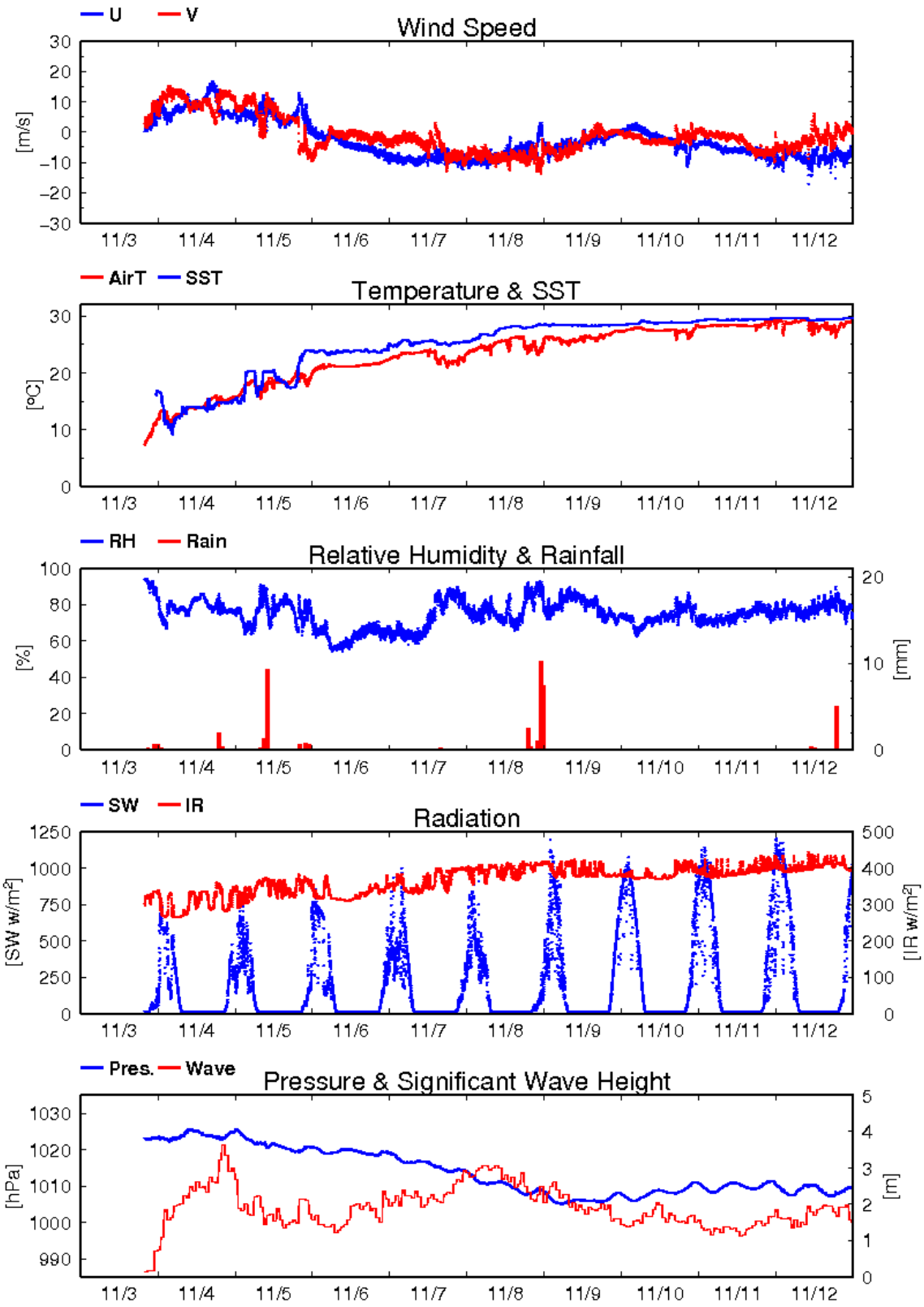

Fig.6.1.1-1 Time series of surface meteorological parameters during the cruise

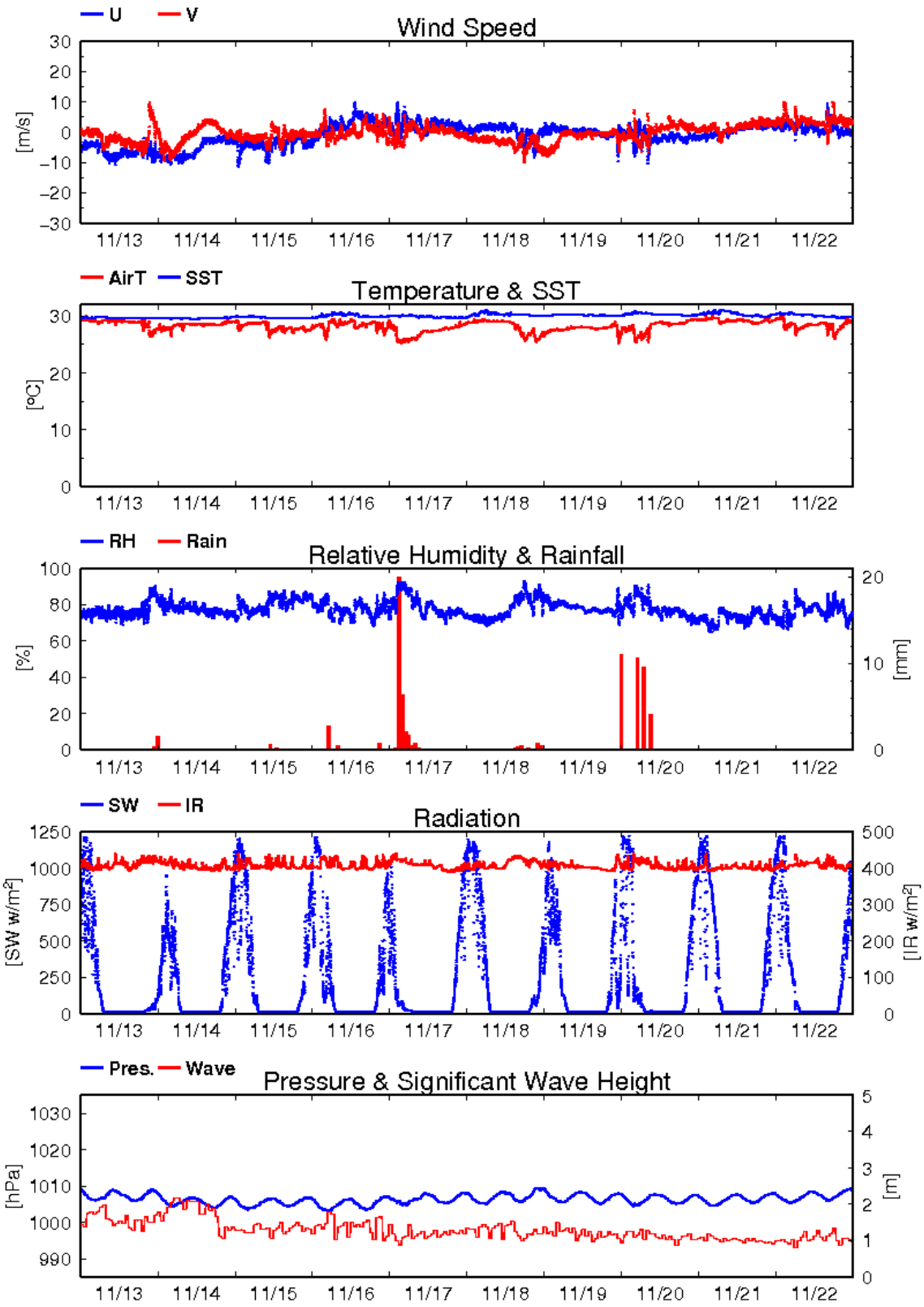

Fig. 6.1.1-1 (Continued)

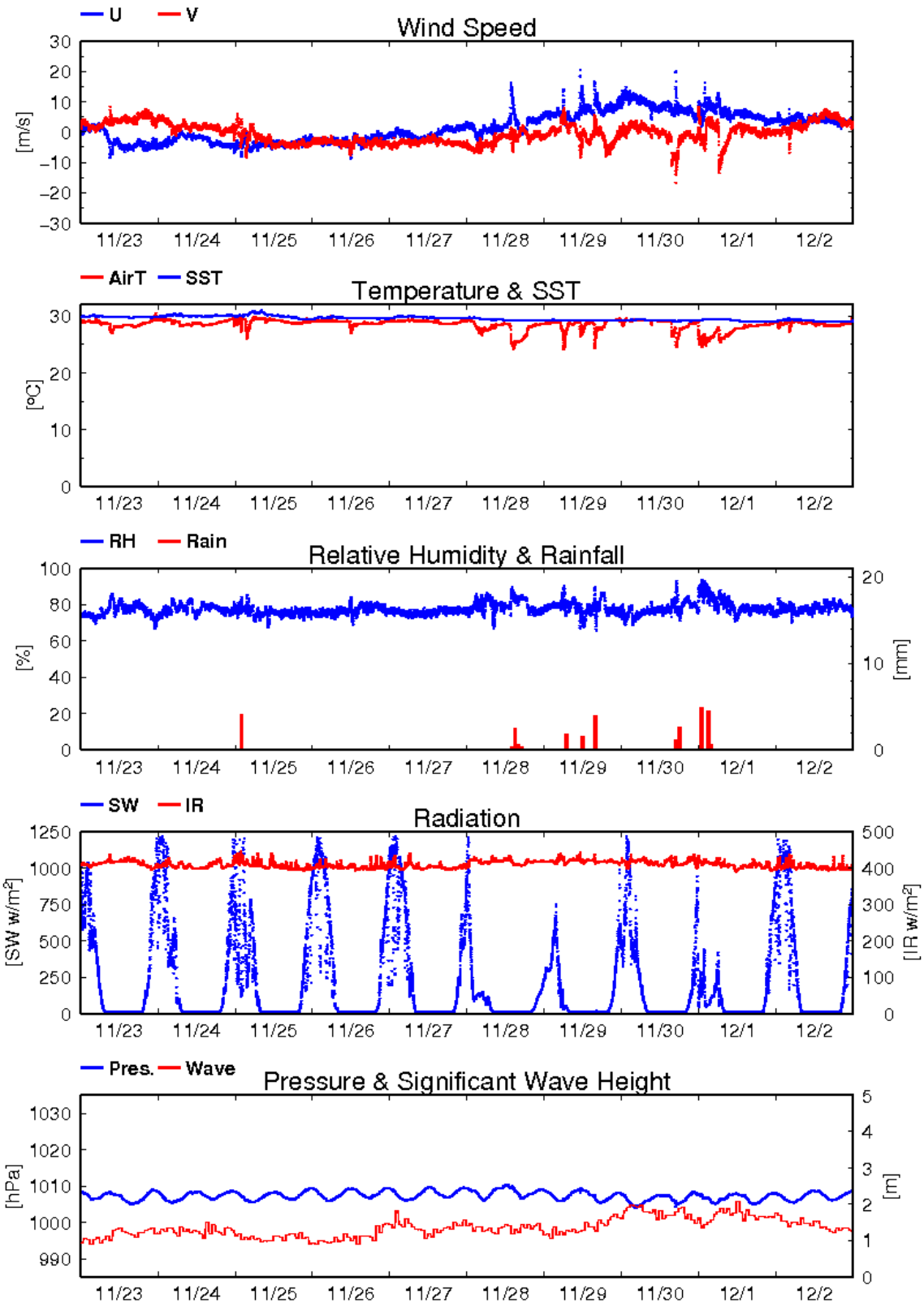

Fig. 6.1.1-1 (Continued)

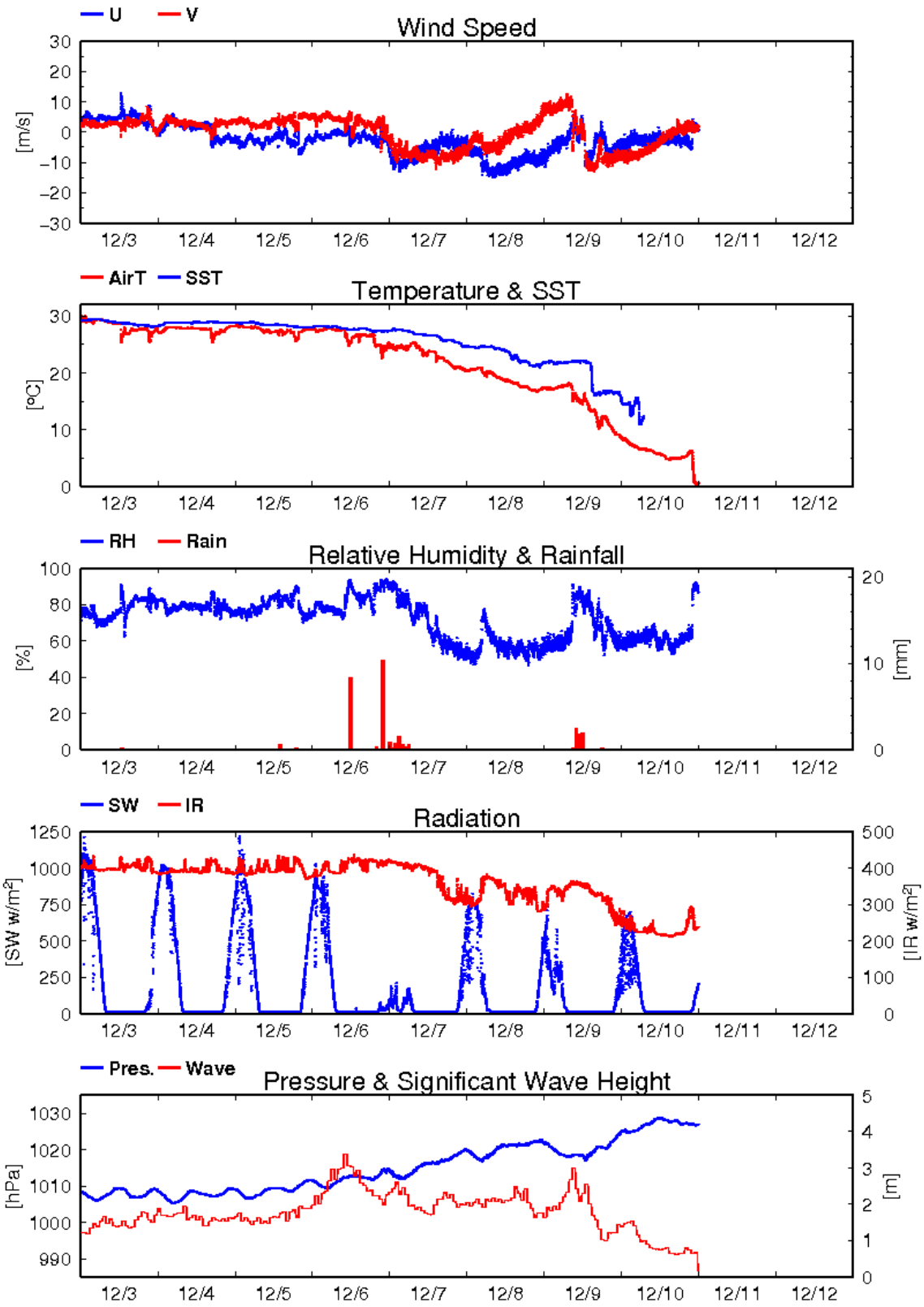

Fig. 6.1.1-1 (Continued)

6.1.2 Ceilometer observation

(1) Personnel

Kunio Yoneyama	(JAMSTEC): Principal Investigator (not on-board)
Souichiro Sueyoshi	(Global Ocean Development Inc., GODI)
Ryo Kimura	(GODI)
Ryo Ohyama	(MIRAI Crew)

(2) Objectives

The information of cloud base height and the liquid water amount around cloud base is important to understand the process on formation of the cloud. As one of the methods to measure them, the ceilometer observation was carried out.

(3) Paramters

1. Cloud base height [m].
2. Backscatter profile, sensitivity and range normalized at 30 m resolution.
3. Estimated cloud amount [oktas] and height [m]; Sky Condition Algorithm.

(4) Methods

We measured cloud base height and backscatter profile using ceilometer (CT-25K, VAISALA, Finland) throughout the MR09-04 cruise.

Major parameters for the measurement configuration are as follows;

Laser source:	Indium Gallium Arsenide (InGaAs) Diode
Transmitting wavelength:	905±5 nm at 25 degC
Transmitting average power:	8.9 mW
Repetition rate:	5.57 kHz
Detector:	Silicon avalanche photodiode (APD)
	Responsibility at 905 nm: 65 A/W
Measurement range:	0 ~ 7.5 km
Resolution:	50 ft in full range
Sampling rate:	60 sec
Sky Condition	0, 1, 3, 5, 7, 8 oktas (9: Vertical Visibility)
	(0: Sky Clear, 1:Few, 3:Scattered, 5-7: Broken, 8: Overcast)

On the archive dataset, cloud base height and backscatter profile are recorded with the resolution of 30 m (100 ft).

(5) Preliminary results

Fig.6.1.2-1 shows the time series of the lowest, second and third cloud base height during the cruise.

(6) Data archives

The raw data obtained during this cruise will be submitted to the Data Integration and Analysis

Group (DIAG) in JAMSTEC.

(7) Remarks

1. Window cleaning;

20:45UTC 10 Nov. 2009

19:45UTC 18 Nov. 2009

22:07UTC 23 Nov. 2009

05:37UTC 02 Dec. 2009

05:59UTC 09 Dec. 2009

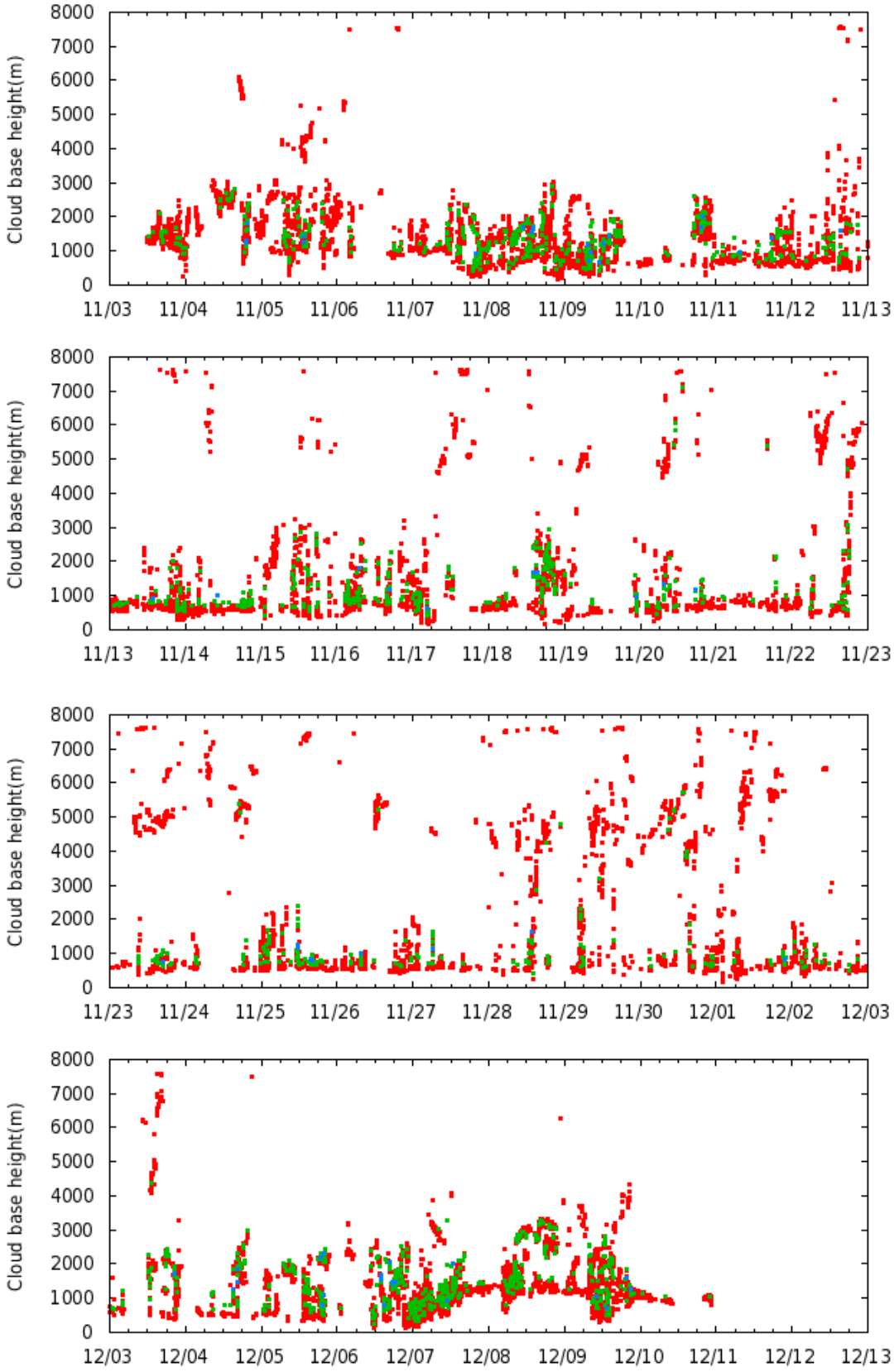

Fig. 6.1.2-1 Lowest(red), 2nd(green) and 3rd(blue) cloud base height during the cruise

6.2 CTD/XCTD

6.2.1 CTD

Personnel	Yuji Kashino	(JAMSTEC): Principal investigator
	Tomoyuki Takamori	(MWJ): Operation leader
	Yuichi Sonoyama	(MWJ)

(1) Objective

Investigation of oceanic structure and water sampling

(2) Parameters

Temperature (Primary and Secondary)
Conductivity (Primary and Secondary)
Pressure
Dissolved Oxygen

(3) Instruments and Methods

CTD/Carousel Water Sampling System, which is a 36-position Carousel water sampler (CWS) with Sea-Bird Electronics, Inc. CTD (SBE9plus), was used during this cruise. 12-litter Niskin Bottles were used for sampling seawater. The sensors attached on the CTD were temperature (Primary and Secondary), conductivity (Primary and Secondary), pressure, dissolved oxygen, altimeter, Fluorescence. Salinity was calculated by measured values of pressure, conductivity and temperature. The CTD/CWS was deployed from starboard on working deck.

The CTD raw data were acquired on real time using the Seasave-Win32 (ver.7.17a) provided by Sea-Bird Electronics, Inc. and stored on the hard disk of the personal computer. Seawater was sampled during the up cast by sending fire commands from the personal computer. We sampled seawater for analysis of salinity, dissolved oxygen and nutrients (routine cast).

The package was lowered into the water from the starboard side and held 10 m beneath the surface for about 1 minute in order to activate the pump. After the pump was activated the package was lifted to the surface, and the package was lowered again at a rate of about 1.0 m/s to 1.2m/s. For the up cast, the package was lifted at a rate of 1.2 m/s except for bottle firing stops. At each bottle firing stops, the bottle was fired.

Data processing procedures and used utilities of SBE Data Processing-Win32 (ver.7.17a) and SEASOFT were as follows:

(The process in order)

DATCNV : Convert the binary raw data to engineering unit data. DATCNV also extracts bottle information where scans were marked with the bottle confirm bit during acquisition.

TCORP (original module) : Corrected the pressure sensitivity of the temperature (SBE3) sensor.

S/N 1359 : -1.8386e-007 (degC/dbar)

S/N 1525 : 5.92243e-009(degC/dbar)

BOTTLESUM : Create a summary of the bottle data. The data were averaged over 3 seconds.

ALIGNCTD : Convert the time-sequence of sensor outputs into the pressure sequence to ensure that all calculations were made using measurements from the same parcel of water. Oxygen data are systematically delayed with respect to depth mainly because of the long time constant of the oxygen sensor and of an additional delay from the transit time of water in the pumped pluming line. This delay was compensated by 6 seconds advancing oxygen sensor output (oxygen voltage) relative to the temperature data.

WILDEDIT : Mark extreme outliers in the data files. The first pass of WILDEDIT obtained an accurate estimate of the true standard deviation of the data. The data were read in blocks of 1000 scans. Data greater than 10 standard deviations were flagged. The second pass computed a standard deviation over the same 1000 scans excluding the flagged values. Values greater than 20 standard deviations were marked bad. This process was applied to all variables.

CELLTM : Remove conductivity cell thermal mass effects from the measured conductivity. Typical values used were thermal anomaly amplitude alpha = 0.03 and the time constant 1/beta = 7.0.

FILTER : Perform a low pass filter on pressure with a time constant of 0.15 second. In order to produce zero phase lag (no time shift) the filter runs forward first then backwards.

SECTIONU (original module of SECTION) : Select a time span of data based on scan number in order to reduce a file size. The minimum number was set to be the starting time when the CTD package was beneath the sea-surface after activation of the pump. The maximum number of was set to be the end time when the package came up from the surface. Data for estimation of the CTD pressure drift were prepared before SECTION.

LOOPEDIT：Mark scans where the CTD was moving less than the minimum velocity of 0.0 m/s (traveling backwards due to ship roll).

DESPIKE (original module)：Remove spikes of the data. A median and mean absolute deviation was calculated in 1-dbar pressure bins for both down and up cast, excluding the flagged values. Values greater than 4 mean absolute deviations from the median were marked bad for each bin. This process was performed 2 times for temperature, conductivity, oxygen voltage (SBE43).

DERIVE：Compute oxygen (SBE43)

BINAVG：Average the data into 1-dbar pressure bins.

DERIVE：Compute salinity, potential temperature, and sigma-theta.

SPLIT：Separate the data from an input cnv file into down cast and up cast files.

Configuration file

MR0904A.con (File name; C01M01～C10M01)

MR0904B.con (File name; C11M01～C36M02)

Specifications of the sensors are listed below.

CTD：SBE911plus CTD system

Under water unit：

SBE9plus (S/N 09P9833-0357, Sea-Bird Electronics, Inc.)

Pressure sensor：Digiquartz pressure sensor (S/N 42423)

Calibrated Date：24 Jul. 2009

Temperature sensors：

Primary：SBE03-04/F (S/N 031359, Sea-Bird Electronics, Inc.)

Calibrated Date：07 Jul. 2009

Secondary：SBE03-04F (S/N 031525, Sea-Bird Electronics, Inc.)

Calibrated Date：07 Jul. 2009

Conductivity sensors：

Primary：SBE04C (S/N 043036, Sea-Bird Electronics, Inc.)

Calibrated Date：08 Jul. 2009

Secondary：SBE04-04/O (S/N 041203, Sea-Bird Electronics, Inc.)

Calibrated Date：08 Jul. 2009

SBE04-02/O (S/N 041088, Sea-Bird Electronics, Inc.)

Calibrated Date：08 Jul. 2009

Dissolved Oxygen sensors：

Primary：SBE43 (S/N 430949, Sea-Bird Electronics, Inc.)

Calibrated Date：21 Nov. 2008

Altimeter：Benthos PSA-916T (S/N 1100, Teledyne Benthos, Inc.)

Carousel water sampler：

SBE32 (S/N 3227443-0391, Sea-Bird Electronics, Inc.)

Deck unit：SBE11plus (S/N 11P7030-0272, Sea-Bird Electronics, Inc.)

(4) Preliminary results

Total 43 casts of CTD measurements have been carried out (see table6.2.1 below). Vertical profile (down cast) of primary temperature, salinity, dissolved oxygen with pressure are shown in Figure 6.2.1-1-6.2.1-43

(5) Data Policy

All raw and processed CTD data files were copied onto DVD-ROM. The data will be submitted to the Data Integration and Analyses Group (DIAG), JAMSTEC, and will be opened to public via “R/V MIRAI Data Web Page” in JAMSTEC home page.

Table 6.2.1-1 CTD Casttable

Stnnbr	Castno	Date(UTC)	Time(UTC)		BottomPosition		Depth	Wire Out	HT Above Bottom	Max Depth	Max Pressure	CTD Filename	Remark
		(mmddyy)	Start	End	Latitude	Longitude							
C01	1	110509	07:02	08:06	38-06.59N	146-30.29E	5394.0	2025.4	-	1976.3	2001.7	C01M01	
C02	1	110609	19:30	20:36	32-15.19N	144-32.99E	5631.0	2057.5	-	1977.7	2002.1	C02M01	pH/pCO2 LADCP
C03	1	111209	02:28	03:37	10-00.42N	154-51.08E	5551.0	2049.8	-	1980.1	2000.5	C03M01	pH/pCO2 LADCP
C04	1	111209	19:16	19:50	08-01.29N	155-55.86E	4845.0	804.8	-	795.2	801.4	C04M01	LADCP
C04	2	111309	02:10	05:21	08-02.96N	155-51.78E	4843.0	4836.5	46.2	4764.3	4844.8	C04M02	pH/pCO2
C05	1	111409	18:42	19:21	04-58.32N	156-03.86E	3596.0	802.1	-	794.3	801.0	C05M01	LADCP
C05	2	111509	02:10	04:40	04-56.70N	156-06.36E	3592.0	3583.5	27.3	3607.6	3556.7	C05M02	pH/pCO2
C06	1	111609	02:48	03:10	04-29.92N	156-00.24E	3555.0	503.1	-	497.9	501.7	C06M01	LADCP
C07	1	111609	06:39	07:00	04-00.04N	156-00.14E	3474.0	497.9	-	500.1	497.6	C07M01	LADCP
C08	1	111609	10:06	10:27	03-30.08N	156-00.14E	3247.0	497.8	-	500.0	496.6	C08M01	LADCP
C09	1	111609	18:08	18:31	03-00.33N	156-00.23E	2870.0	499.4	-	498.2	501.5	C09M01	LADCP
C10	1	111609	21:48	22:09	02-30.18N	156-00.08E	2675.0	499.2	-	497.6	501.3	C10M01	LADCP
C11	1	111709	06:32	06:53	02-00.53N	155-55.74E	2566.0	507.5	-	496.8	499.7	C11M01	secondary coductivitys senser chenge(S/N041203→041088) LADCP
C11	2	111709	18:06	20:06	01-57.79N	155-59.67E	2568.0	2565.4	35.6	2527.5	2557.5	C11M02	pH/pCO2
C12	1	111809	02:31	02:52	01-30.02N	156-00.16E	2383.0	498.5	-	497.4	501.2	C12M01	LADCP
C13	1	111809	06:37	06:58	01-00.00N	155-59.99E	2262.0	498.9	-	498.4	500.7	C13M01	LADCP
C14	1	111809	10:02	10:23	00-30.04N	156-00.09E	2142.0	500.5	-	498.7	501.4	C14M01	LADCP
C15	1	111809	18:17	18:37	00-01.76N	156-02.24E	1956.0	498.3	-	496.6	500.1	C15M01	LADCP
C15	2	111909	04:37	06:15	00-01.77S	155-58.49E	1943.0	1946.8	30.4	1908.0	1928.0	C15M02	pH/pCO2
C16	1	112009	06:32	06:53	00-30.18S	155-59.78E	1953.0	498.5	-	497.0	500.4	C16M01	LADCP
C17	1	112009	09:50	10:12	00-59.91S	155-59.73E	2084.0	501.4	-	496.7	500.7	C17M01	LADCP
C18	1	112009	21:05	21:26	01-29.98S	155-59.79E	1813.0	497.8	-	496.7	500.4	C18M01	LADCP
C19	1	112109	05:03	05:38	01-59.02S	155-59.43E	1747.0	815.6	-	797.4	803.9	C19M01	pH/pCO2 LADCP
C20	1	112209	06:37	06:57	02-30.14S	155-59.73E	1742.0	498.9	-	497.3	501.0	C20M01	LADCP
C21	1	112209	09:56	10:18	03-00.06S	155-59.93E	1814.0	498.5	-	497.1	500.5	C21M01	LADCP
C25	1	112309	01:31	02:04	04-57.69S	156-01.95E	1496.0	801.5	-	794.6	801.2	C25M01	pH/pCO2 LADCP
C24	1	112309	04:46	05:06	04-29.77S	155-59.83E	1723.0	507.6	-	497.5	501.1	C24M01	LADCP
C23	1	112309	08:01	08:21	03-59.67S	156-00.09E	1783.0	502.3	-	497.1	500.0	C23M01	LADCP
C22	1	112409	05:32	05:53	03-29.88S	156-00.12E	1893.0	499.0	-	497.5	500.3	C22M01	pH/pCO2 LADCP
C26	1	112509	22:41	01:42	00-01.29S	147-01.63E	4535.0	4504.0	31.0	4474.1	4547.1	C26M01	pH/pCO2
C26	2	112609	07:37	08:11	00-04.49N	147-01.55E	4470.0	806.7	-	796.5	803.5	C26M02	LADCP
C27	1	112809	02:51	03:12	00-29.80N	147-00.02E	4483.0	501.6	-	496.4	500.5	C27M01	LADCP
C28	1	112809	06:14	06:34	00-59.97N	146-59.94E	4510.0	497.6	-	497.6	500.5	C28M01	LADCP
C29	1	112809	09:38	09:58	01-29.83N	146-59.91E	4510.0	501.2	-	496.8	501.0	C29M01	LADCP
C30	1	112809	19:16	19:50	01-58.55N	147-01.82E	4519.0	807.2	-	796.5	802.8	C30M01	LADCP
C30	2	112909	03:08	06:13	01-58.48N	147-02.07E	4516.0	4521.9	30.4	4477.5	4550.0	C30M02	pH/pCO2
C31	1	113009	04:54	05:15	02-29.82N	147-00.38E	4402.0	515.3	-	496.5	500.5	C31M01	LADCP
C32	1	113009	19:45	20:06	02-59.42N	147-01.18E	4413.0	500.3	-	497.6	500.5	C32M01	LADCP
C33	1	113009	23:21	23:40	03-29.65N	147-00.54E	4274.0	510.2	-	497.6	501.5	C33M01	LADCP
C34	1	120109	02:52	03:14	03-59.67N	147-00.31E	4698.0	516.8	-	497.2	501.2	C34M01	LADCP
C35	1	120109	06:24	06:46	04-29.68N	147-00.37E	3903.0	502.7	-	497.5	501.1	C35M01	LADCP
C36	1	120209	03:06	06:00	05-01.85N	146-58.74E	4261.0	4257.9	29.0	4211.2	4277.9	C36M01	pH/pCO2
C36	2	120309	03:07	03:41	04-57.96N	147-03.73E	4215.0	802.3	-	795.5	801.6	C36M02	pH/pCO2 LADCP

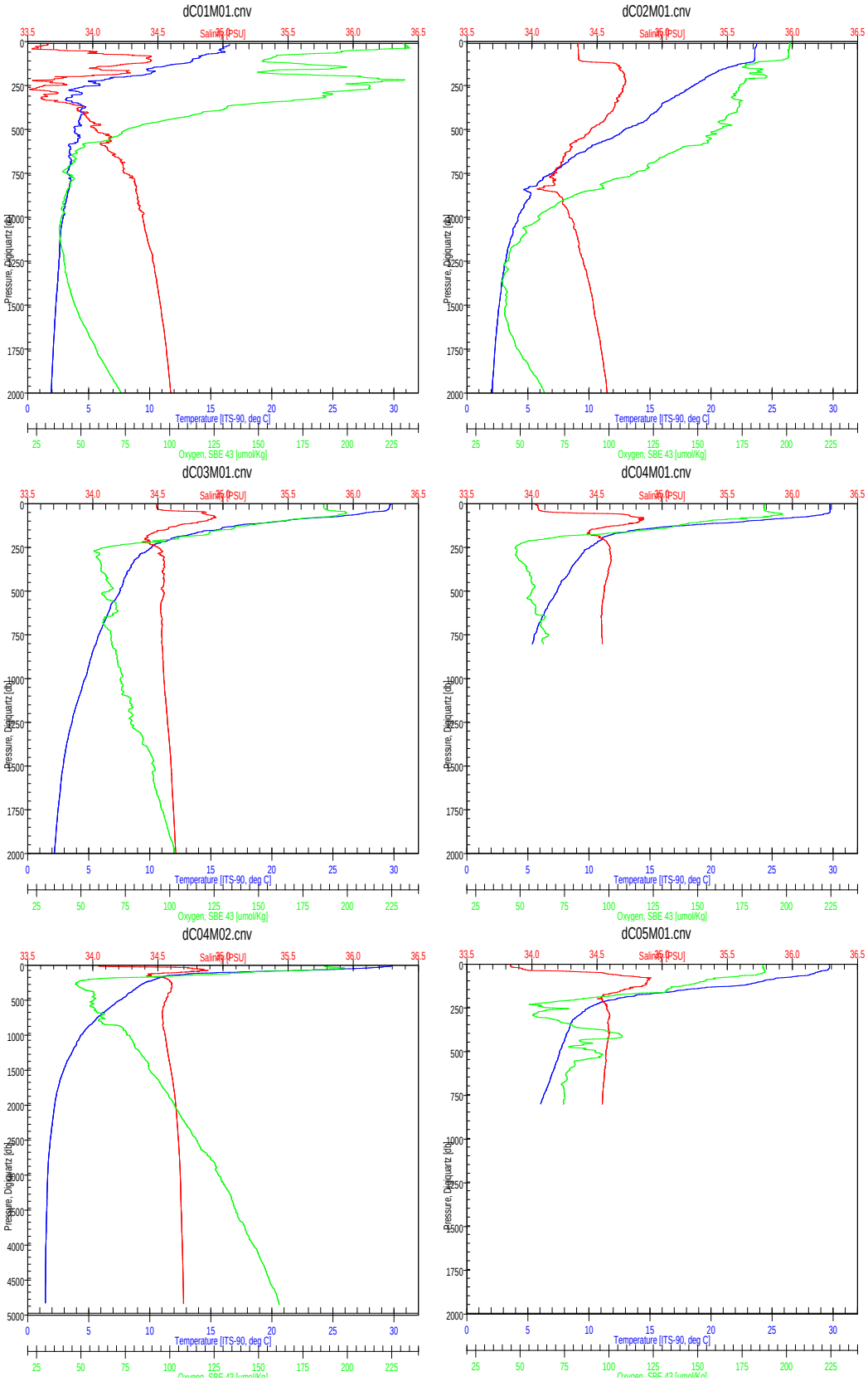

Figure 6.2.1-1～-6 CTD profile

(C01M01, C02M01, C03M01, C04M01, C04M02 and C05M01)

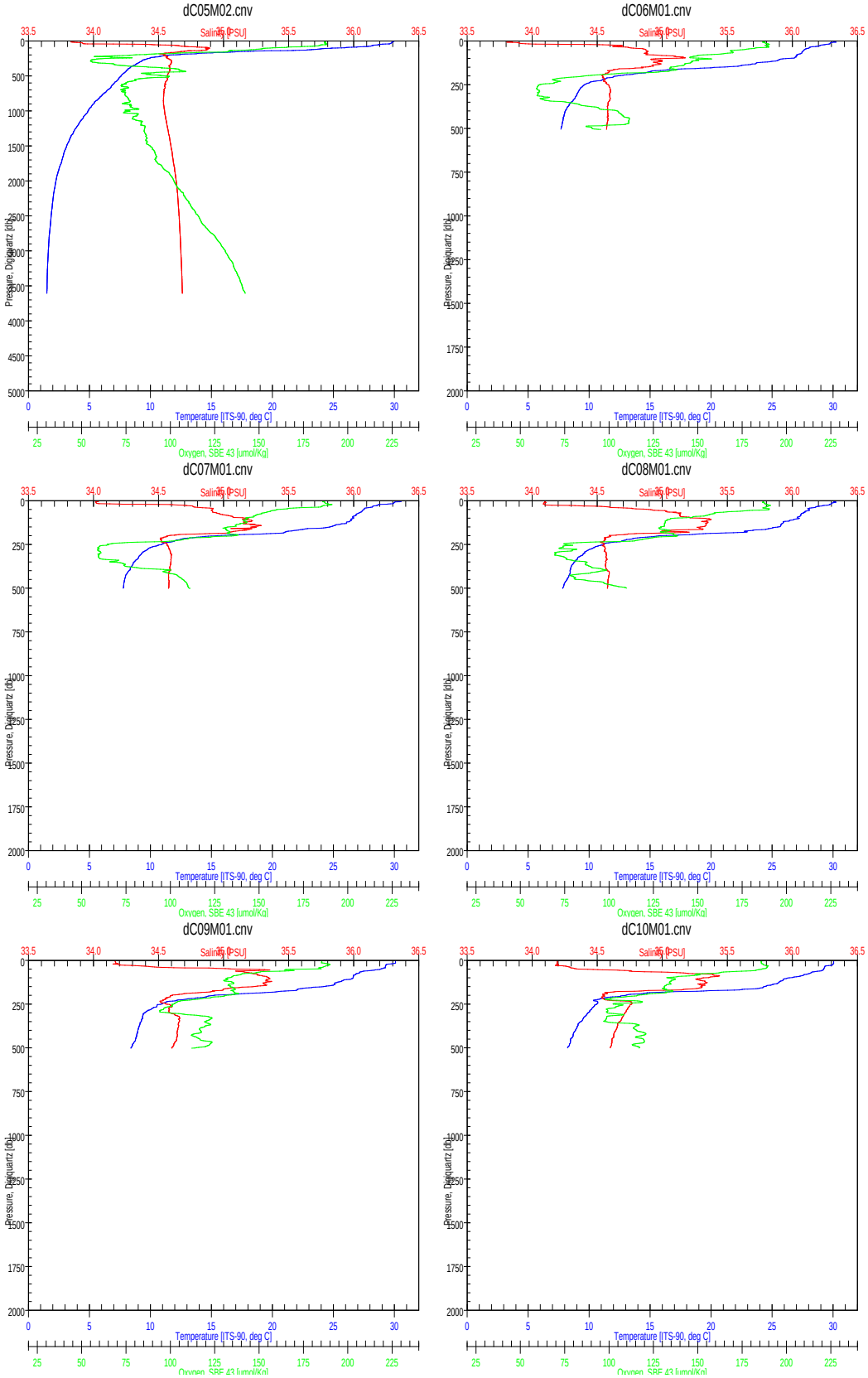

Figure 6.2.1-7～-12 CTD profile

(C05M02, C06M01, C07M01, C08M01, C09M01 and C10M01)

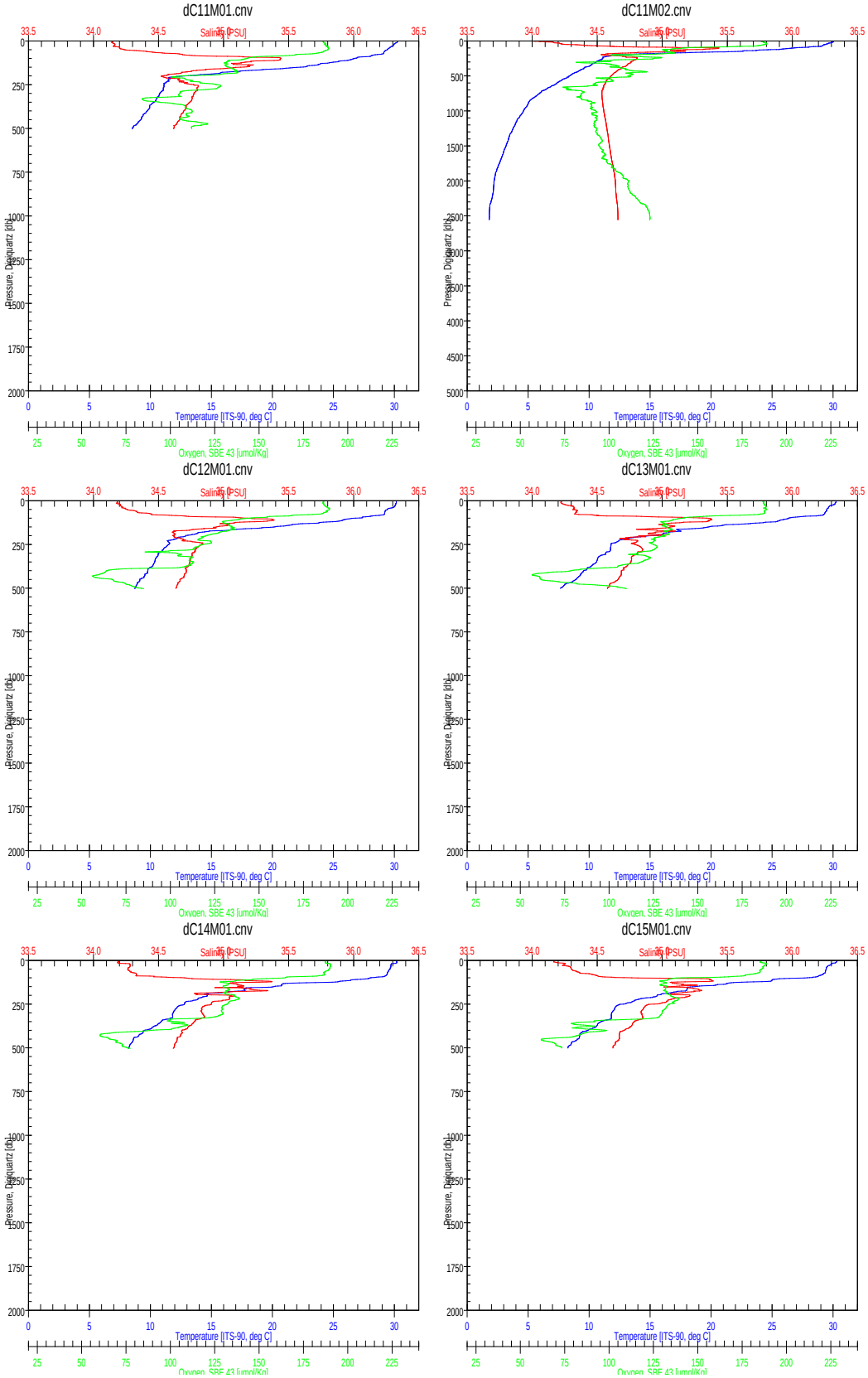

Figure 6.2.1-13～-18 CTD profile

(C11M01, C11M02, C12M01, C13M01, C14M01 and C15M01)

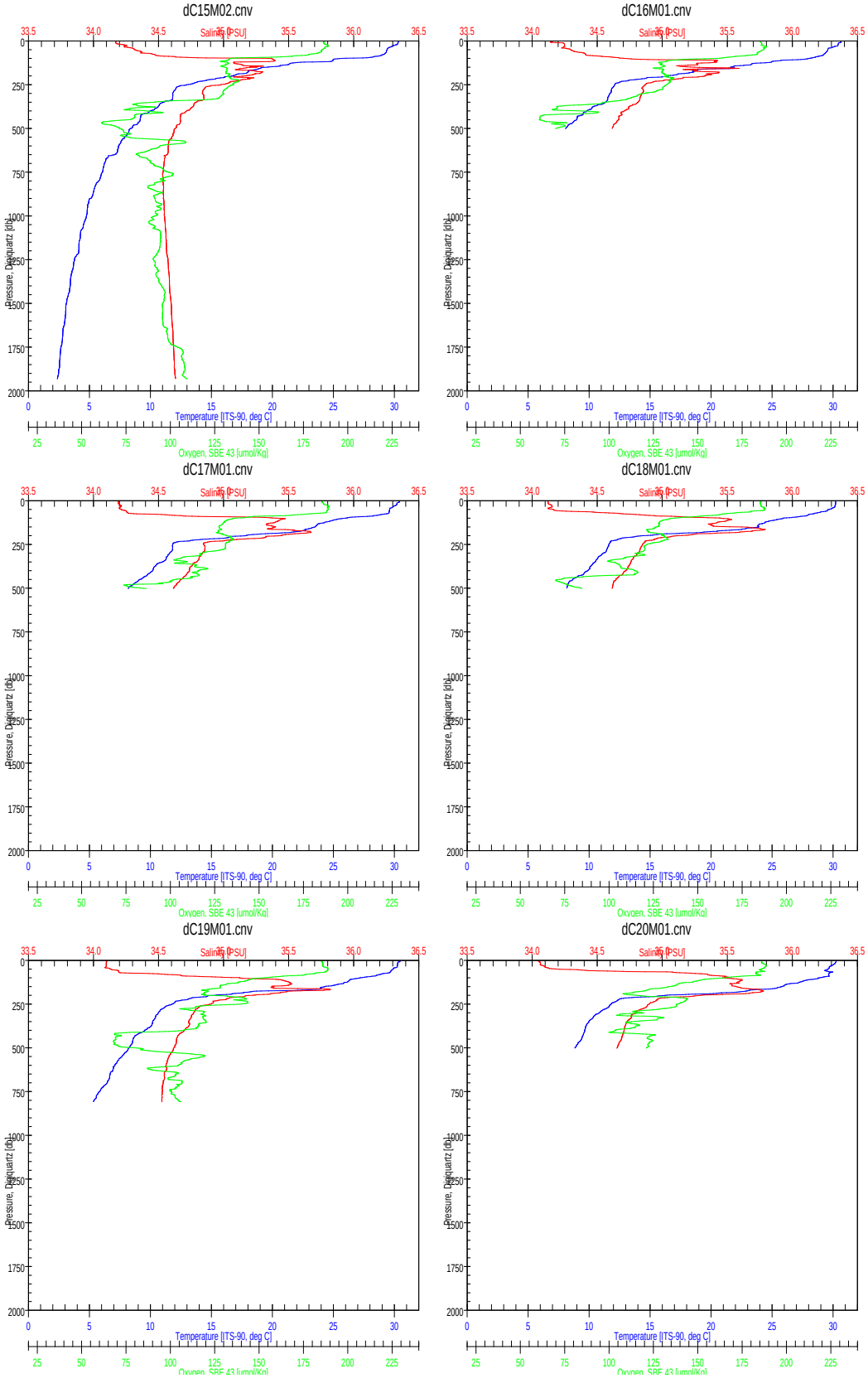

Figure 6.2.1-19～-24 CTD profile

(C15M02, C16M01, C17M01, C18M01, C19M01 and C20M01)

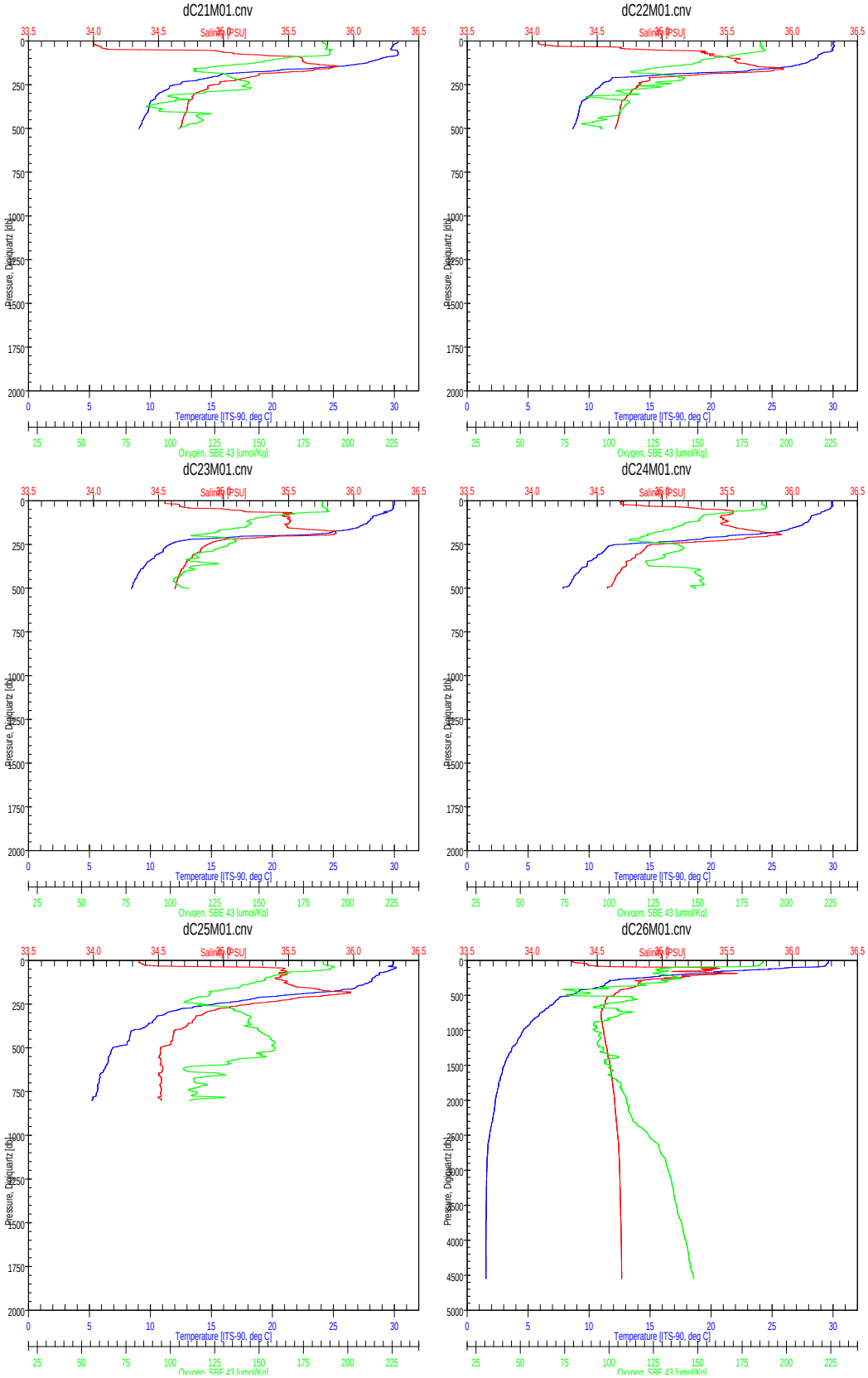

Figure 6.2.1-25～-30 CTD profile

(C21M01, C22M01, C23M01, C24M01, C25M01 and C26M01)

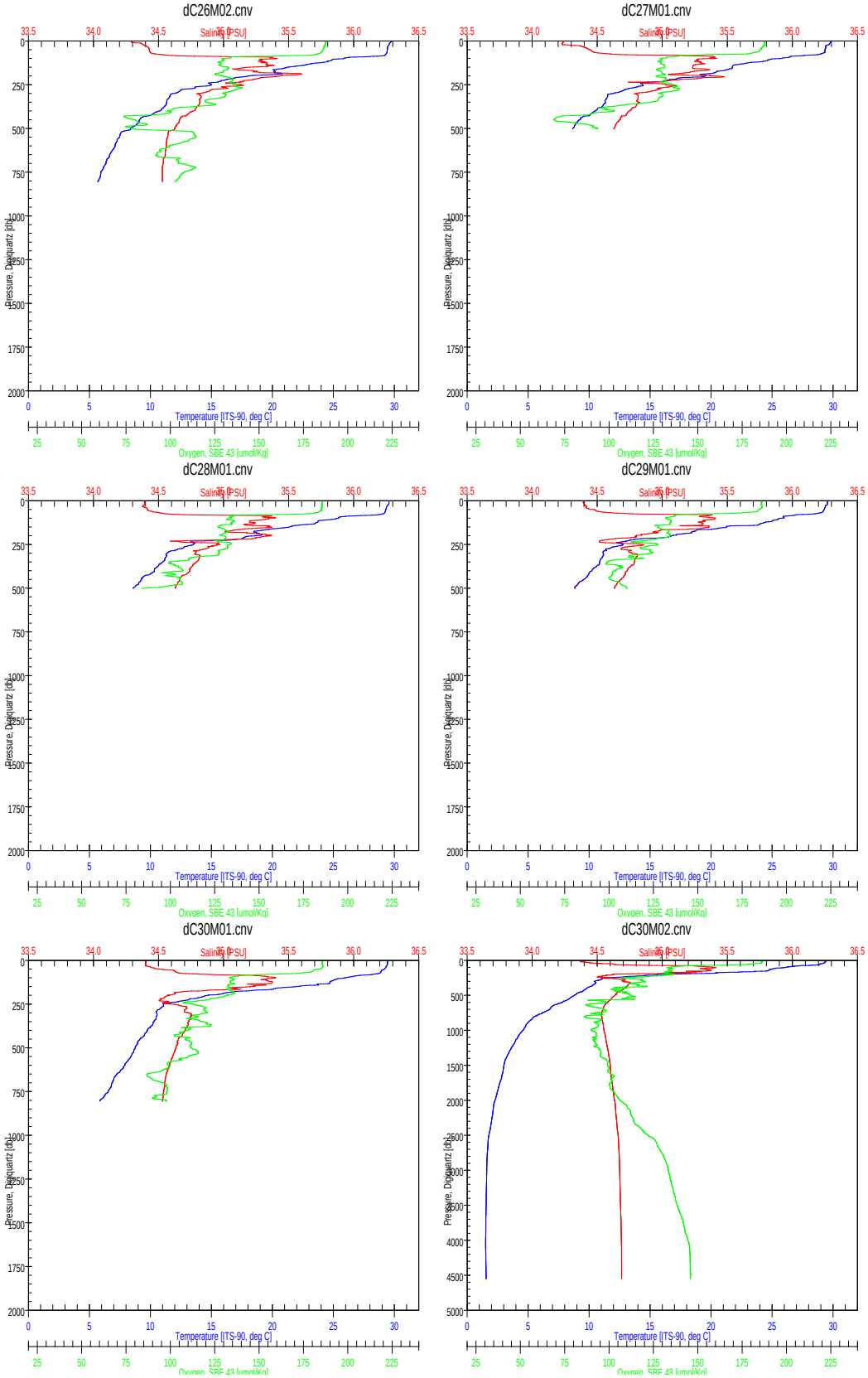

Figure 6.2.1-31～-36 CTD profile

(C26M02, C27M01, C28M01, C29M01, C30M01 and C30M02)

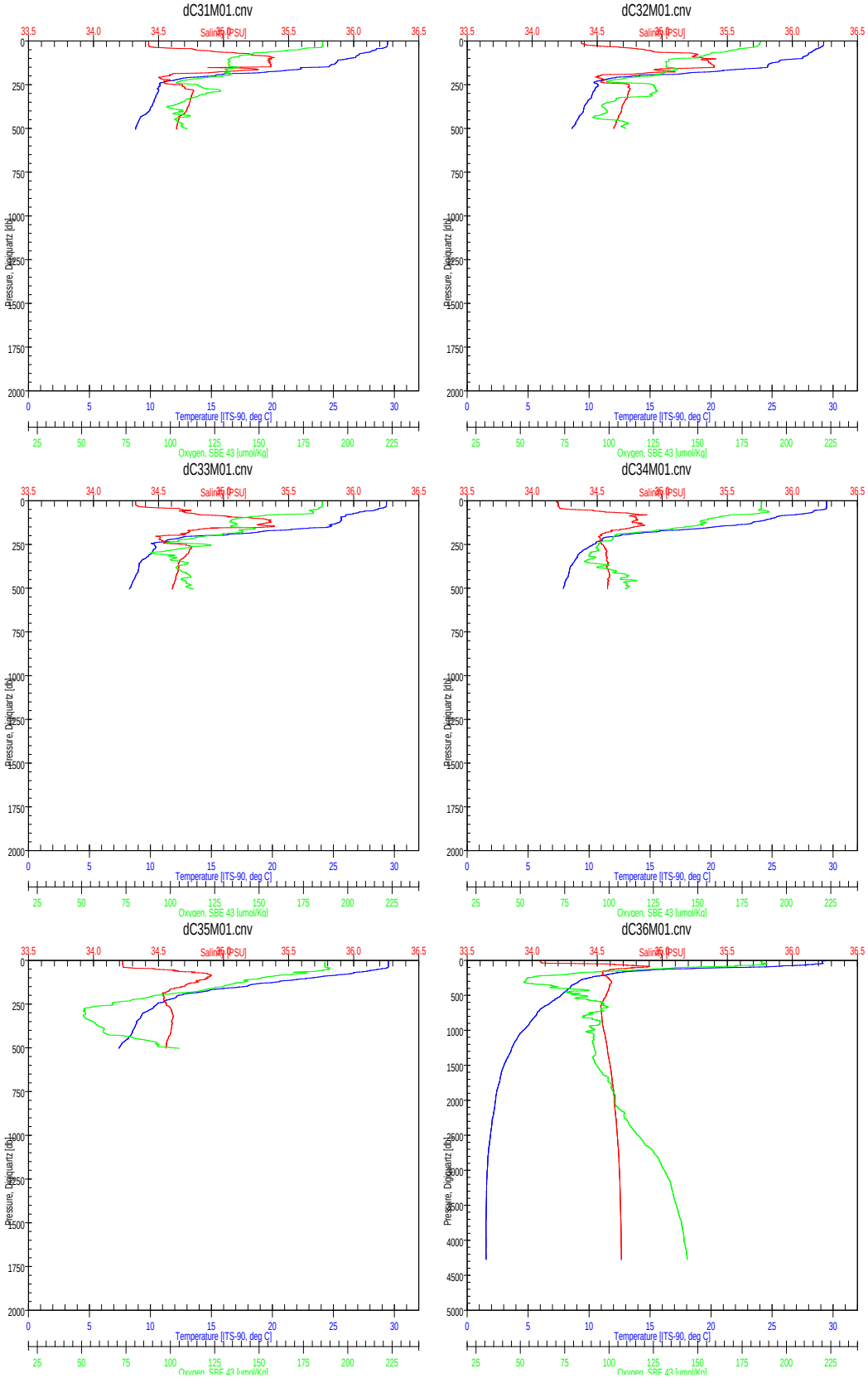

Figure 6.2.1-37～-42 CTD profile

(C31M01, C32M01, C33M01, C34M01, C35M01 and C36M01)

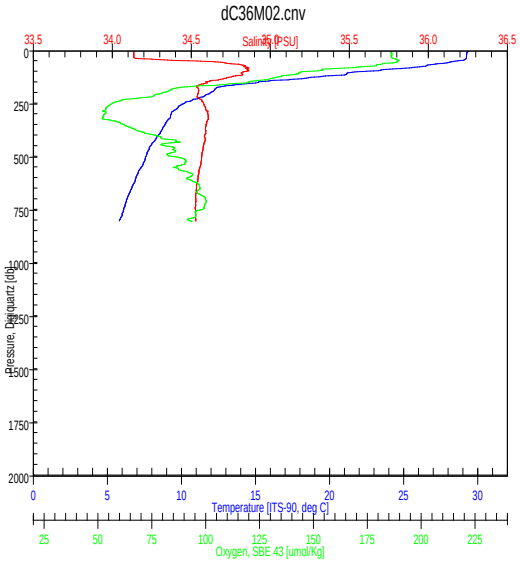

Figure 6.2.1-43 CTD profile

(C36M02)

6.2.2 XCTD

(1) Personnel

Yuji Kashino	(JAMSTEC): Principal Investigator
Souichiro Sueyoshi	(Global Ocean Development Inc.: GODI)
Ryo Kimura	(GODI)
Ryo Ohyama	(MIRAI Crew)
Not on-board	
Hiroshi Ichikawa	(JAMSTEC)
Masashisa Kubota	(Tokai Univ.)

(2) Objectives

Investigation of oceanic structure.

(3) Parameters

According to the manufacturer's nominal specifications, the range and accuracy of parameters measured by the XCTD (eXpendable Conductivity, Temperature & Depth profiler) are as follows;

Parameter	Range	Accuracy
Conductivity	0 ~ 60 [mS/cm]	+/- 0.03 [mS/cm]
Temperature	-2 ~ 35 [deg-C]	+/- 0.02 [deg-C]
Depth	0 ~ 1000 [m]	5 [m] or 2 [%] (either of them is major)

(4) Methods

We observed the vertical profiles of the sea water temperature and salinity measured by XCTD-1 manufactured by Tsurumi-Seiki Co.. The signal was converted by MK-130, Tsurumi-Seiki Co. and was recorded by MK-130 software (Ver.3.07) provided by Tsurumi-Seiki Co.. We launched 35 probes (X01-X35) by using automatic launcher. The summary of XCTD observations and launching log were shown in Table 6.2.2. SST (Sea Surface Temperature) and SSS (Sea Surface Salinity) in the table were got from EPCS at launching.

(5) Preliminary results

Position map of XCTD observations, Vertical sections of temperature and salinity were shown in Fig. 6.2.2-1 to 6.2.2-4

(6) Data archive

These data obtained in this cruise will be submitted to the Data Integration and Analysis Group (DIAG) of JAMSTEC, and will be opened to the public via "R/V Mirai Data Web Page" in JAMSTEC home page.

Table 6.2.2 Summary of XCTD observation and launching log

No.	Station No.	Date	Time	Latitude	Longitude	Depth [m]	SST [deg-C]	SSS [PSU]	Probe S/N
X01	E01	2009/11/05	00:14	39-00.07N	147-06.00E	5438	15.351	33.600	09064691
X02	E02	2009/11/05	02:31	38-30.24N	146-54.11E	5421	15.960	33.510	09064697
X03	E03	2009/11/05	05:06	38-00.20N	146-42.08E	5392	20.303	34.216	09064695
X04	E04	2009/11/05	11:40	37-29.97N	146-29.98E	5635	20.196	34.147	09064686
X05	E05	2009/11/05	14:23	37-00.08N	146-18.02E	5505	18.663	33.867	09064696
X06	E06	2009/11/05	15:46	36-45.05N	146-12.02E	5577	18.266	33.767	09064693
X07	E07	2009/11/05	17:08	36-30.12N	146-06.05E	5530	17.326	33.425	09064692
X08	E08	2009/11/05	18:30	36-15.13N	146-00.02E	5560	17.519	33.405	09064688
X09	E09	2009/11/05	19:50	36-00.17N	145-54.11E	5731	21.695	34.253	09064694
X10	E10	2009/11/05	21:12	35-45.12N	145-47.98E	5843	23.444	34.429	09074918
X11	E11	2009/11/05	22:33	35-30.12N	145-42.04E	5843	23.912	34.430	09064687
X12	E12	2009/11/05	23:58	35-15.27N	145-36.09E	4776	23.743	34.446	09064685
X13	E13	2009/11/06	01:23	35-00.23N	145-30.10E	5839	23.634	34.350	09064681
X14	E14	2009/11/06	02:48	34-45.27N	145-24.08E	5846	23.933	34.366	09064679
X15	E15	2009/11/06	04:11	34-30.23N	145-18.09E	5865	23.465	34.340	09064586
X16	E16	2009/11/06	05:34	34-15.26N	145-12.15E	5819	23.579	34.250	09064684
X17	E17	2009/11/06	06:56	34-00.23N	145-06.06E	5729	23.414	34.206	09064682
X18	E18	2009/11/06	09:42	33-30.24N	144-54.12E	5718	23.830	34.329	09064584
X19	E19	2009/11/06	12:48	33-00.09N	144-42.03E	5673	23.738	34.371	09064690
X20	E20	2009/11/06	16:49	32-30.16N	144-30.03E	5702	24.064	34.344	09064689
X21	E21	2009/11/06	22:54	32-00.21N	144-18.16E	5672	24.212	34.341	09064680
X22	E22	2009/11/07	04:13	31-00.24N	143-54.10E	5836	25.789	34.588	09064680
X23	E23	2009/11/07	09:35	30-00.18N	143-29.97E	5634	25.392	34.547	09064678
X24	1	2009/11/14	02:53	08-00.50N	155-57.34E	4851	29.703	34.048	09075028
X25	2	2009/11/14	05:11	07-30.22N	155-59.98E	4397	29.705	33.998	09075022
X26	3	2009/11/14	07:24	07-00.25N	155-59.95E	4447	29.602	33.894	09064587
X27	4	2009/11/14	09:34	06-30.19N	156-00.20E	4412	29.660	34.048	09064585
X28	5	2009/11/14	11:48	06-00.19N	156-00.04E	4142	29.603	33.957	09075025
X29	6	2009/11/14	14:06	05-30.13N	156-00.00E	3736	29.714	33.917	09075019
X30	7	2009/11/16	00:34	04-58.06N	156-02.82E	3596	29.845	33.858	09075027
X31	8	2009/11/17	05:04	02-03.17N	156-01.37E	2584	30.141	33.798	09075024
X32	9	2009/11/18	23:36	00-00.28N	156-02.65E	1953	30.165	34.161	09075021
X33	10	2009/11/21	04:30	02-00.59S	155-56.88E	1746	30.984	34.111	09075018
X34	11	2009/11/22	23:20	05-01.77S	156-01.02E	1525	29.947	34.150	09075017
X35	12	2009/11/30	01:48	01-59.70N	147-01.83E	4520	29.341	34.403	09075020

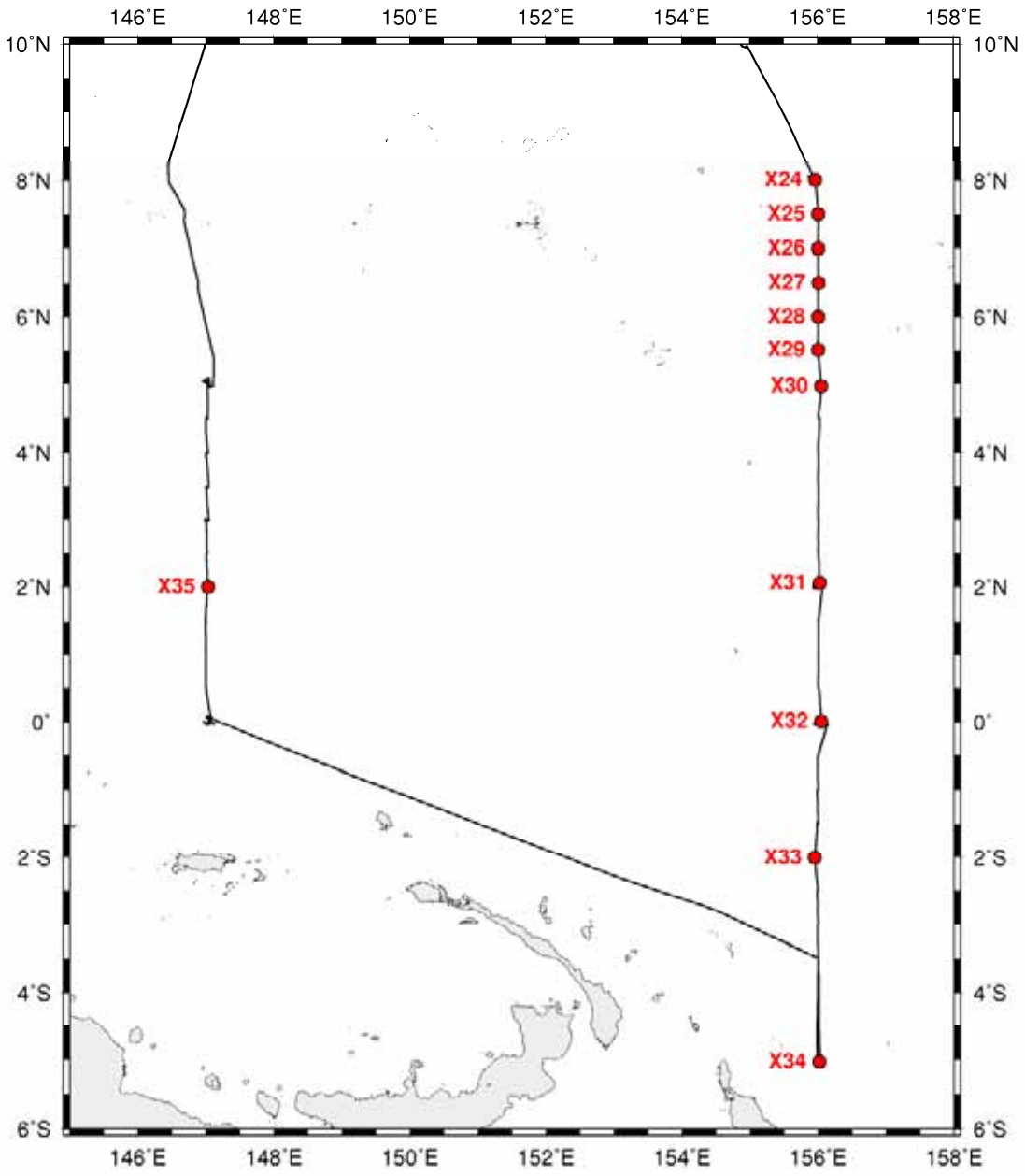

Fig. 6.2.2-1 Position map of XCTD observations (Tropical region).

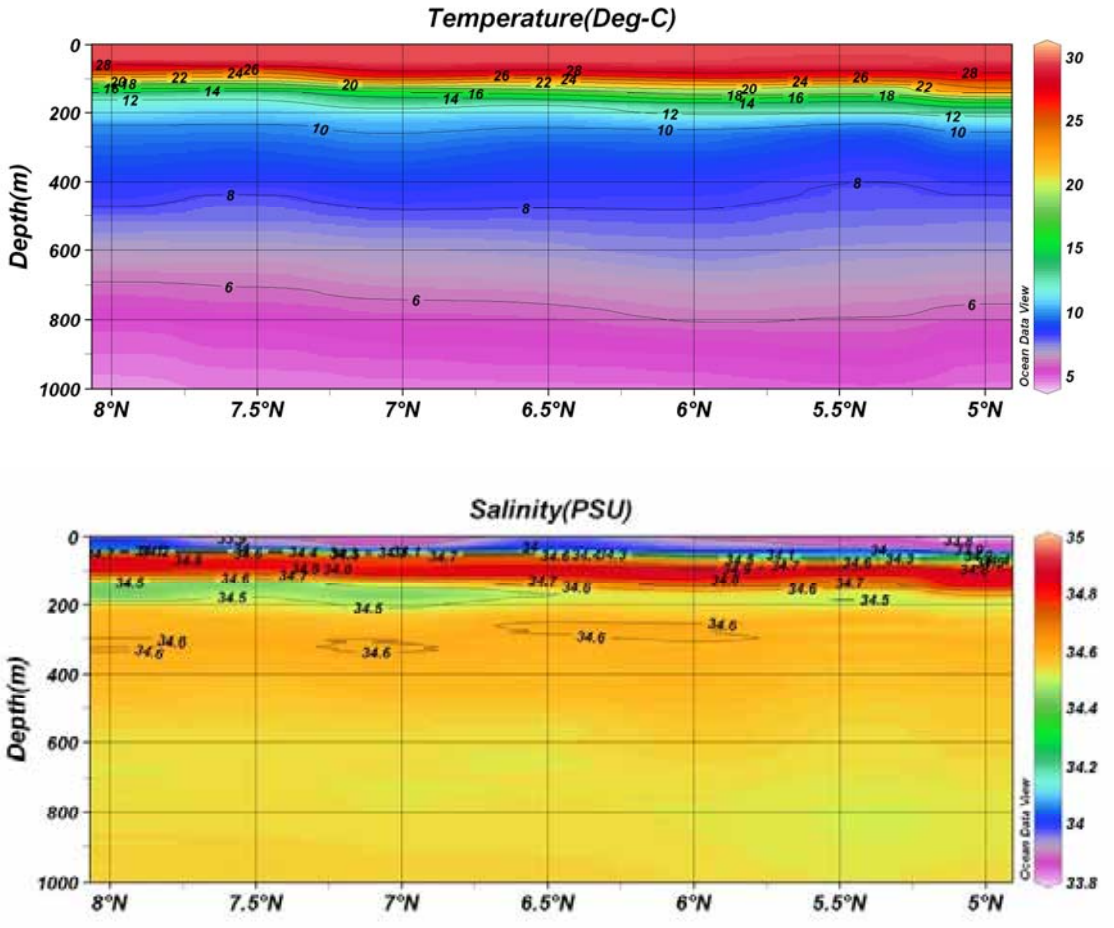

Fig. 6.2.2-2 Vertical section of temperature (upper) and salinity (lower) along 156E line (8N to 5N)

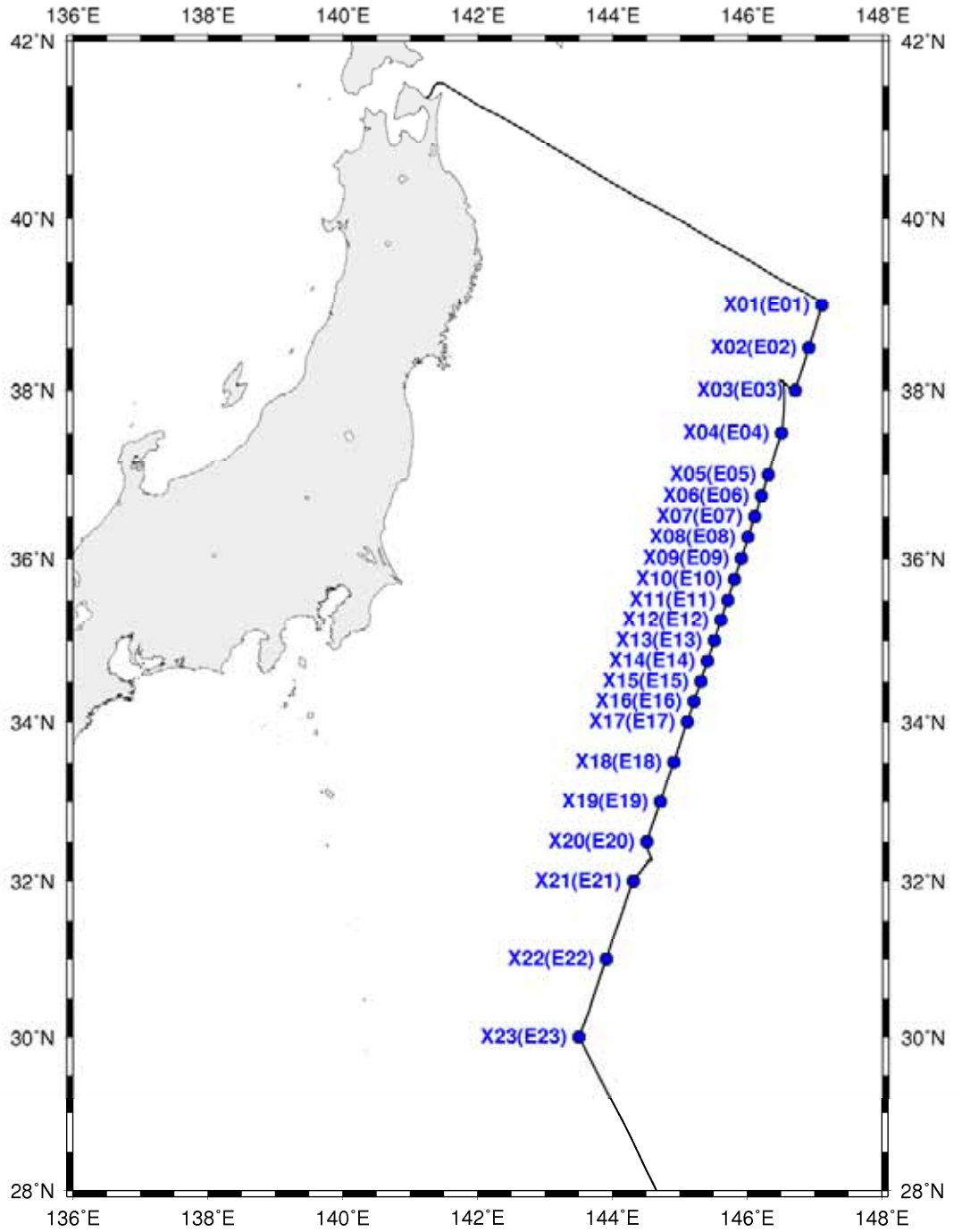

Fig. 6.2.2-3 Position map of XCTD observations (Kuroshio region)

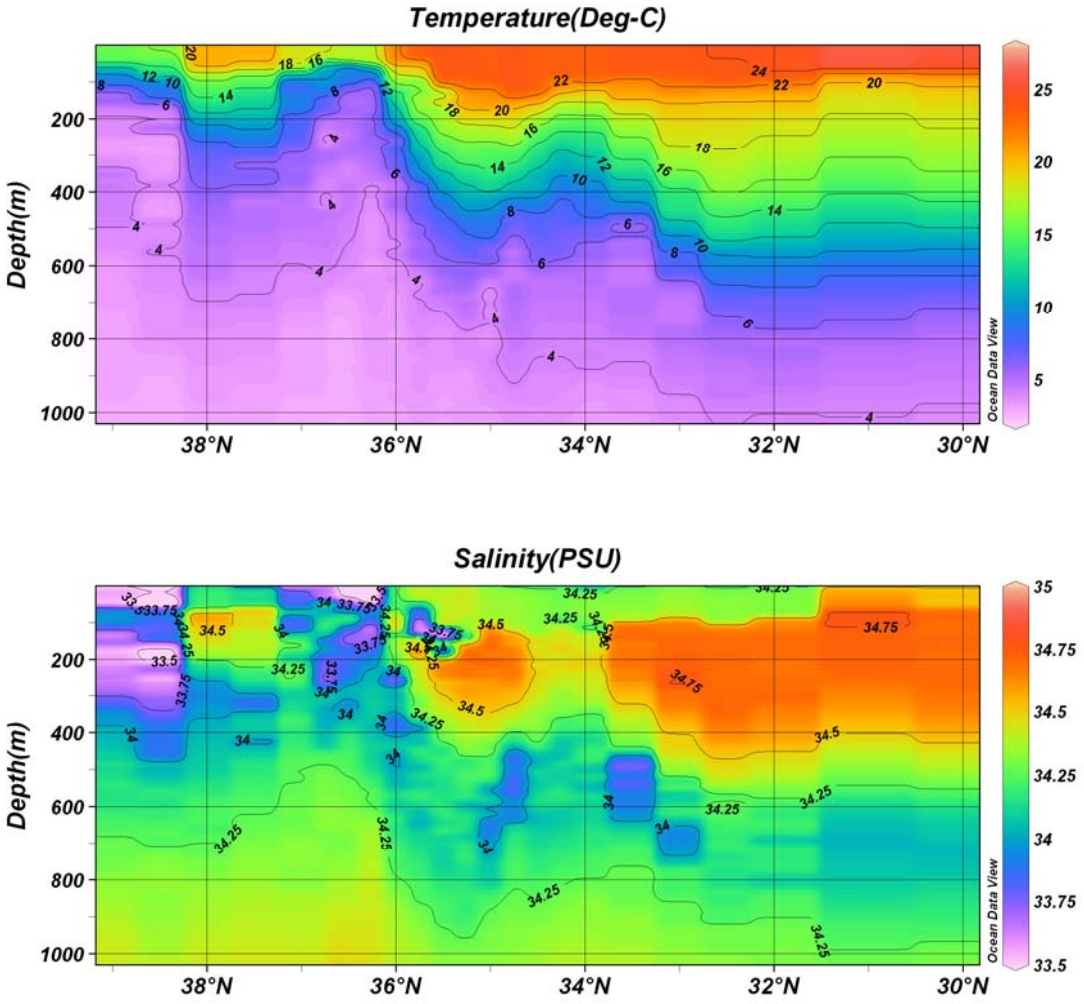

Fig. 6.2.2-4 Vertical section of temperature (top) and salinity (middle) along Kuroshio observation line.

6.3 Water sampling

6.3.1 Salinity

(1) Personnel

Yuji KASHINO (JAMSTEC) :Principal Investigator
Tatsuya TANAKA (MWJ)

(2) Objective

To provide a calibration for the measurement of salinity of bottle water collected on the CTD casts and EPCS

(3) Method

a. Salinity Sample Collection

Seawater samples were collected with 12 liter Niskin-X bottles, bucket and EPCS. The salinity sample bottle of the 250ml brown glass bottle with screw cap was used for collecting the sample water. Each bottle was rinsed three times with the sample water, and was filled with sample water to the bottle shoulder. The sample bottle was sealed with a plastic insert thimble and a screw cap. The thimble was thoroughly rinsed with the sample water before use. The bottle was stored for more than 18 hours in the laboratory before the salinity measurement.

The kind and number of samples taken are shown as follows ;

Table 5.14-1 Kind and number of samples

Kind of Samples	Number of Samples
Samples for CTD and bucket	347
Samples for EPCS	48
Total	395

b. Instruments and Method

The salinity analysis was carried out on R/V MIRAI during the cruise of MR09-04 using the salinometer (Model 8400B “AUTOSAL” ; Guildline Instruments Ltd.: S/N 62556) with an additional peristaltic-type intake pump (Ocean Scientific International, Ltd.). A pair of precision digital thermometers (Model 9540 ; Guildline Instruments Ltd.) were used. The thermometer monitored the ambient temperature and the other monitored a bath temperature.

The specifications of the AUTOSAL salinometer and thermometer are shown as follows ;

Salinometer (Model 8400B “AUTOSAL” ; Guildline Instruments Ltd.)
- Measurement Range : 0.005 to 42 (PSU)
- Accuracy : Better than ±0.002 (PSU) over 24 hours without re-standardization
- Maximum Resolution : Better than ±0.0002 (PSU) at 35 (PSU)

Thermometer (Model 9540 ; Guildline Instruments Ltd.)
- Measurement Range : -40 to +180 deg C
- Resolution : 0.001
- Limits of error ±deg C : 0.01 (24 hours @ 23 deg C ±1 deg C)
- Repeatability : ±2 least significant digits

The measurement system was almost the same as Aoyama *et al.* (2002). The salinometer was operated in the air-conditioned ship's laboratory at a bath temperature of 24 deg C. The ambient temperature varied from approximately 20 deg C to 24 deg C, while the bath temperature was very stable and varied within +/- 0.003 deg C on rare occasion.

The measurement for each sample was done with a double conductivity ratio and defined as the median of 31 readings of the salinometer. Data collection was started 10 seconds after filling the cell with the sample and it took about 15 seconds to collect 31 readings by a personal computer. Data were taken for the sixth and seventh filling of the cell after rinsing 5 times. In the case of the difference between the double conductivity ratio of these two fillings being smaller than 0.00002, the average value of the double conductivity ratio was used to calculate the bottle salinity with the algorithm for the practical salinity scale, 1978 (UNESCO, 1981). If the difference was greater than or equal to 0.00003, an eighth filling of the cell was done. In the case of the difference between the double conductivity ratio of these two fillings being smaller than 0.00002, the average value of the double conductivity ratio was used to calculate the bottle salinity. In the case of the double conductivity ratio of eighth filling did not satisfy the criteria above, I measured a ninth filling of the cell and calculated the bottle salinity above. The measurement was conducted in about 8 hours per day and the cell was cleaned with soap after the measurement of the day.

(4) Results

a. Standard Seawater

Standardization control of the salinometer was set to 640 on Nov 9. The value of STANDBY was 5483 +/- 0001 and that of ZERO was 0.0-0001 +/- 0001. The double conductivity ratio changed about +0.00010 caused by the suddenly shift of salinometer on Dec 4. The value of STANDBY was 5484 +/- 0001 and that of ZERO was 0.0-0001 +/- 0001 after Dec 4, the standardization control was not changed. The conductivity ratio of IAPSO Standard Seawater batch P150 was 0.99978 (double conductivity ratio was 1.99956) and was used as the standard for salinity. I measured 26 bottles of P150 before Dec 4 and 10 bottles after Dec 4, except 6 bad bottles. Data of these 6 bad bottles are not taken into consideration hereafter. The average of the double conductivity ratio of 30 bottles except 6 bad bottles during the cruise was 1.99959 and the standard deviation was 0.00006, which is equivalent to 0.0012 in salinity.

Fig.6.3.1-1 shows the history of the double conductivity ratio of the Standard Seawater batch P150. The average of the double conductivity ratio before Dec 4 was 1.99956 and the standard deviation was 0.00002, which is equivalent to 0.0003 in salinity. The average of the double conductivity ratio after Dec 4 was 1.99968 and the standard deviation was smaller than 0.00001, which is equivalent to 0.0002 in salinity.

Fig.6.3.1-2 shows the history of the double conductivity ratio of the Standard Seawater batch P150 after correction. The average of the double conductivity ratio after correction before Dec 4 was 1.99956 and the standard deviation was 0.00001, which is equivalent to 0.0002 in salinity. The average of the double conductivity ratio after correction after Dec 4 was 1.99956 and the standard deviation was smaller than 0.00001, which is equivalent to 0.0002 in salinity.

The specifications of SSW used in this cruise are shown as follows ;

batch	:	P150
conductivity ratio	:	0.99978
salinity	:	34.991
preparation date	:	22nd May 2008

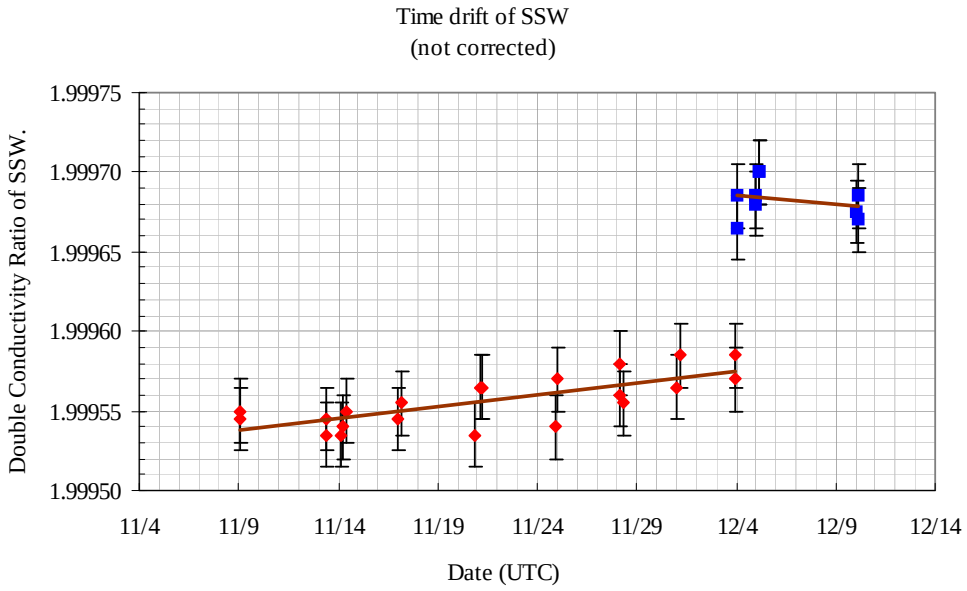

Fig. 6.3.1-1 History of double conductivity ratio for the Standard Seawater batch P150 (before correction)

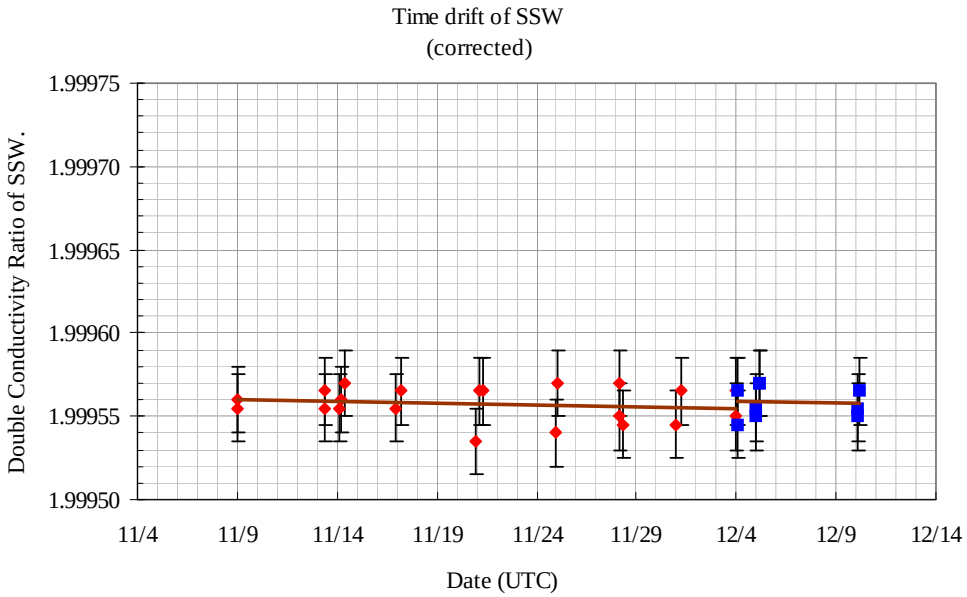

Fig. 6.3.1-2 History of double conductivity ratio for the Standard Seawater batch P150 (after correction)

b. Sub-Standard Seawater

Sub-standard seawater was made from deep-sea water filtered by a pore size of 0.45 micrometer and stored in a 20 liter container made of polyethylene and stirred for at least 24 hours before measuring. It was measured about every 6 samples in order to check for the possible sudden drifts of the salinometer.

c. Replicate Samples

I estimated the precision of this method using 72 pairs of replicate samples taken from the same Niskin bottle. The average and the standard deviation of absolute difference among 72 pairs of replicate samples were 0.0003 and 0.0002 in salinity, respectively.

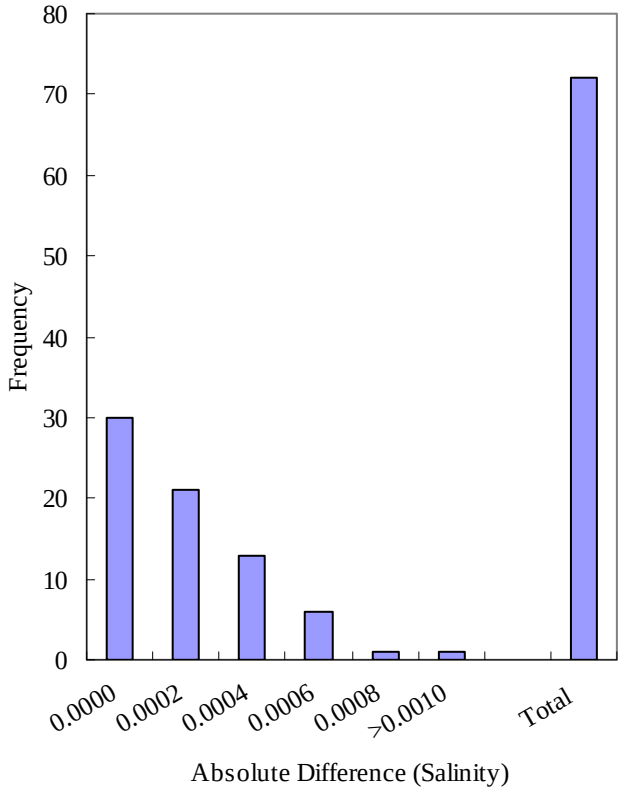

Fig. 6.3.1-3 Absolute difference of Replicate Samples

(5) Data Policy

These data will be submitted to Data Integration and Analyses Group (DIAG) of JAMSTEC just after the cruise.

(6) Reference

・Aoyama, M., T. Joyce, T. Kawano and Y. Takatsuki : Standard seawater comparison up to P129. Deep-Sea Research, I, Vol. 49, 1103～1114, 2002

・UNESCO : Tenth report of the Joint Panel on Oceanographic Tables and Standards. UNESCO Tech. Papers in Mar. Sci., 36, 25 pp., 1981

6.3.2 Dissolved oxygen

(1) Personnel

Yuji KASHINO (JAMSTEC): Principal Investigator
Hironori SATO (Marine Works Japan Co. Ltd.): Operation Leader
Masanori ENOKI(Marine Works Japan Co. Ltd.)

(2) Objective

Dissolved oxygen is important parameter to identify water masses of intermediate and deep water in the Arctic Ocean. We measured dissolved oxygen in seawater by Winkler titration.

(3) Parameters

Dissolved oxygen

(4) Instruments and Methods

a. Reagents

Pickling Reagent I: Manganese chloride solution (3 mol/dm^3)
Pickling Reagent II: Sodium hydroxide (8 mol/dm^3) / sodium iodide solution (4 mol/dm^3)
Sulfuric acid solution (5 mol/dm^3)
Sodium thiosulfate (0.025 mol/dm^3)
Potassium iodate (0.001667 mol/dm^3)

b. Instruments:

Burette for sodium thiosulfate;
APB-510 manufactured by Kyoto Electronic Co. Ltd. / 10 cm^3 of titration vessel
Burette for potassium iodate;
APB-510 manufactured by Kyoto Electronic Co. Ltd. / 10 cm^3 of titration vessel
Detector and Software;
Automatic photometric titrator (DOT-01) manufactured by Kimoto Electronic Co. Ltd.

c. Sampling

Following procedure is based on the WHP Operations and Methods (Dickson, 1996). Seawater samples were collected with Niskin bottle attached to the CTD-system. Seawater for oxygen measurement was transferred from Niskin sampler bottle to a volume calibrated flask (ca. 100 cm^3). Three times volume of the flask of seawater was overflowed. Temperature was measured by digital thermometer during the overflowing. Then two reagent solutions (Reagent I and II) of 0.5 cm^3 each were added immediately into the sample flask and the stopper was inserted carefully into the flask. The sample flask was then shaken vigorously to mix the contents and to disperse the precipitate finely throughout. After the precipitate has settled at least halfway down the flask, the flask was shaken again vigorously to disperse the precipitate. The sample flasks containing pickled samples were stored in a laboratory until they were titrated.

d. Sample measurement

At least two hours after the re-shaking, the pickled samples were measured on board.

A magnetic stirrer bar and 1 cm^3 sulfuric acid solution were added into the sample flask and stirring began. Samples were titrated by sodium thiosulfate solution whose morality was determined by potassium iodate solution. Temperature of sodium thiosulfate during titration was recorded by a digital thermometer. During this cruise, we measured dissolved oxygen concentration using 2 sets of the titration apparatus. Dissolved oxygen concentration ($\mu mol\ kg^{-1}$) was calculated by sample temperature during seawater sampling, salinity of the sample, and titrated volume of sodium thiosulfate solution without the blank.

e. Standardization and determination of the blank

Concentration of sodium thiosulfate titrant (ca. 0.025 mol/dm^3) was determined by potassium iodate solution. Pure potassium iodate was dried in an oven at 130°C. 1.7835g potassium iodate weighed out accurately was dissolved in deionized water and diluted to final volume of 5 dm^3 in a calibrated volumetric flask (0.001667 mol/dm^3). 10 cm^3 of the standard potassium iodate solution was added to a flask using a calibrated dispenser. Then 90 cm^3 of deionized water, 1 cm^3 of sulfuric acid solution, and 0.5 cm^3 of pickling reagent solution II and I were added into the flask in order. Amount of sodium thiosulfate titrated gave the morality of sodium thiosulfate titrant.

The blank from the presence of redox species apart from oxygen in the reagents was determined as follows. Firstly, 1 cm^3 of the standard potassium iodate solution was added to a flask using a calibrated dispenser. Then 100 cm^3 of deionized water, 1 cm^3 of sulfuric acid solution, and 0.5 cm^3 of pickling reagent solution II and I were added into the flask in order. Secondary, 2 cm^3 of the standard potassium iodate solution was added to a flask using a calibrated dispenser. Then 100 cm^3 of deionized water, 1 cm^3 of sulfuric acid solution, and 0.5 cm^3 of pickling reagent solution II and I were added into the flask in order. The blank was determined by difference between the first and second titrated volumes of the sodium thiosulfate.

Table6.3.2-1 shows results of the standardization and the blank determination during this cruise.

Table6.3.2-1 Results of the standardization and the blank determinations during this cruise.

Date	KIO_3	$Na_2S_2O_3$	DOT-01(No.1)		DOT-01(No.2)	
			E.P.	Blank	E.P.	Blank
2009/11/5	CSK	20080704-19-1				
2009/11/5	20081204-19-01	20080704-19-1	3.970	-0.002	3.972	-0.001
2009/11/7	20081204-18-07	20080704-19-1	3.969	-0.001	3.971	0.002
2009/11/7	20081204-19-02	20080704-19-1	3.970	-0.001	3.973	-0.001
2009/11/11	20081204-19-03	20080704-19-1	3.969	0.000	3.971	0.003
2009/11/17	20081204-19-04	20080704-19-1	3.969	-0.001	3.971	0.001
2009/11/21	20081204-19-04	20080704-19-1	3.970	-0.001	3.972	0.001
2009/11/21	20081204-19-05	20080704-19-2	3.969	-0.003	3.971	-0.001
2009/11/25	20081204-19-06	20080704-19-2	3.968	-0.003	3.972	0.000
2009/12/1	20081204-19-07	20080704-19-2	3.967	-0.002	3.972	0.002
2009/12/5	20081204-19-08	20080704-19-2	3.970	-0.003	3.974	0.001
2009/12/5	20081204-20-01	20080704-19-2	3.969	-0.003	3.972	0.001
2009/12/9	CSK	20080704-19-2				
2009/12/9	20081204-19-09	20080704-19-2	3.970	-0.003	3.973	0.000

f. Repeatability of sample measurement

During this cruise we measured oxygen concentration in 272 seawater samples at 7 stations. Replicate samples were taken at every CTD casts. Results of replicate samples were shown in Table6.3.2-2 and this diagram shown in Fig6.3.2-1. The standard deviation was calculated by a procedure in Guide to best practices for ocean CO2 measurements Chapter4 SOP23 Ver.3.0 (2007).

Table6.3.2-2 Results of the replicate sample measurements

Layer	Number of replicate sample pairs	Oxygen concentration (μmol/kg) Standard Deviation.
1000m>=	14	0.08
>1000m	19	0.13
All	33	0.11

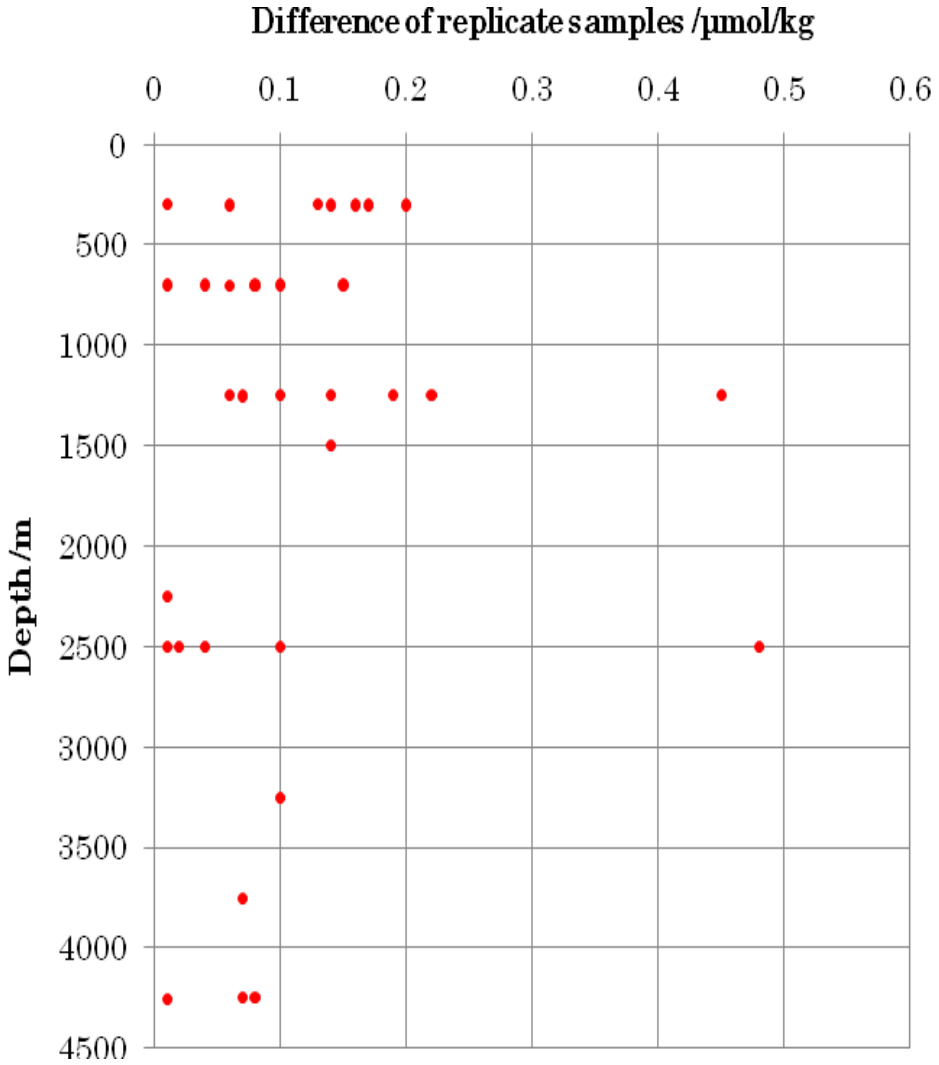

Fig.6.3.2-1 Differences of replicate samples against sampling depth.

(5) Data policy and citation

All data will be submitted to Chief Scientist.

(6) Reference

Dickson, A.G., Determination of dissolved oxygen in sea water by Winkler titration. (1996)
Dickson, A.G., Sabine, C.L. and Christian, J.R. (Eds.), Guide to best practices for ocean CO2 measurements. (2007)
Culberson, C.H., WHP Operations and Methods July-1991 “Dissolved Oxygen”, (1991)
Japan Meteorological Agency, Oceanographic research guidelines(Part 1). (1999)
KIMOTO electric CO. LTD., Automatic photometric titrator DOT-01 Instruaction manual

6.3.3 Nutrients

(1) Personnel

Yasuroh KURUSU (University of Ibaraki): Principal Investigator

Junji MATSUSHITA, Kimiko NISHIJIMA (Marine Works Japan)

(2) Objectives

The vertical and horizontal distributions of nutrients are one of most important factors on the primary production. On the other hand, nutrients data are used to study of climate changes as chemical tracers of sweater mass movement. During this cruise, nutrients measurements will give us the important information on the mechanism of the primary production and/or seawater circulation.

(3) Parameter

Nitrate, Nitrite, Silicate (although silicic acid is correct, we use silicate because a term of silicate is widely used in oceanographic community), Phosphate and Ammonia. See below for further details.

(4) Instruments and Methods

Nutrient analysis was performed on two QuAAtro systems produced by SEAL. Silicon heater panels at 40 deg C for stable chemical reaction heated each console on QuAAtro. Cells of detector using on this method was 1 cm flow cell. The laboratory temperature was maintained between 21 to 24 deg C.

a. Measured Parameters

Nitrate + nitrite and nitrite are analyzed to the modification method of Grasshoff (1970). The sample nitrate is reduced to nitrite in a cadmium tube inside of which is coated with metallic copper. The seawater sample stream with its equivalent nitrite is treated with an acidic, sulfanilamide reagent and the nitrite forms nitrous acid, which reacts with the sulfanilamide to produce a diazonium ion. N1-Naphthylethylene-diamine added to the sample stream then couples with the diazonium ion to produce a red, azo dye. With reduction of the nitrate to nitrite, both nitrate and nitrite react and are measured; without reduction, only nitrite reacts. Thus, for the nitrite analysis, no reduction is performed and the alkaline buffer is not necessary. Nitrate is computed by difference. Wavelength using nitrate and nitrite analysis is 550 nm, which is absorbance of azo dye.

The phosphate analysis is a modification of the procedure of Murphy and Riley (1962).

Molybdic acid is added to the seawater sample to form phosphomolybdic acid, which is in turn reduced to phosphomolybdous acid or “molybdenum blue” using L-ascorbic acid as the reductant. Wavelength using phosphate analysis is 880 nm, which is absorbance of phosphomolybdous acid.

The silicate method is analogous to that described for phosphate. The method used is essentially that of Grasshoff et al. (1983), wherein silicomolybdic acid is first formed from the silicic acid in the seawater sample and added molybdic acid; then the silicomolybdic acid is reduced to silicomolybdous acid, or “molybdenum blue” using L-ascorbic acid as the reductant. Wavelength using silicate analysis is 630 nm, which is absorbance of silicomolybdous acid.

b. Standard

For nitrate standard, we used potassium nitrate 99.995 SupraPUR®, CAS No. 7757-91-1, provided by Merck.

For phosphate standard, we used potassium dihydrogen phosphate anhydrous 99.995 SupraPUR®, CAS No. 7778-77-0, provided by Merck.

For nitrite standard, we used sodium nitrite, CAS No. 7632-00-0, provided by Wako chemical Co. Assay of nitrite salt was determined according to JIS K8019 and purity was 98.77%.

For silicate standard, we used silicon standard solution SiO_2 in NaOH 0.5 mol/l CertiPUR®, CAS No. 1310-73-2, provided by Merck of which lot number is HC814662. The silicate concentration was certified by NIST-SRM 3150 with the uncertainty of 0.5%.

c. Low Nutrients Sea Water (LNSW)

Surface water having low nutrients concentration was taken and filtered using 0.45 μm pore size membrane filter. This water is stored in 20-liter cubitainer with paper box. The concentrations of nutrients of LNSW were measured carefully in July 2008.

d. Sampling Procedures

Samples were drawn into virgin 10 ml polyacrylate vials that were rinsed three times before sampling without sample drawing tubes.

e. Analysis Procedures

Working standards for calibration were prepared at on board before every analysis. The calibration curves for each run were obtained using four levels, and fitted by second order approximation. The standard of highest concentration was measured every 11 samples for correction of sensitivity and evaluation of precision. We also used reference material for nutrients in seawater, RMNS (KANSO Co., Ltd., lot AX), for every runs to secure comparability on nutrient

analysis throughout this cruise. We made duplicate measurement at all layer samples.

(5) Results

Analytical precisions in this cruise were less than 0.10% (55.1 μM) for nitrate, 0.14% (1.2 μM) for nitrite, 0.09% (170.8 μM) for silicate, 0.15% (3.6 μM) for phosphate, respectively. Results of RMNS are shown in table 6.3.3-1.

(6) Archive

All raw and processed nutrients data files were copied on HD provided Data Integration and Analyses Group (DIAG), JAMSTEC and will be opened to public via “R/V Mirai Data Web Page” in JAMSTEC home page.

(7) Reference

Grasshoff, K. (1970), Technicon paper, 691-57.

Grasshoff, K., Ehrhardt, M., Kremling, K. et al. (1983), Methods of seawater analysis. 2nd rev. Weinheim: Verlag Chemie, Germany, West.

Murphy, J. and Riley, J.P. (1962), Analytical chim. Acta 27, 31-36.

Table 6.3.3-1 Summary of RMNS concentration during this cruise.

unit: μmol/kg

RMNS Lot.		Nitrate	Nitrite	Silicate	Phosphate
AX	average	21.54	0.36	58.21	1.619
	S.D.	0.02	0.00	0.09	0.004
	n	14	14	14	14

6.4 Continuous monitoring of surface seawater

6.4.1 Temperature, salinity, dissolved oxygen

(1) Personnel

Yuji KASHINO (JAMSTEC): Principal Investigator
Hironori SATO (Marine Works Japan Co. Ltd.): Operation Leader
Masanori ENOKI(Marine Works Japan Co. Ltd.)

(2) Objective

Measurements of temperature, salinity and dissolved oxygen of the sea surface water in the Arctic Sea.

(3) Instruments and methods

The *Continuous Sea Surface Water Monitoring System* (Nippon Kaiyo Co. Ltd.) that equips five sensors of 1) salinity, 2) temperatures (two sensors) and 3) dissolved oxygen can continuously measure their values in near-sea surface water. Salinity is calculated by conductivity on the basis of PSS78. Specifications of these sensors are listed below.

This system is settled in the "*sea surface monitoring laboratory*" on R/V MIRAI, and near-surface water was continuously pumped up to the system through a vinyl-chloride pipe. The flow rate for the system is manually controlled by several valves with its value of 12 L min^{-1}. Flow rate is monitored with respective flow meter. The system is connected to shipboard LAN-system, and measured data is stored in a hard disk of PC every 1-minute together with time (UTC) and position of the ship.

a) Temperature and Conductivity sensor
Model: SBE-21, SEA-BIRD ELECTRONICS, INC.
Serial number: 2126391-3126
Measurement range: Temperature -5 to +35℃, Conductivity 0 to 7 S m^{-1}
Resolution: Temperatures 0.001℃, Conductivity 0.0001 S m^{-1}
Stability: Temperature 0.01℃ 6 $months^{-1}$, Conductivity 0.001 S m^{-1} $month^{-1}$

b) Bottom of ship thermometer
Model: SBE 3S, SEA-BIRD ELECTRONICS, INC.
Serial number: 032607
Measurement range: -5 to +35℃
Resolution: ±0.001℃
Stability: 0.002℃ $year^{-1}$

c) Dissolved oxygen sensor
Model: 2127A, Hach Ultara Analytics Japan, INC.
Serial number: 61230
Measurement range: 0 to 14 ppm
Accuracy: ±1% in ±5℃ of correction temperature
Stability: 5% $month^{-1}$

d) Flow meter
Model: EMARG2W, Aichi Watch Electronics LTD.

Serial number: 8672
Measurement range: 0 to 30 L min^{-1}
Accuracy: <= ±1%
Stability: <= ±1% day^{-1}

The monitoring period (UTC) during this cruise are listed below.
Start: 2009/11/04 00:00 Stop: 2009/12/10 07:00

(4) Preliminary Result

Preliminary data of temperature, salinity and dissolved oxygen at sea surface are shown in Fig.6.4.1-1. We took the surface water samples once a day to compare sensor data with bottle data of salinity and dissolved oxygen. The results are shown in Fig.6.4.1-2, 6.4.1-3. All the salinity samples were analyzed by the Guildline 8400B "AUTOSAL", and dissolve oxygen samples were analyzed by Winkler method.

(5) Date archive

The data were stored on a CD-R, which will be submitted to JAMSTEC, and will be opened to public via "R/V MIRAI Data Web Page" in JAMSTEC homepage.

(6) Remarks

None

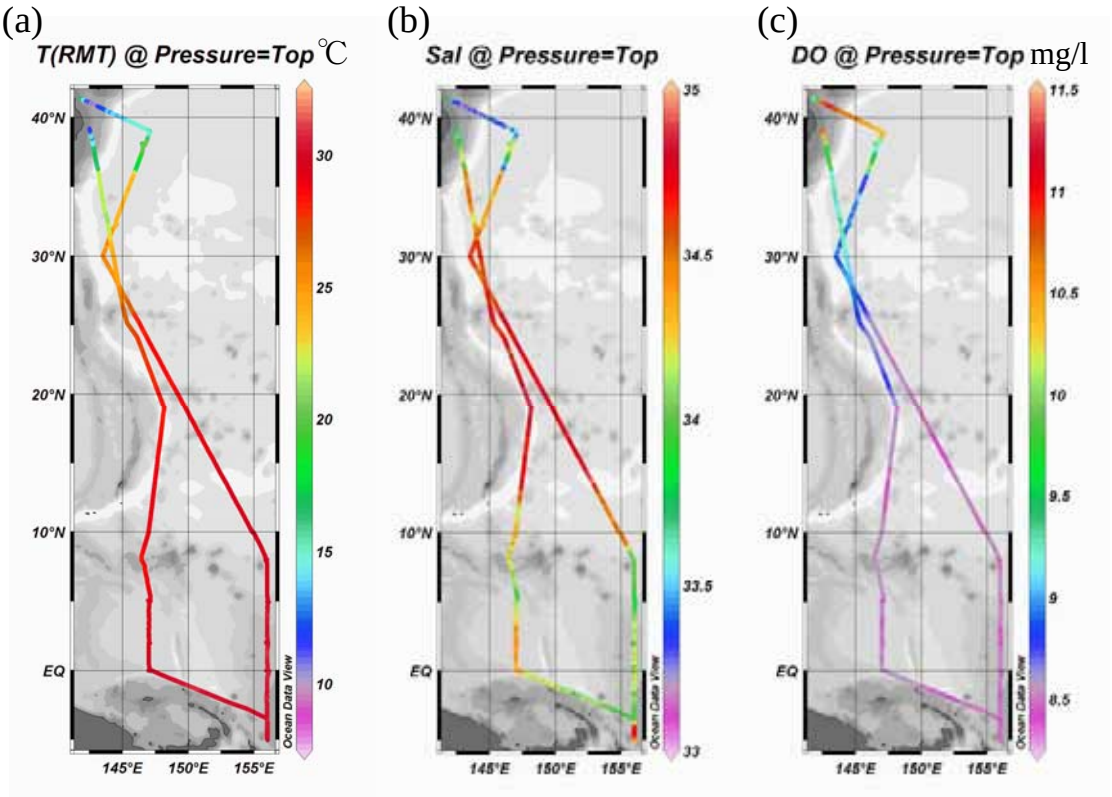

Fig.6.4.1-1 Spatial and temporal distribution of (a) temperature, (b) salinity and (c) dissolved oxygen in MR09-04 cruise.

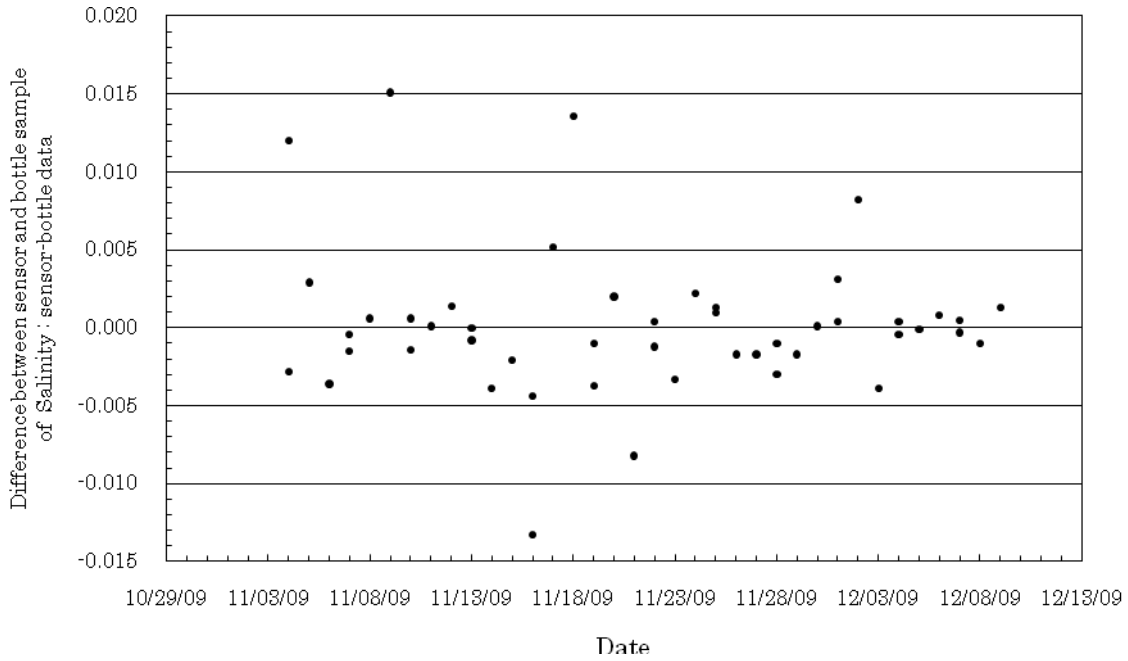

Fig.6.4.1-2 Difference of salinity between sensor data and bottle data. The mean difference is 0.0001psu.

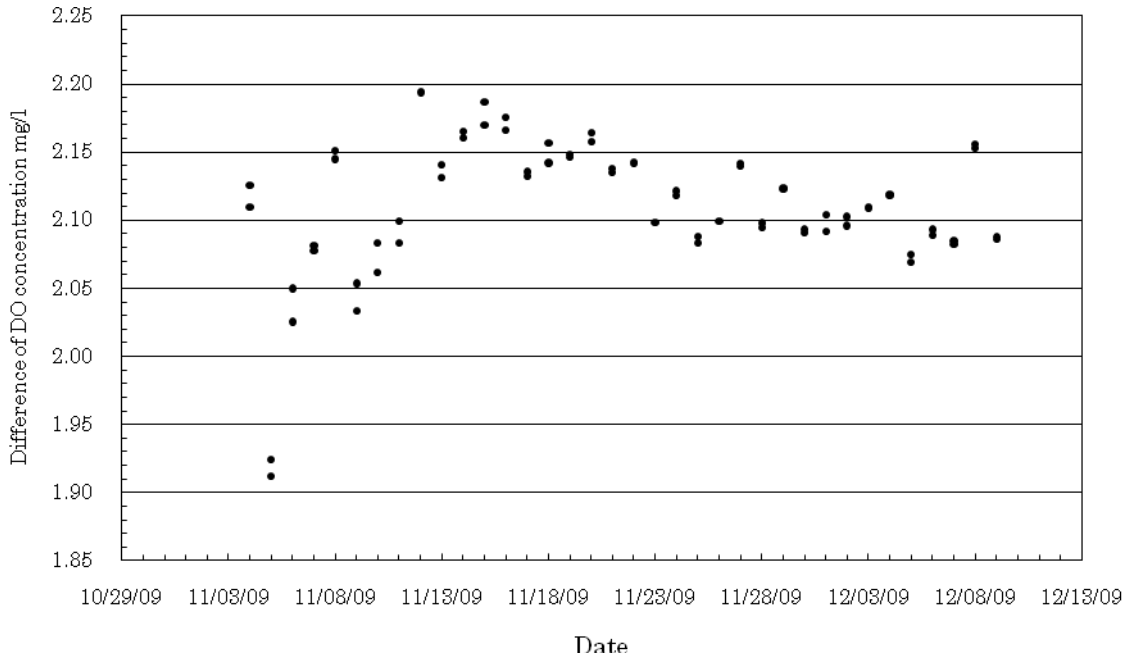

Fig.6.4.1-3 Difference of dissolved oxygen between sensor data and bottle data. The mean difference is 2.11 mg/l.

6.4.2 Underway pCO_2

Shuichi WATANABE and Tetsuichi FUJIKI (JAMSTEC)
Yasuhiro ARII (MWJ)

(1) Objectives

Concentrations of CO_2 in the atmosphere are now increasing at a rate of 1.5 ppmv y^{-1} owing to human activities such as burning of fossil fuels, deforestation, and cement production. It is an urgent task to estimate as accurately as possible the absorption capacity of the oceans against the increased atmospheric CO_2, and to clarify the mechanism of the CO_2 absorption, because the magnitude of the anticipated global warming depends on the levels of CO_2 in the atmosphere, and because the ocean currently absorbs 1/3 of the 6 Gt of carbon emitted into the atmosphere each year by human activities. We here report on board measurements of pCO_2 during MR09-04 cruise.

(2) Methods, Apparatus and Performance

Concentrations of CO_2 in the atmosphere and the sea surface were measured continuously during the cruise using an automated system with a non-dispersive infrared gas analyzer (NDIR; MLT 3T-IR).

The automated system was operated by on one and a half hour cycle. In one cycle, standard gasses, marine air and equilibrated air with surface seawater within the equilibrator were analyzed subsequently. The concentrations of the standard gas were 300.03, 350.14, 400.09 and 450.10 ppm.

To measure marine air concentrations (mol fraction) of CO_2 in dry air (xCO_2-air), marine air sampled from the bow of the ship (approx.30m above the sea level) was introduced into the NDIR by passing through a mass flow controller which controls the air flow rate at about 0.5 L/min, a cooling unit, a perma-pure dryer (GL Sciences Inc.) and a desiccant holder containing $Mg(ClO_4)_2$.

To measure surface seawater concentrations of CO_2 in dry air (xCO_2-sea), marine air equilibrated with a stream of seawater within the equilibrator was circulated with a pump at 0.7-0.8L/min in a closed loop passing through two cooling units, a perma-pure dryer (GL Science Inc.) and a desiccant holder containing $Mg(ClO_4)_2$. The seawater taken by a pump from the intake placed at the approx. 4.5m below the sea surface flowed at a rate of 5-6L/min in the equilibrator. After that, the equilibrated air was introduced into the NDIR.

(3) Preliminary results

Concentrations of CO_2 (xCO_2) of marine air and surface seawater are shown in Fig. 6.4.2-1.

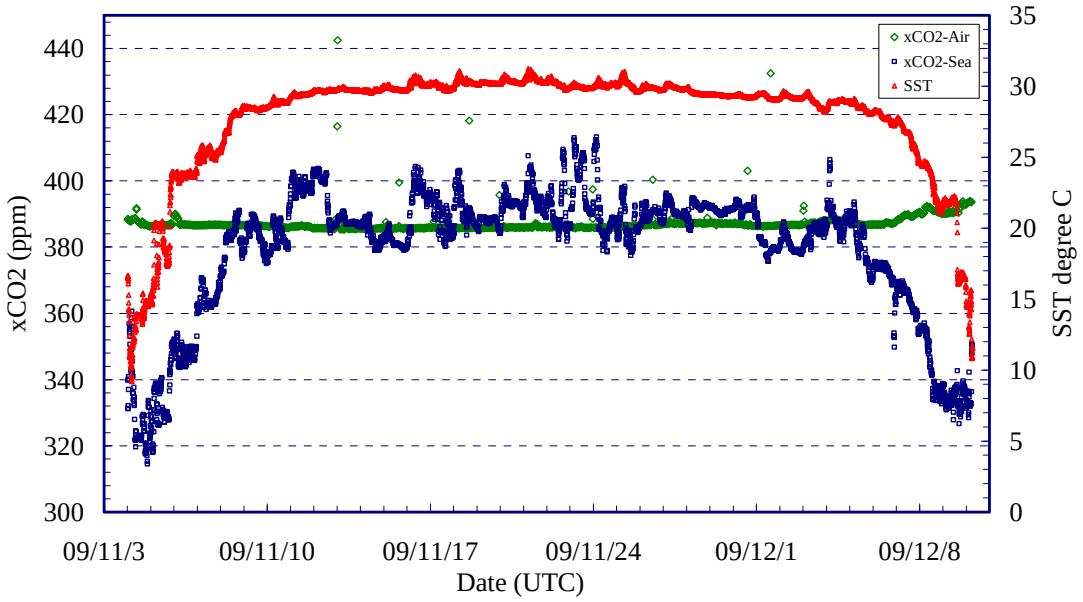

Figure 6.4.2-1 Temporal changes of concentrations of CO_2 (xCO_2) in atmosphere (green) and surface seawater (blue), and SST (red).

(4) Data Archive

All data will be submitted to the Data Integration and Analyses Group (DIAG), JAMSTEC and will be opened to public via “R/V MIRAI Data Web Page” in JAMSTEC home page.

Reference

DOE (1994), Handbook of methods for the analysis of the various parameters of the carbon dioxide system in sea water; version 2, A. G. Dickson & C. Goyet, Eds., ORNS/CDIAC-74

Manual on Oceanographic Observation Part 1 (1999), Japan Meteorological Agency

6.5 Shipboard ADCP

(1) Personnel

Yuji Kashino	(JAMSTEC) :Principal Investigator
Souichiro Sueyoshi	(Global Ocean Development Inc.)
Ryo Kimura	(GODI)
Ryo Ohyama	(MIRAI Crew)

(2) Objective

To obtain continuous measurement of the current profile along the ship's track.

(3) Methods

Upper ocean current measurements were made in MR09-04 cruise, using the hull-mounted Acoustic Doppler Current Profiler (ADCP) system. For most of its operation the instrument was configured for water-tracking mode. Bottom-tracking mode, interleaved bottom-ping with water-ping, was made to get the calibration data for evaluating transducer misalignment angle. The system consists of following components;

1) R/V MIRAI has installed the Ocean Surveyor for vessel-mount (acoustic frequency 75 kHz; Teledyne RD Instruments). It has a phased-array transducer with single ceramic assembly and creates 4 acoustic beams electronically. We mounted the transducer head rotated to a ship-relative angle of 45 degrees azimuth from the keel
2) For heading source, we use ship's gyro compass (Tokimec, Japan), continuously providing heading to the ADCP system directory. Additionally, we have Inertial Navigation System (INS) which provide high-precision heading, attitude information, pitch and roll, are stored in ".N2R" data files with a time stamp.
3) DGPS system (Trimble SPS751 & StarFixXP) providing position fixes.
4) We used VmDas version 1.4.2 (TRD Instruments) for data acquisition.
5) To synchronize time stamp of ping with GPS time, the clock of the logging computer is adjusted to GPS time every 1 minute
6) We have placed ethylene glycol into the fresh water to prevent freezing in the sea chest.
7) The sound speed at the transducer does affect the vertical bin mapping and vertical velocity measurement, is calculated from temperature, salinity (constant value; 35.0 psu) and depth (6.5 m; transducer depth) by equation in Medwin (1975).

Data was configured for 16-m intervals starting 23-m below the surface. Every ping was recorded as raw ensemble data (.ENR). Also, 60 seconds and 300 seconds averaged data were recorded as short term average (.STA) and long term average (.LTA) data, respectively. Major parameters for the measurement (Direct Command) are shown in Table 6.5-1.

(4) Preliminary results

Fig. 6.5-1 shows vector plot of surface (50-100m) water current in the Triton Buoy area. In this cruise, the data quality was not in good condition. When cruising speed is faster than 12 knot, current profile deeper than 250m was bad. The reason of this phenomenon is not cleared, but some problem might be occurred on a transducer system. Paying attention for using shipboard ADCP data is highly recommended to check the status data (correlation, echo amplitude and error velocity).

(5) Data archive

These data obtained in this cruise will be submitted to the Data Integration and Analysis Group (DIAG) of JAMSTEC, and will be opened to the public via “R/V MIRAI Data Web Page” in JAMSTEC home page.

Table 6.5-1 Major parameters

Bottom-Track Commands	
BP = 001	Pings per Ensemble (almost less than 1000m depth)
Environmental Sensor Commands	
EA = +04500	Heading Alignment (1/100 deg)
EB = +00000	Heading Bias (1/100 deg)
ED = 00065	Transducer Depth (0 - 65535 dm)
EF = +001	Pitch/Roll Divisor/Multiplier (pos/neg) [1/99 - 99]
EH = 00000	Heading (1/100 deg)
ES = 35	Salinity (0-40 pp thousand)
EX = 00000	Coord Transform (Xform:Type; Tilts; 3Bm; Map)
EZ = 10200010	Sensor Source (C; D; H; P; R; S; T; U)
	C (1): Sound velocity calculates using ED, ES, ET (temp.)
	D (0): Manual ED
	H (2): External synchro
	P (0), R (0): Manual EP, ER (0 degree)
	S (0): Manual ES
	T (1): Internal transducer sensor
	U (0): Manual EU
Timing Commands	
TE = 00:00:02.00	Time per Ensemble (hrs:min:sec.sec/100)
TP = 00:02.00	Time per Ping (min:sec.sec/100)
Water-Track Commands	
WA = 255	False Target Threshold (Max) (0-255 count)
WB = 1	Mode 1 Bandwidth Control (0=Wid, 1=Med, 2=Nar)
WC = 120	Low Correlation Threshold (0-255)
WD = 111 100 000	Data Out (V; C; A; PG; St; Vsum; Vsum^2;#G;P0)
WE = 1000	Error Velocity Threshold (0-5000 mm/s)
WF = 0800	Blank After Transmit (cm)
WG = 001	Percent Good Minimum (0-100%)
WI = 0	Clip Data Past Bottom (0 = OFF, 1 = ON)
WJ = 1	Rcvr Gain Select (0 = Low, 1 = High)
WM = 1	Profiling Mode (1-8)
WN = 40	Number of depth cells (1-128)
WP = 00001	Pings per Ensemble (0-16384)
WS= 1600	Depth Cell Size (cm)
WT = 000	Transmit Length (cm) [0 = Bin Length]
WV = 0390	Mode 1 Ambiguity Velocity (cm/s radial)

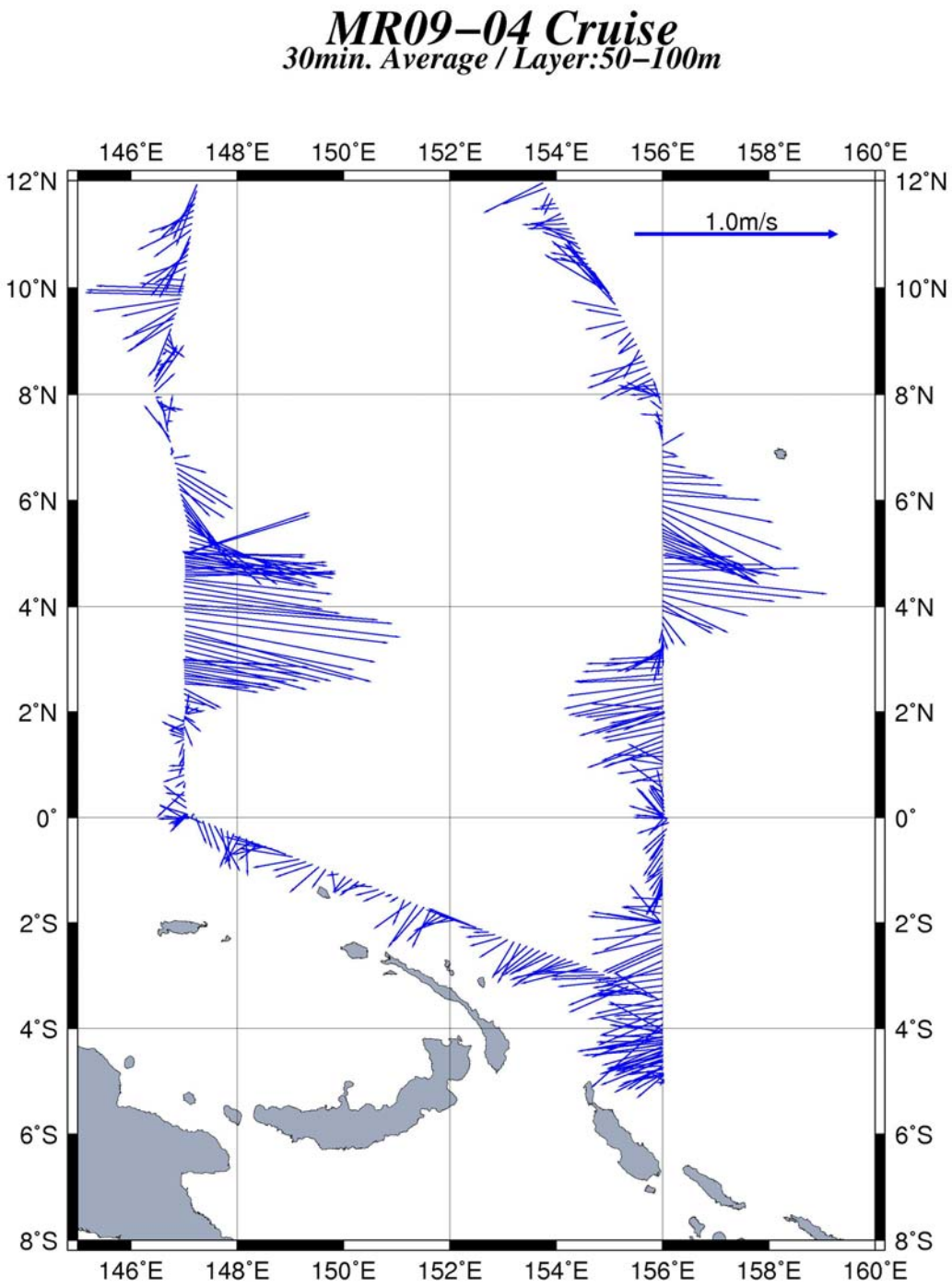

Fig 6.5-1 Vector plot of surface (50-100m) water current in the Triton Buoy area.

6.6 Underway geophysics

6.6.1. Sea surface gravity

(1) Personnel

Takeshi Matsumoto	(University of the Ryukyus)	: Principal Investigator (Not on-board)
Masao Nakanishi	(Chiba University)	: Principal Investigator (Not on-board)
Souichiro Sueyoshi	(Global Ocean Development Inc., GODI)	
Ryo Kimura	(GODI)	
Ryo Ohyama	(MIRAI Crew)	

(2) Introduction

The local gravity is an important parameter in geophysics and geodesy. We collected gravity data at the sea surface.

(3) Parameters

Relative Gravity [CU: Counter Unit]

[mGal] = (coef1: 0.9946) * [CU]

(4) Data Acquisition

We measured relative gravity using LaCoste and Romberg air-sea gravity meter S-116 (Micro-g LaCoste, LLC) during the MR09-04 cruise from 3rd November 2009 to 12th December 2009.

To convert the relative gravity to absolute one, we measured gravity, using portable gravity meter (Scintrex gravity meter CG-3M), at Sekinehama as the reference point.

(5) Preliminary Results

Absolute gravity table is shown in Tabel 6.6.1

(6) Data Archives

Surface gravity data obtained during this cruise will be submitted to the Data Integration and Analysis Group (DIAG) in JAMSTEC, and will be archived there.

Table 6.6.1

No	Date	UTC	Port	Absolute Gravity [mGal]	Sea Level [cm]	Draft [cm]	Gravity at Sensor *[1] [mGal]	L&R*[2] Gravity [mGal]
#1	Oct/25	02:35	Sekinehama	980,371.95	256	628	980,372.78	12,642.05
#2	Dec/12	05:25	Sekinehama	980,371.93	239	630	980,372.71	12,641.67

*1: Gravity at Sensor = Absolute Gravity + Sea Level*0.3086/100 + (Draft-530)/100*0.0431

*2: LaCoste and Romberg air-sea gravity meter S-116

Differential	G at sensor	L&R value
#2 - #1	-0.07 mGal ---(a)	-0.38 mGal ---(b)
L&R drift value (b) - (a)	-0.310 mGal	49.12 days
Daily drift ratio	-0.0063 mGal/day	

6.6.2 Sea surface magnetic field

1) Three-component magnetometer

(1) Personnel

Takeshi Matsumoto	(University of the Ryukyus)	: Principal Investigator (Not on-board)
Masao Nakanishi	(Chiba University)	: Principal Investigator (Not on-board)
Souichiro Sueyoshi	(Global Ocean Development Inc., GODI)	
Ryo Kimura	(GODI)	
Ryo Ohyama	(MIRAI Crew)	

(2) Introduction

Measurement of magnetic force on the sea is required for the geophysical investigations of marine magnetic anomaly caused by magnetization in upper crustal structure. We measured geomagnetic field using a three-component magnetometer during the MR09-04 cruise from Sekinehama on 3rd November 2009 to Sekinehama on 12th December 2009.

(3) Principle of ship-board geomagnetic vector measurement

The relation between a magnetic-field vector observed on-board, **H**ob, (in the ship's fixed coordinate system) and the geomagnetic field vector, **F**, (in the Earth's fixed coordinate system) is expressed as:

$$\mathbf{H}ob = \tilde{\mathbf{A}}\ \tilde{\mathbf{R}}\ \tilde{\mathbf{P}}\ \tilde{\mathbf{Y}}\ \mathbf{F} + \mathbf{H}p \qquad (a)$$

where $\tilde{\mathbf{R}}$, $\tilde{\mathbf{P}}$ and $\tilde{\mathbf{Y}}$ are the matrices of rotation due to roll, pitch and heading of a ship, respectively. $\tilde{\mathbf{A}}$ is a 3 x 3 matrix which represents magnetic susceptibility of the ship, and **H**p is a magnetic field vector produced by a permanent magnetic moment of the ship's body. Rearrangement of Eq. (a) makes

$$\tilde{\mathbf{R}}\ \mathbf{H}ob + \mathbf{H}bp = \tilde{\mathbf{R}}\ \tilde{\mathbf{P}}\ \tilde{\mathbf{Y}}\ \mathbf{F} \qquad (b)$$

where $\tilde{\mathbf{R}} = \tilde{\mathbf{A}}^{-1}$, and $\mathbf{H}bp = -\tilde{\mathbf{R}}\ \mathbf{H}p$. The magnetic field, **F**, can be obtained by measuring $\tilde{\mathbf{R}}$, $\tilde{\mathbf{P}}$, $\tilde{\mathbf{Y}}$ and **H**ob, if $\tilde{\mathbf{R}}$ and **H**bp are known. Twelve constants in $\tilde{\mathbf{R}}$ and **H**bp can be determined by measuring variation of **H**ob with $\tilde{\mathbf{R}}$, $\tilde{\mathbf{P}}$ and $\tilde{\mathbf{Y}}$ at a place where the geomagnetic field, **F**, is known.

(4) Instruments on R/V MIRAI

A shipboard three-component magnetometer system (Tierra Tecnica SFG1214) is equipped on-board R/V MIRAI. Three-axes flux-gate sensors with ring-cored coils are fixed on the fore mast. Outputs from the sensors are digitized by a 20-bit A/D converter (1 nT/LSB), and sampled at 8 times per second. Ship's heading, pitch, and roll are measured by the Inertial Navigation System (INS) for controlling attitude of a Doppler radar. Ship's position (GPS) and speed data are taken from LAN every second.

(5) Data Archives

These data obtained in this cruise will be submitted to the Data Integration and Analysis Group (DIAG) of JAMSTEC.

(6) Remarks

1) For calibration of the ship's magnetic effect, we made a "figure-eight" turn (a pair of clockwise and anti-clockwise rotation). This calibration was carried out as below.

08th Nov. 2009, 19:49 to 20:17UTC around at 24-03N, 146-53E

23th Nov. 2009, 09:11 to 09:37UTC around at 04-00N, 156-00E

10th Dec. 2009, 01:00 to 01:28UTC around at 38-15N, 142-43E

2) Cesium magnetometer

(1) Personnel

Masao Nakanishi	(Chiba University)	: Principal investigator / Not on-board
Takeshi Matsumoto	(University of the Ryukyus)	: Principal investigator / Not on-board
Souichiro Sueyoshi	(GODI)	
Ryo Kimura	(GODI)	
Ryo Ohyama	(MIRAI Crew)	

(2) Introduction

Measurement of magnetic force on the sea is required for the geophysical investigations of marine magnetic anomaly caused by magnetization in upper crustal structure.

(3) Data Period

20:36UTC 08th Nov. 2009 - 12:43UTC 10th Nov. 2009

23:21UTC 05th Dec. 2009 - 03:27UTC 07th Dec. 2009

(4) Specification

We measured total geomagnetic field using a cesium marine magnetometer (Geometrics Inc., G-882) and recorded by G-882 data logger (Clovertech Co., Ver.1.0.0). The G-882 magnetometer uses an optically pumped Cesium-vapor atomic resonance system. The sensor fish towed 500 m behind the vessel to minimize the effects of the ship's magnetic field.

Table 6.6.2-1 shows system configuration of MIRAI cesium magnetometer system.

Table 6.6.2-1 System configuration of MIRAI cesium magnetometer system.

Dynamic Operating Range:		20,000 to 100,000 nT
Absolute Accuracy:		<±2 nT throughout range
Setting:	Cycle rate;	0.1 sec
	Sensitivity;	0.02 nT at a 0.1 second cycle rate
	Sampling rate;	1 sec

(5) Data Archive

Total magnetic force data obtained during this cruise was submitted to the Data Integration and Analysis Group (DIAG) of JAMSTEC, and archived there.

6.6.3. Swath bathymetry

(1) Personnel

Takeshi Matsumoto	(University of the Ryukyus)	: Principal Investigator (Not on-board)
Masao Nakanishi	(Chiba University)	: Principal Investigator (Not on-board)
Souichiro Sueyoshi	(Global Ocean Development Inc., GODI)	
Ryo Kimura	(GODI)	
Ryo Ohyama	(MIRAI Crew)	

(2) Introduction

R/V MIRAI is equipped with a Multi narrow Beam Echo Sounding system (MBES), SEABEAM 2112 (SeaBeam Instruments Inc.). The objective of MBES is collecting continuous bathymetric data along ship's track to make a contribution to geological and geophysical investigations and global datasets.

(3) Data Acquisition

The "SEABEAM 2100" on R/V MIRAI was used for bathymetry mapping during the MR09-04 cruise from 3rd November 2009 to 10th December 2009.

To get accurate sound velocity of water column for ray-path correction of acoustic multibeam, we used Surface Sound Velocimeter (SSV) data to get the sea surface (6.2m) sound velocity, and the deeper depth sound velocity profiles were calculated by temperature and salinity profiles from CTD, XCTD and ARGO float data by the equation in Del Grosso (1974) during the cruise.

Table 6.6.3 shows system configuration and performance of SEABEAM 2112.004 system.

Table 6.6.3 System configuration and performance

SEABEAM 2112 (12 kHz system)	
Frequency:	12 kHz
Transmit beam width:	2 degree
Transmit power:	20 kW
Transmit pulse length:	3 to 20 msec.
Depth range:	100 to 11,000 m
Beam spacing:	1 degree athwart ship
Swath width:	150 degree (max)
	120 degree to 4,500 m
	100 degree to 6,000 m
	90 degree to 11,000 m
Depth accuracy:	Within < 0.5% of depth or +/-1m,
	whichever is greater, over the entire swath.
	(Nadir beam has greater accuracy;
	typically within < 0.2% of depth or +/-1m, whichever is greater)

(4) Preliminary Results

The results will be published after primary processing.

(5) Data Archives

Bathymetric data obtained during this cruise will be submitted to the Data Integration and Analysis Group (DIAG) in JAMSTEC, and will be archived there.

7. Special Observations

7.1 TRITON buoys

7.1.1 Operation of the TRITON buoys

(1) Personnel

Yuji Kashino	(JAMSTEC): Principal Investigator
Tomohide Noguchi	(MWJ): Operation Leader
Keisuke Matsumoto	(MWJ): Technical Leader
Masaki Taguchi	(MWJ): Technical Staff
Masaki Furuhata	(MWJ): Technical Staff
Masaki Yamada	(MWJ): Technical Staff
Tomoyuki Takamori	(MWJ): Technical Staff
Tatsuya Tanaka	(MWJ): Technical Staff
Akira Watanabe	(MWJ): Technical Staff
Shungo Oshitani	(MWJ): Technical Staff
Yuichi Sonoyama	(MWJ): Technical Staff
Masanori Enoki	(MWJ): Technical Staff
Kimiko Nishijima	(MWJ): Technical Staff
Junji Matsushita	(MWJ): Technical Staff
Yasuhiro Arii	(MWJ): Technical Staff
Hironori Satoh	(MWJ): Technical Staff

(2) Objectives

The large-scale air-sea interaction over the warmest sea surface temperature region in the western tropical Pacific Ocean called warm pool that affects the global atmosphere and causes El Nino phenomena. The formation mechanism of the warm pool and the air-sea interaction over the warm pool have not been well understood. Therefore, long term data sets of temperature, salinity, currents and meteorological elements have been required at fixed locations. The TRITON program aims to obtain the basic data to improve the predictions of El Nino and variations of Asia-Australian Monsoon system.

TRITON buoy array is integrated with the existing TAO(Tropical Atmosphere Ocean) array, which is presently operated by the Pacific Marine Environmental Laboratory/National Oceanic and Atmospheric Administration of the United States. TRITON is a component of international research program of CLIVAR (Climate Variability and Predictability), which is a major component of World Climate Research Program sponsored by the World Meteorological Organization, the International Council of Scientific Unions, and the Intergovernmental Oceanographic Commission of UNESCO. TRITON will also contribute to the development of GOOS (Global Ocean Observing System) and GCOS (Global Climate Observing System).

Nine TRITON buoys have been successfully recovered and deployed during this R/V MIRAI cruise (MR09-04).

(3) Measured parameters

Meteorological parameters:	wind speed, direction, atmospheric pressure, air temperature, relative humidity, radiation, precipitation.
Oceanic parameters:	water temperature and conductivity at 1.5m, 25m, 50m, 75m, 100m, 125m, 150m, 200m, 300m, 500m 750m, depth at 300m and 750m, currents at 10m.

(4) Instrument

1) CTD and CT

SBE-37 IM MicroCAT

A/D cycles to average : 4

Sampling interval : 600sec

Measurement range, Temperature : -5～+35 deg-C

Measurement range, Conductivity : 0～+7 S/m

Measurement range, Pressure : 0～full scale range

2) CRN(Current meter)

SonTek Argonaut ADCM

Sensor frequency : 1500kHz

Sampling interval : 1200sec

Average interval : 120sec

3) Meteorological sensors

Precipitation

R.M.YOUNG COMPANY MODEL50202/50203

Atmospheric pressure

PAROPSCIENTIFIC.Inc. DIGIQUARTZ FLOATING BAROMETER 6000SERIES

Relative humidity/air temperature,Shortwave radiation, Wind speed/direction

Woods Hole Institution ASIMET

Sampling interval : 60sec

Data analysis : 600sec averaged

(5) Locations of TRITON buoys deployment

Nominal location	8N, 156E
ID number at JAMSTEC	01012
Number on surface float	T09
ARGOS PTT number	28868
ARGOS backup PTT number	24229
Deployed date	14 Nov. 2009
Exact location	08-01.00N, 155-57.17E
Depth	4,836 m

Nominal location	5N, 156E
ID number at JAMSTEC	02012
Number on surface float	T12
ARGOS PTT number	20374
ARGOS backup PTT number	24230
Deployed date	16 Nov. 2009
Exact location	04-58.39N, 156-02.04E
Depth	3,600 m

Nominal location	2N, 156E
ID number at JAMSTEC	03013
Number on surface float	T17
ARGOS PTT number	3780

ARGOS backup PTT number	24240
Deployed date	17 Nov. 2009
Exact location	02-2.26N, 156-01.29 E
Depth	2,573 m

Nominal location	EQ, 156E
ID number at JAMSTEC	04013
Number on surface float	T19
ARGOS PTT number	23470
ARGOS backup PTT number	27409
Deployed date	18 Nov. 2009
Exact location	00-00.97N, 156-02.44 E
Depth	1,953 m

Nominal location	2S, 156E
ID number at JAMSTEC	05011
Number on surface float	T22
ARGOS PTT number	20439
ARGOS backup PTT number	27410
Deployed date	21 Nov. 2009
Exact location	02-01.00S, 155-57.50 E
Depth	1,749 m

Nominal location	5S, 156E
ID number at JAMSTEC	06011
Number on surface float	T24
ARGOS PTT number	20392
ARGOS backup PTT number	13067
Deployed date	22 Nov. 2009
Exact location	05-01.73S, 156-01.44 E
Depth	1,517m

Nominal location	5N, 147E
ID number at JAMSTEC	07011
Number on surface float	T25
ARGOS PTT number	7898
ARGOS backup PTT number	11592
Deployed date	02 Dec. 2009
Exact location	04-57.66N, 147-01.83 E
Depth	4,290 m

Nominal location	2N, 147E
ID number at JAMSTEC	08010
Number on surface float	T27
ARGOS PTT number	9793
ARGOS backup PTT number	29698
Deployed date	30 Nov. 2009

Exact location	01-59.51N, 147-01.24E
Depth	4,519 m

Nominal location	EQ, 147E
ID number at JAMSTEC	09011
Number on surface float	T28
ARGOS PTT number	3779
ARGOS backup PTT number	24715
Deployed date	26 Nov. 2009
Exact location	00-03.59E, 147-00.64E
Depth	4,474 m

(6) TRITON recovered

Nominal location	8N, 156E
ID number at JAMSTEC	01011
Number on surface float	T01
ARGOS PTT number	23511
ARGOS backup PTT number	29738
Deployed date	26 Jul. 2008
Recovered date	13 Nov. 2009
Exact location	08-00.94N, 155-57.08E
Depth	4,834 m

Nominal location	5N, 156E
ID number at JAMSTEC	02011
Number on surface float	T06
ARGOS PTT number	3595
ARGOS backup PTT number	29708
Deployed date	23 Jul. 2008
Recovered date	15 Nov. 2009
Exact location	04-58.35N, 156-02.01E
Depth	3,599 m

Nominal location	2N, 156E
ID number at JAMSTEC	03012
Number on surface float	T07
ARGOS PTT number	9426
ARGOS backup PTT number	24243
Deployed date	21 Jul. 2008
Recovered date	18 Nov. 2009
Exact location	01-57.36N, 155-59.98E
Depth	2,565 m

Nominal location	EQ, 156E
ID number at JAMSTEC	04012

Number on surface float	T10
ARGOS PTT number	7883
ARGOS backup PTT number	24244
Deployed date	19 Jul. 2008
Recovered date	20 Nov. 2009
Exact location	00-01.02S, 155-57.42 E
Depth	1,940 m

Nominal location	2S, 156E
ID number at JAMSTEC	05010
Number on surface float	T11
ARGOS PTT number	9771
ARGOS backup PTT number	7861
Deployed date	13 Jul. 2008
Recovered date	21 Nov. 2009
Exact location	01-59.04S, 156-01.90 E
Depth	1,756 m

Nominal location	5S, 156E
ID number at JAMSTEC	06010
Number on surface float	T14
ARGOS PTT number	3593
ARGOS backup PTT number	7864
Deployed date	15 Jul. 2008
Recovered date	23 Nov. 2009
Exact location	04-58.03S, 156-00.94 E
Depth	1,510m

Nominal location	5N, 147E
ID number at JAMSTEC	07010
Number on surface float	T18
ARGOS PTT number	23510
ARGOS backup PTT number	7871
Deployed date	05 Jul. 2008
Recovered date	03 Dec. 2009
Exact location	05-02.51N, 146-56.99 E
Depth	4,255 m

Nominal location	2N, 147E
ID number at JAMSTEC	08009
Number on surface float	T23
ARGOS PTT number	23719
ARGOS backup PTT number	7878
Deployed date	08 Jul. 2008
Recovered date	29 Nov. 2009
Exact location	01-59.60N, 147-01.34 E
Depth	4,521 m

Nominal location	EQ, 147E
ID number at JAMSTEC	09010
Number on surface float	T26
ARGOS PTT number	3781
ARGOS backup PTT number	7881
Deployed date	10 Jul. 2008
Recovered date	27 Nov. 2009
Exact location	00-01.49S, 147-00.04E
Depth	4,567 m

*: Dates are UTC and represent anchor drop times for deployments and release time for recoveries, respectively.

(7) Details of deployed

We had deployed nine TRITON buoys, described them details in the list.

Deployment TRITON buoys

Observation No.	Location	Details
01012	8N156E	Deploy with full spec and 1 optional unit. JES-10CTD : 300m
02012	5N156E	Deploy with full spec and 1 optional unit. JES-10CTD : 750m
03013	2N156E	Deploy with full spec and 3 optional sensors. CO2 float type buoy : with TRITON top buoy SBE37 (CT) : 175m pCO2 : 25m
04012	EQ156E	Deploy with full spec and 1 optional unit. SBE37 (CT) : 175m Camera system : with TRITON tower
05010	2S156E	Deploy with full spec and 1 optional unit. Camera system : with TRITON tower
06010	5S156E	Deploy with full spec.
07010	5N147E	Deploy with full spec.
08009	2N147E	Deploy with full spec and 1 optional unit. SBE37 (CT) : 175m
09010	EQ147E	Deploy with full spec.

(8) Data archive

Hourly averaged data are transmitted through ARGOS satellite data transmission system in almost real time. The real time data are provided to meteorological organizations via Global Telecommunication System and utilized for daily weather forecast. The data will be also distributed world wide through Internet from JAMSTEC and PMEL home pages. All data will be archived at The JAMSTEC Mutsu Institute.

TRITON Homepage : http://www.jamstec.go.jp/jamstec/triton

7.1.2 Inter-comparison between shipboard CTD and TRITON transmitted data

(1) Personnel

Yuji Kashino	(JAMSTEC): Principal Investigator
Keisuke Matsumoto	(MWJ): Technical Staff

(2) Objectives

TRITON CTD data validation.

(3) Measured parameters

・Temperature
・Conductivity
・Pressure

(4) Methods

TRITON buoy underwater sensors are equipped along a wire cable of the buoy below sea surface. We used the same CTD (SBE 9/11Plus) system with general CTD observation (See section 5) on R/V MIRAI for this intercomparison. We conducted 1 CTD cast at each TRITON buoy site before recovery, conducted 1 CTD or XCTD cast at each TRITON buoy site after deployment. The cast was performed immediately after the deployment and before recovery. R/V MIRAI was kept the distance from the TRITON buoy within 2 nm.

TRITON buoy data was sampled every 1 hour except for transmission to the ship. We compared CTD observation by R/V MIRAI data with TRITON buoy data using the 1 hour averaged value.

As our temperature sensors are expected to be more stable than conductivity sensors, conductivity data and salinity data are selected at the same value of temperature data. Then, we calculate difference of salinity from conductivity between the shipboard (X)CTD data on R/V MIRAI and the TRITON buoy data for each deployment and recovery of buoys.

Compared site

Observation No.	Latitude	Longitude	Condition
01012	8N	156E	After Deployment
02012	5N	156E	After Deployment
03013	2N	156E	After Deployment
04013	EQ	156E	After Deployment
05011	2S	156E	After Deployment
06011	5S	156E	After Deployment
07011	5N	147E	After Deployment
08010	2N	147E	After Deployment
09011	EQ	147E	After Deployment
01011	8N	156E	Before Recover
03012	2N	156E	Before Recover
04012	EQ	156E	Before Recover
05010	2S	156E	Before Recover
06010	5S	156E	Before Recover
07010	5N	147E	Before Recover
08009	2N	147E	Before Recover
09010	EQ	147E	Before Recover

(5) Results

Most of temperature, conductivity and salinity data from TRITON buoy showed good agreement with CTD cast data in T-S diagrams. See the Figures 7.1.2-1(a) (b).

To evaluate the performance of the conductivity sensors on TRITON buoy, the data from had deployed buoy and shipboard CTD data at the same location were analyzed.

The estimation was calculated as deployed buoy data minus shipboard CTD (9Plus) or XCTD data. The salinity differences are from –0.1078 to 0.1174 for all depths. Below 300db, salinity differences are from –0.0135 to 0.0428 (See the Figures 7.1.2-2 (a)). The average of salinity differences was -0.0126 with standard deviation of 0.0278.

The estimation was calculated as recovered buoy data minus shipboard CTD (9Plus) data. The salinity differences are from –2.7905 to 0.2660 for all depths. Below 300db, salinity differences are from -0.00059 to 0.1495 (See the Figures 7.1.2-2(b)). The average of salinity differences was -0.0261 with standard deviation of 0.3848.

The estimation of time-drift was calculated as recovered buoy data minus deployed buoy data. The salinity changes for 1 year are from –2.7955 to 0.2308, for all depths. Below 300db, salinity changes for 1 year are from -0.0349 to 0.1360 (See the figures 7.1.2-2(c)). The average of salinity differences was -0.0438 with standard deviation of 0.3800.

(6) Data archive

All raw and processed CTD data files were copied on 3.5 inch magnetic optical disks and submitted to JAMSTEC TOCS group of the Ocean Observation and Research Department. All original data will be stored at JAMSTEC Mutsu brunch. (See section 5)

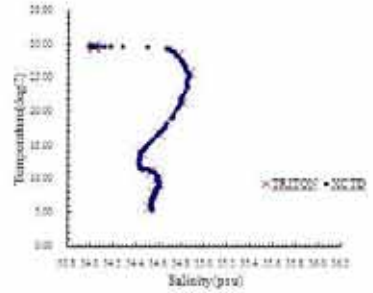

Observation No. 01012 after Deployment

Observation No. 02012 after Deployment

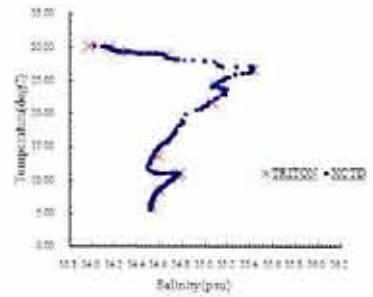

Observation No. 03013 after Deployment

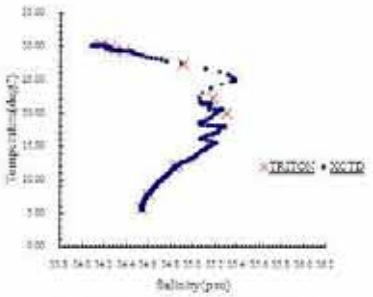

Observation No. 04013 after Deployment

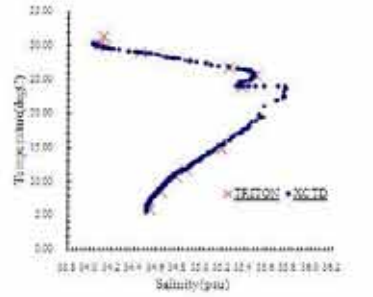

Observation No. 05011 after Deployment

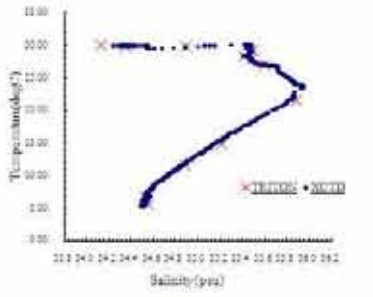

Observation No. 06011 after Deployment

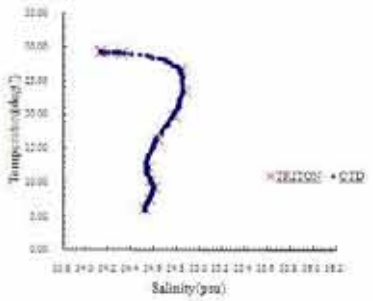

Observation No. 07011 after Deployment

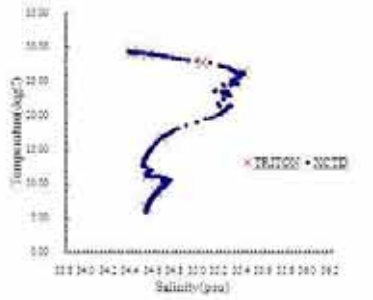

Observation No. 08010 after Deployment

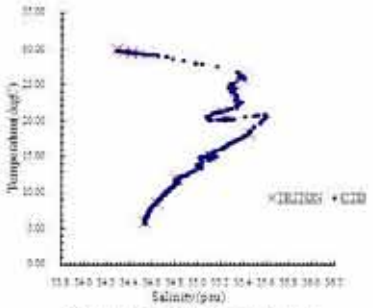

Observation No. 09010 after Deployment

Fig.7.1.2.-1(a) T-S diagram of TRITON buoys data and shipboard (X)CTD data

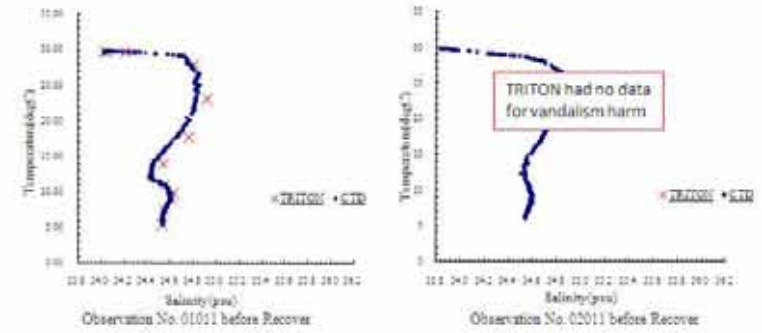

Observation No. 01011 before Recover　　Observation No. 02011 before Recover

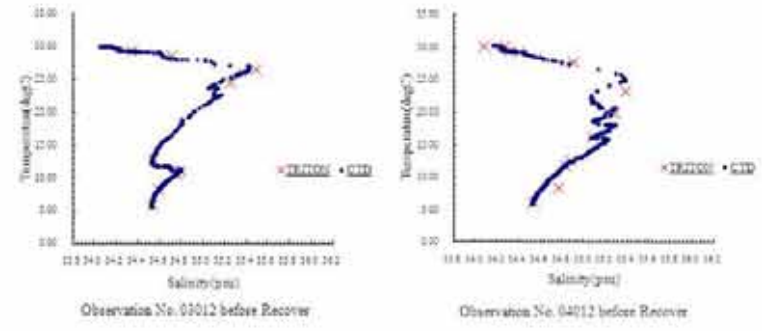

Observation No. 03012 before Recover　　Observation No. 04012 before Recover

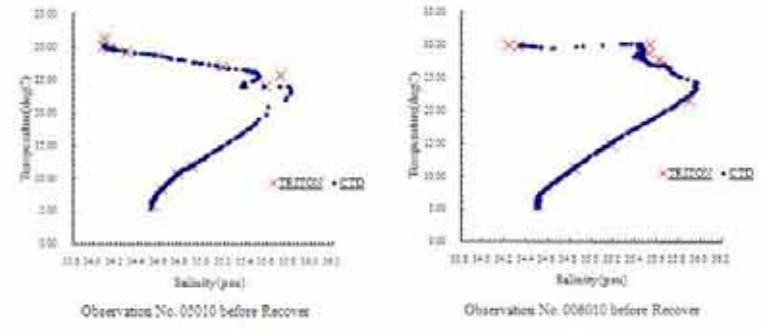

Observation No. 05010 before Recover　　Observation No. 006010 before Recover

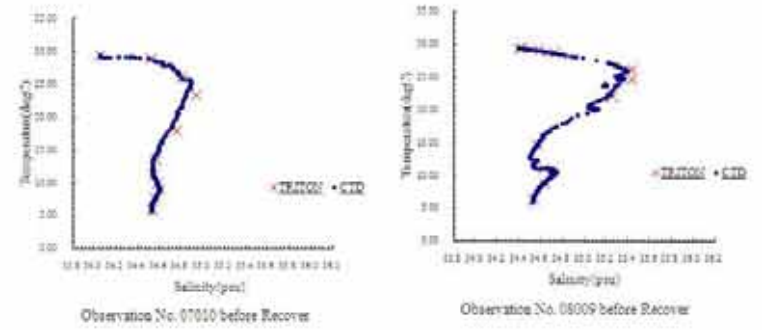

Observation No. 07010 before Recover　　Observation No. 08009 before Recover

Observation No. 09010 before Recover

Fig. 7.1.2.-1(b) T-S diagram of TRITON buoys data and shipboard CTD data

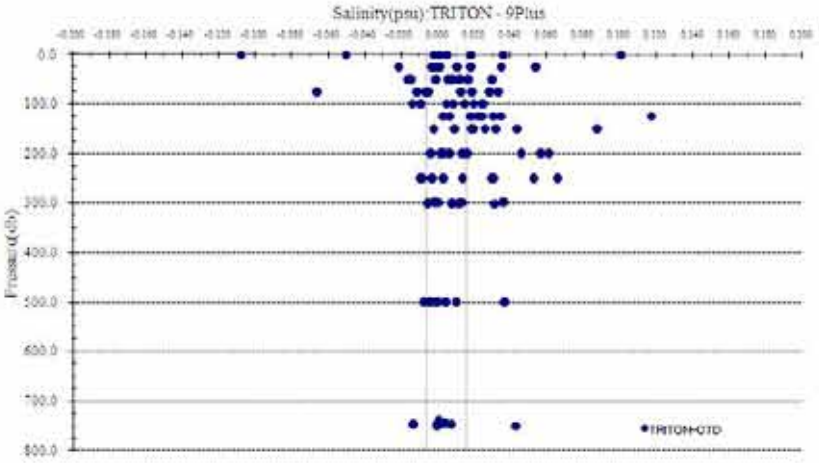

Fig.7.1.2.-2 (a) Salinity differences between TRITON buoys data and shipboard (X) CTD data after deployment

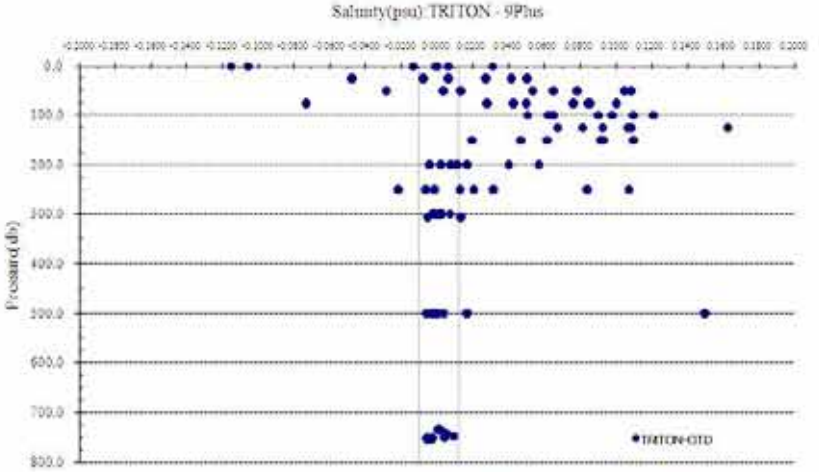

Fig.7.1.2.-2 (b) Salinity differences between TRITON buoys data and shipboard CTD data before recovery

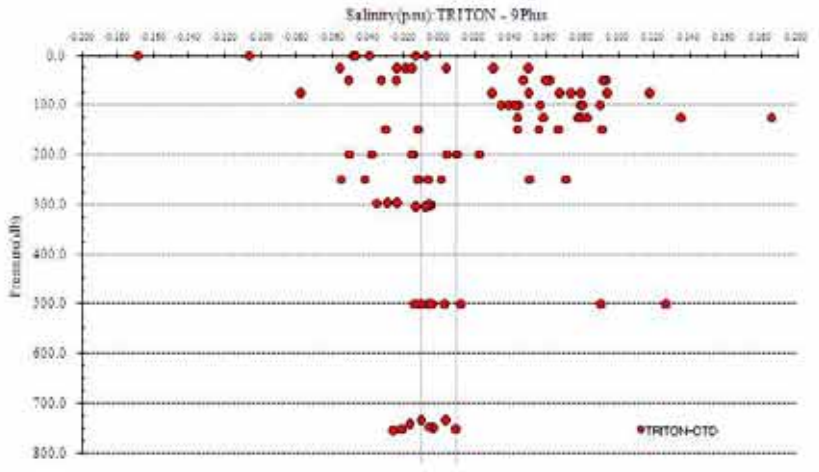

Fig.7.1.2.-2 (c) Salinity differences between deployment data and recovery data for 1year

7.2 Subsurface ADCP moorings

(1) Personnel

Yuji Kashino	(JAMSTEC): Principal Investigator
Tomohide Noguchi	(MWJ): Operation leader
Tashuya Tanaka	(MWJ): Technical staff
Akira Watanabe	(MWJ): Technical staff
Shungo Oshitani	(MWJ): Technical staff
Kimiko Nishijima	(MWJ): Technical staff

(2) Objectives

The purpose of this ADCP observation is to get knowledge of physical process underlying the dynamics of oceanic circulation in the western equatorial Pacific Ocean. We have been observing subsurface currents using ADCP moorings along the equator. In this cruise (MR09-04), we recovered two subsurface ADCP moorings at Eq-147E/Eq-156E and deployed two ADCP moorings at Eq-147E/Eq-156E.

(3) Parameters

- Current profiles
- Echo intensity
- Pressure, Temperature and Conductivity

(4) Methods

Two instruments are mounted at the top float of the mooring. One is ADCP (Acoustic Doppler Current Profiler) to observe upper-ocean currents from subsurface down to around 300m depths. The second instrument mounted below the float is CTD, which observes pressure, temperature and salinity for correction of sound speed and depth variability. Details of the instruments and their parameters are as follows:

1) ADCP

Self-Contained Broadband ADCP 150 kHz (Teledyne RD Instruments, Inc.)
Distance to first bin : 8 m
Pings per ensemble : 16
Time per ping : 2.00 seconds
Bin length : 8.00 m
Sampling Interval : 3600 seconds

Recovered ADCP

- Serial Number : 1222 (Mooring No.080711-00147E)
- Serial Number : 1154 (Mooring No.080720-00156E)

Deployed ADCP

- Serial Number : 1150 (Mooring No.091127-00147E)
- Serial Number : 1225 (Mooring No.091120-00156E)

2) CTD

SBE-16 (Sea Bird Electronics Inc.)

Sampling Interval : 1800 seconds

Recovered CTD

- Serial Number : 1278 (Mooring No.080711-00147E)
- Serial Number : 1274 (Mooring No.080720-00156E)

Deployed CTD

- Serial Number : 1283 (Mooring No.091127-00147E)
- Serial Number : 2611 (Mooring No.091120-00156E)

3) Other instrument

(a) Acoustic Releaser (BENTHOS,Inc.)

Recovered Acoustic Releaser

- Serial Number : 632 (Mooring No.080711-00147E)
- Serial Number : 693 (Mooring No.080711-00147E)
- Serial Number : 667 (Mooring No.080720-00156E)
- Serial Number : 634 (Mooring No.080720-00156E)

Deployed Acoustic Releaser

- Serial Number : 663 (Mooring No.091127-00147E)
- Serial Number : 694 (Mooring No.091127-00147E)
- Serial Number : 716 (Mooring No.091120-00156E)
- Serial Number : 719 (Mooring No.091120-00156E)

(b) Transponder (BENTHOS,Inc.)

Recovered Transponder

- Serial Number : 57069 (Mooring No.080711-00147E)
- Serial Number : 57491 (Mooring No.080720-00156E)

Deployed Transponder

- Serial Number : 57068 (Mooring No.091127-00147E)
- Serial Number : 46472 (Mooring No.091120-00156E)

(5) Deployment

The ADCP mooring deployed at Eq-147E and Eq-156E was planned to play the ADCP at about 300m depths. After we dropped the anchor, we monitored the depth of the acoustic releaser.

The position of the mooring No. 091127-00147E

Date: 27 Nov. 2009 Lat: 00-00.28S Long: 147-04.53E Depth: 4,485m

The position of the mooring No. 091120-00156E

Date: 20 Nov. 2009 Lat: 00-02.22S Long: 156-08.02E Depth: 1,950m

(6) Recovery

We recovered two ADCP moorings. One was deployed on 18 Jun.2007 and the other was deployed on 28 Jun. 2007 (MR07-03cruise). After the recovery, we uploaded ADCP and CTD data into a computer, then raw data were converted into ASCII code. The CTD recovered at Eq-156E was broken down. It's not known exactly why.

Results were shown in the figures in the following pages. Fig.7-2-1 shows the ADCP velocity data (zonal and meridional component / Eq-147E). Fig.7-2-2 shows CTD pressure, temperature and salinity data (Eq-147E). Fig.7-2-3 shows the ADCP velocity data (zonal and meridional component / Eq-156E).

(7) Data archive

All data will be submitted to JAMSTEC Data Management Office and is currently under its control.

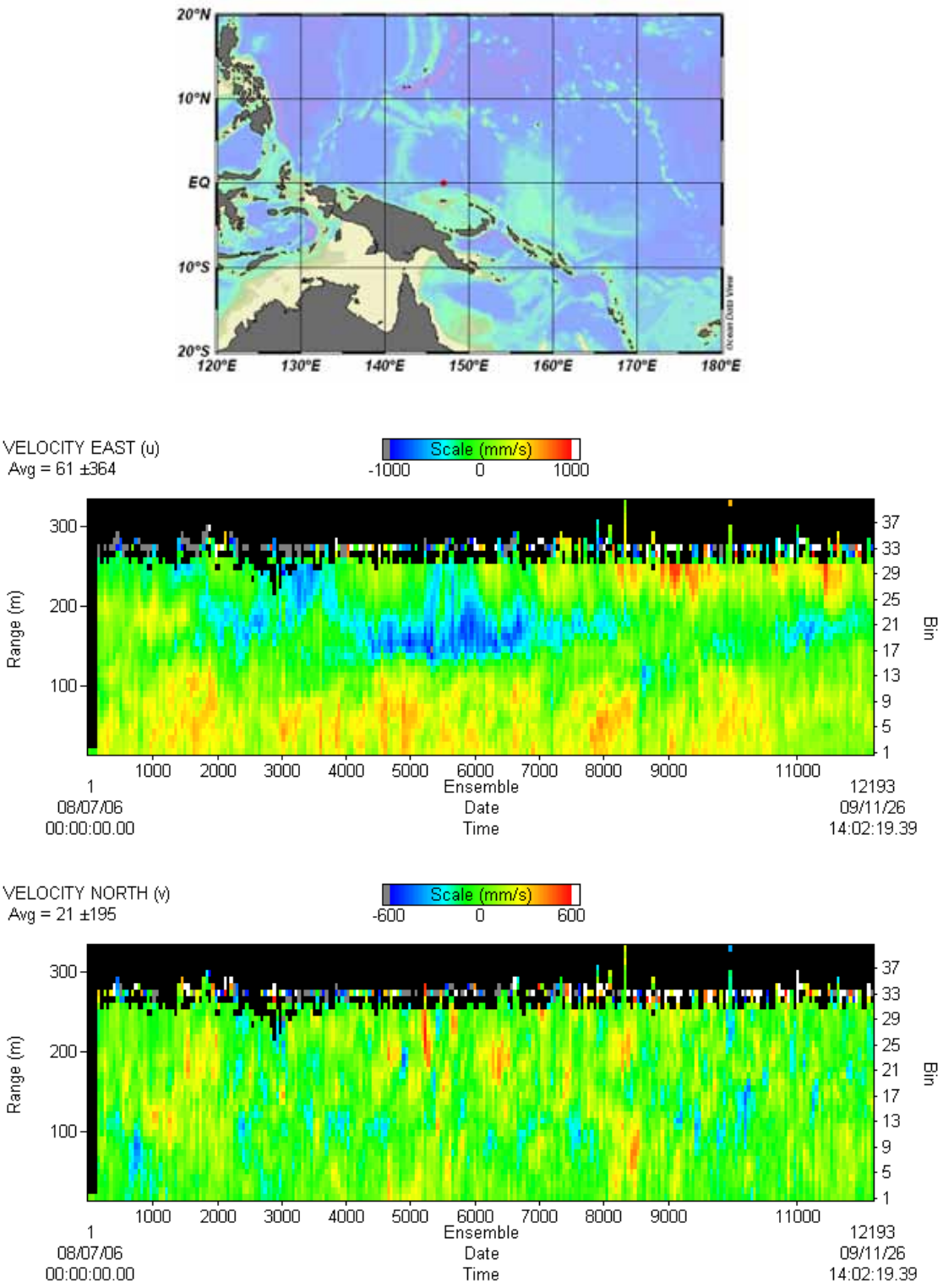

Fig.7-2-1 Time Series of zonal and meridional velocities of EQ-147E mooring
(2008/7/14-2009/11/27)

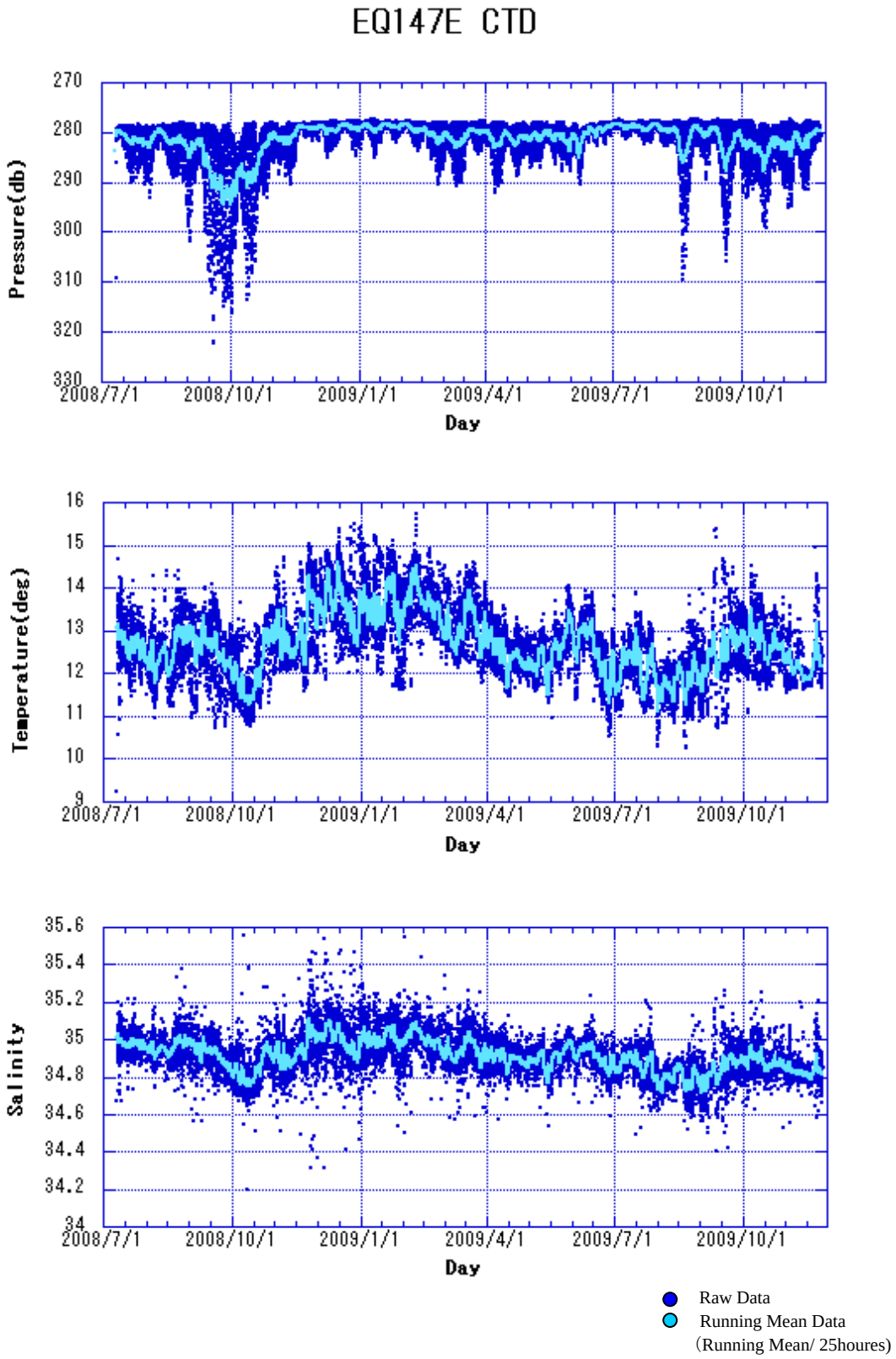

Fig.7-2-2 Time Series of pressure, temperature, salinity of obtained with CTD of EQ-147E mooring (2008/7/14-2009/11/27)

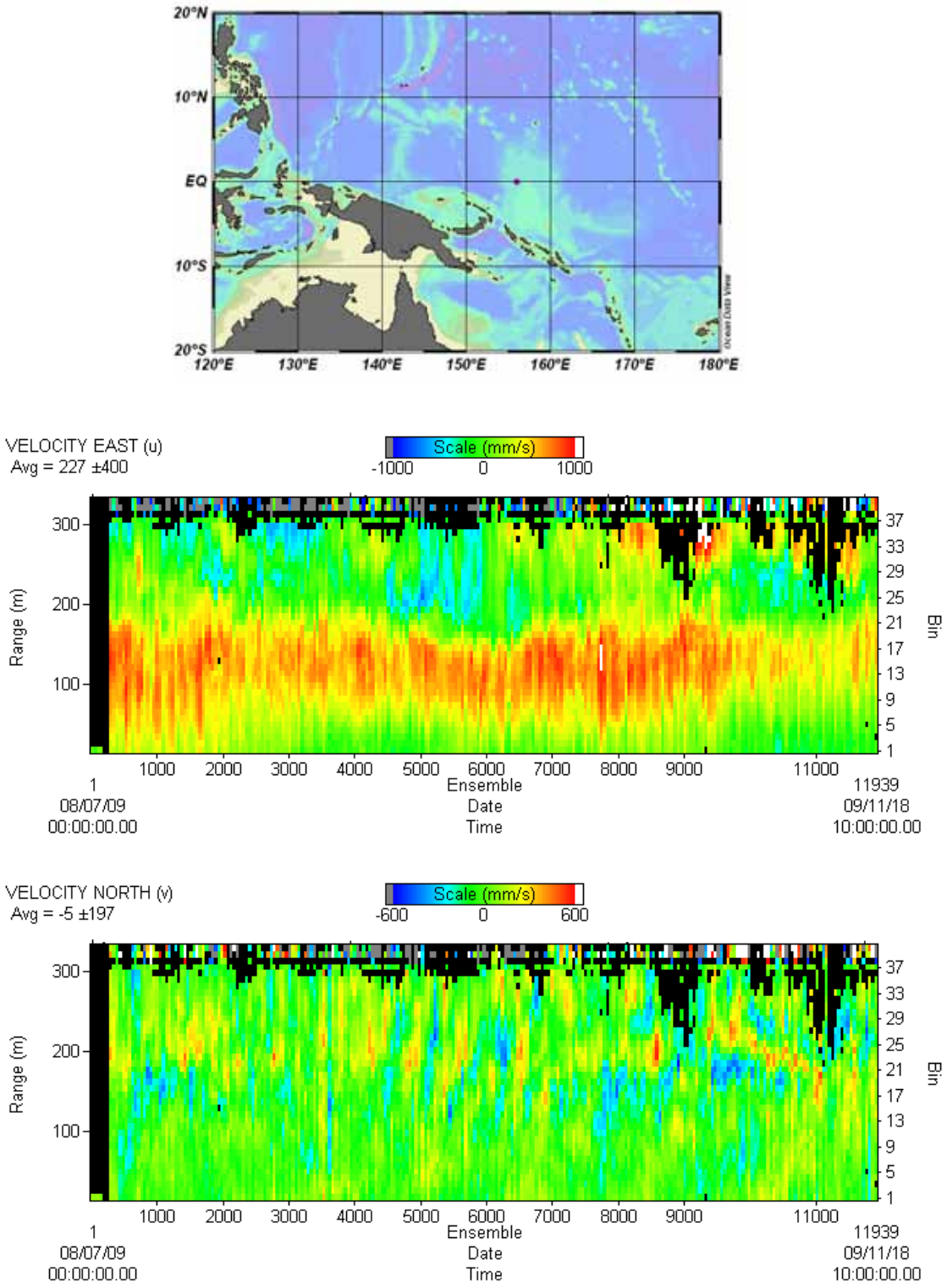

Fig.7-2-3 Time Series of zonal and meridional velocities of EQ-156E mooring

(2008/7/20-2009/11/19)

7.3 Current profile observations using a high frequency lowered acoustic Doppler current profiler

Personnel Kelvin Richards (IPRC, University of Hawaii)

(1) Objective

To measure small vertical scale (SVS) velocity structures in the upper ocean.

(2) Overview of instrument and operation

In order to measure the velocity structure at fine vertical scales a high frequency ADCP was used in lowered mode (LADCP). The instrument was a Teledyne RDI Workhorse Sentinel 600kHz ADCP rated for 1000m depth. The instrument was attached to the frame of the CTD system using a plastic collar and two retaining bolts. A rope was tied to the top end of the instrument to minimize vertical slippage and for added safety (see Figure 7-3-1). The instrument was deployed on all 500m and 800m casts at CTD stations C5-C36. The instrument performed well throughout its use.

Fig 7-3-1. Mounting of LADCP on the CTD System

The instrument is self-contained with an internal battery pack. The health of the battery is monitored by the recorded voltage count. Direct measurements of the battery voltage were taken before the first and after the last deployments and compared to the recorded voltage count:

	Battery Voltage (V)	Voltage Count (VC)	ratio (V/VC)
Before	44.5	149	0.299
After	40.8	134	0.304

Implying, as in other cruises, an almost constant relationship of V~=0.30VC. RDI recommend the battery is changed when V gets below 30V.

(3) Setup and Parameter settings

The LADCP was controlled at deploy and recover stages by a Linux PC using the python script **ladcp600.py** (written by Eric Firing, University of Hawai`i) The commands sent to the instrument at setup were contained in **ladcp600.cmd**. For most of the casts the instrument was setup to have a relatively small bin depth (2m) and a fast ping rate (every 0.25 sec). The full list of commands sent to the instrument were:

```
CR1                 # Retrieve parameter (default)
TC2                 # Ensemble per burst
WP1                 # Pings per ensemble
TE 00:00:00.00      # Time per ensemble (time between data collection cycles)
TP 00:00.25         # Time between pings in mm:ss
WN25                # Number of Depth cells
WS0200              # Depth cell size (in cms)
WF0088    # Blank after transit (recommended setting for 600kHz)
WB0                 # Mode 1 bandwidth control (default - wide)
WV250               # Ambiguity velocity (in cm/s)
EZ0111101           # Sensor source (speed of sound excluded)
EX00000             # Beam coordinates
CF11101             # Data flow control parameters
```

(see the RDI Workhorse "Commands and Data Output Format" document for details.)

(4) Data processing

An initial sampling of the data was made using the following scripts to check that the instrument was performing correctly

scanbb	integrity check
plot_PTCV.py	plot pressure, temperature, voltage and current counts
plot_vel.py	plot velocity from all 4 beams

The principal onboard data processing was performed using the Lamont Doherty Earth Observatory (LDEO, Columbia University) LADCP software package (available at ftp://ftp/ldeo.columbia.edu/pub/ant/LADCP). The package is based on a number of matlab scripts. The package performs an inverse of the LADCP data, incorporating CTD (for depth) and GPS data, to provide a vertical profile of the horizontal components of velocity, U and V (eastward and northward, respectively), that is a best fit to specified constraints. The down- and up-casts are solved separately, as well as the full cast inverse. The package also calculates U and V from the vertical shear of velocity.

The software is run using the matlab script **process_cast.m** with the configuration file **set_cast_params.m.** Frequent CTD data are required. Files of 1 second averaged CTD data were prepared for each station. Accurate time keeping is also required, particularly between the CTD and GPS data. To ensure this the CTD data records also included the GPS position. The LDEO software allows the ship's ADCP data (SADCP) to be included in the inverse calculation. The SADCP data were not included in this case so as to provide an independent check on the functioning of the LADCP.

Because of the short range of the 600 kHz instrument (20-40m in this case) the analysis is very sensitive to the presence of the wake of the CTD system on up-casts. Individual beams can be affected; indicated by a reduced velocity over the top few bins shown in the velocity plot produced by plot_vel.py. In most cases only one out of the four beams was severely affected. Calculating a 3-beam solution, by ignoring the affected beam, produced much better results than the full 4 beam solution.

On-station SADCP velocity profiles were produced by averaging the five minute averaged profiles (mr090400x_000000.LTA produced using VmDAS) over the period of the CTD/LADCP cast. Care was taken to ensure the average did not contain any spurious data from periods when the ship was maneuvering.

(5) Preliminary results

An example of the on-board processed data is presented in Figure 7-3-2. Figure 7-3-2 compares the full cast inverse, up- and down-cast inverse, and the shear solutions for the zonal (U) and meridional (V) components of the velocity vector with the corresponding SADCP profile for Station C07M01. The LADCP velocity has been fitted to the mean and linear shear of the SADCP velocity. There is a very good correspondence between the general structure of all velocity profiles. While the large vertical scale flow is in a good agreement with the SADCP data (gray line), the LADCP solutions show a lot of smaller scale structure, not resolved by the SADCP. Especially noticeable in Figure 7-3-2 are features in V between 50-300m that are barely resolved by the SADCP.

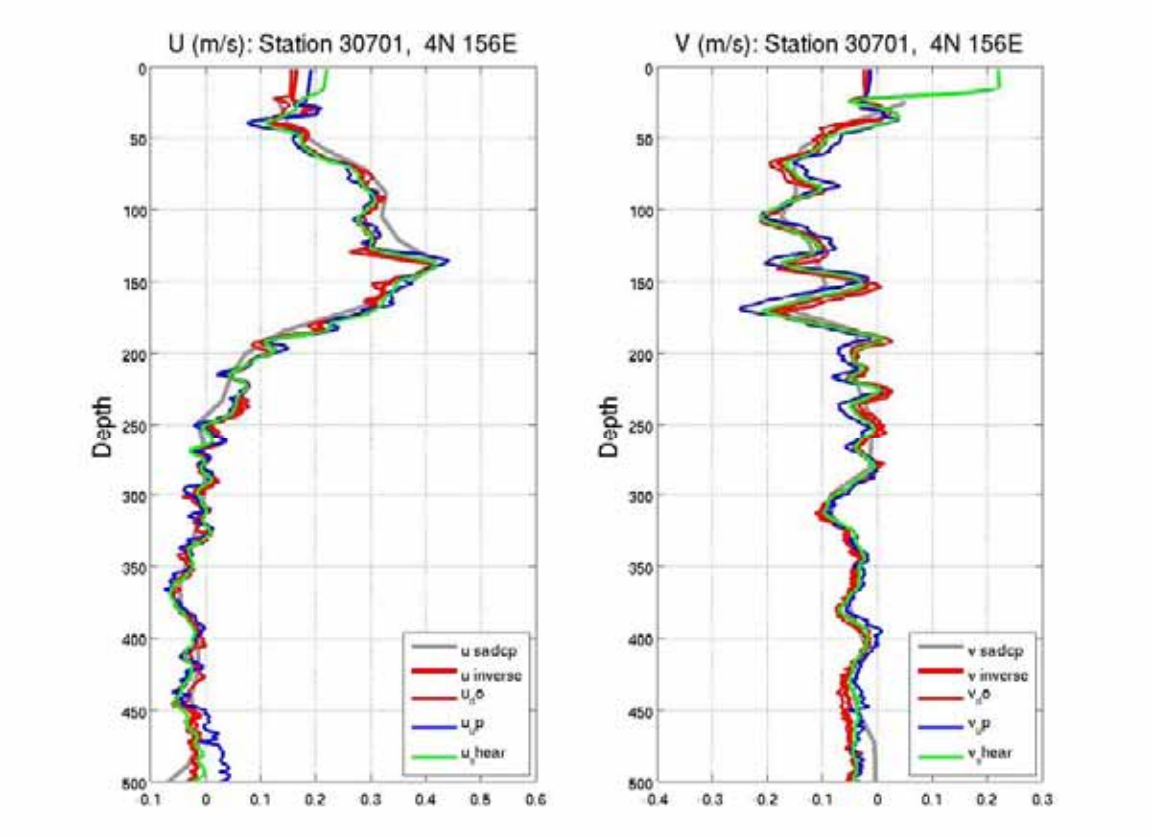

Figure 7-3-2. CTD Station C07M01: Vertical profiles of U and V calculated by a number of methods using LADCP data. Full cast inverse (u inverse), down-cast only inverse (u_do), up-cast only inverse (u_up) and shear solution (u_shear). Also shown are the profiles using SADCP data (u sadcp).

The measurements at individual stations are combined to produce latitudinal sections of the velocity fields. Figures 7-3-3 and 7-3-4 show the zonal component of the velocity as a function of latitude and depth along 147E and 156E, respectively. Both plots show an abundance of features with vertical scales 30 – 60 m. Smaller scale features, not evident in the plots shown, are present and resolved by the LADCP. In the 156E section, as well as the EUC and NECC centered on the equator and 4.5N, respectively, note the strong subsurface current between 4-5S.

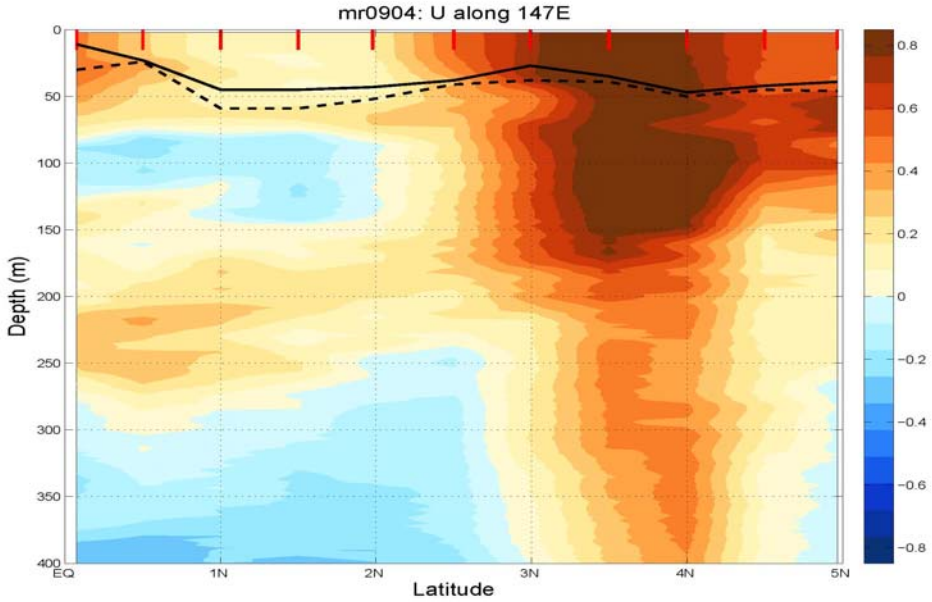

Figure 7-3-3. Latitudinal section of the zonal component of the velocity at 147E. Solid and dashed black lines are the mixed layer depth based on density and temperature, respectively.

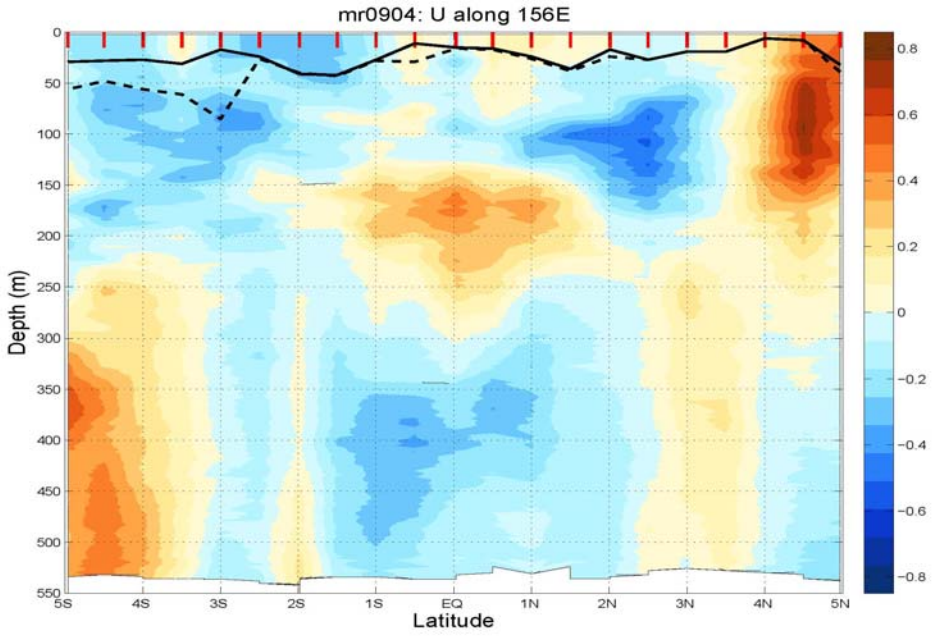

Figure 7-3-4. Latitudinal section of the zonal component of the velocity along 156E. Solid and dashed black lines are the mixed layer depth based on density and temperature, respectively.

7.4 Observation of ocean turbulence

Personnel Yuji Kashino (RIGC, JAMSTEC)
Kelvin Richards (IPRC, Univ. of Hawaii)
Souichiro Sueyoshi (Global Ocean Development Inc.)
Ryo Kimura (Global Ocean Development Inc.)

(1) Introduction

The western equatorial Pacific is called “Water Mass Crossroad” (Fine et al., 1994) because of complicated ocean structure due to various water masses from the northern and southern Pacific oceans. Small structure associated with ocean mixing such as interleaving was sometimes observed. Because this mixing effect is not fully implemented in the ocean general circulation model presently, it should be evaluated by in-situ observation. Considering this background, JAMSTEC started collaboration research with IPRC of Univ. of Hawaii since 2007, and observations using lowered acoustic Doppler current profiler (LADCP) with high frequency were carried out during MR07-07 Leg 1 and MR08-03. These observations revealed interesting fine structures with vertical scale of order 10m and horizontal scale of order 100km. For better understanding of ocean fine structures involving this phenomenon, we observe ocean turbulence using a Turbulence Ocean Microstructure Acquisition Profiles, Turbo Map-L, developed by JFE Alec Co Ltd. during this cruise.

(2) Measurement parameters

Using the Turbo Map-L, we measured following parameters:

Parameter	Type	Range	Accuracy	Sample Rate
$\partial u/\partial z$	Shear probe	0～10 /s	5%	512Hz
$T+\partial T/\partial z$	EPO-7 thermistor	−5～45℃	±0.01℃	512Hz
T	Platinum wire thermometer	−5～45℃	±0.01℃	64Hz
Conductivity	Inductive Cell	0～70mS	±0.01mS	64Hz
Depth	Semiconductor strain gauge	0～1000m	±0.2%	64Hz
x- acceleration	Solid-state fixed mass	±2G	±1%	256Hz
y- acceleration	Solid-state fixed mass	±2G	±1%	256Hz
z- acceleration	Solid-state fixed mass	±2G	±1%	64Hz
Chlorophyll	Fluorescence	0～100 μg/Lm	0.5 μg/L or ±1%	256Hz
Turbidity	Backscatter	0～100ppm	1ppm or ±2%	256Hz
$\partial u/\partial z$	Shear probe	0～10 /s	5%	512Hz

We use following twin shear probes for measuring current shear:

Primary: S/N 502

Secondary: S/N 503 (St.3 – 20 and 22 – 33), S/N 504 (St.21 and 34 – 36)

Because data from the secondary probe shows large noise below 300m after St.32, we changed it from S/N 503 to S/N 504. At st.21, we used S/N 504 for data check.

(3) Observation stations.

Station ID	Date	Observation Start			Max Depth	
		Time	Latitude	Longitude	Time	Depth(m)
St.03	2009/11/12	04:38	154-53.98E	09-57.63N	04:50	505
St.05	2009/11/14	19:37	156-04.27E	04-58.35N	19:51	546
St.06	2009/11/16	03:23	156-00.48E	04-29.82N	03:41	585
St.07	2009/11/16	07:14	156-00.26E	03-59.95N	07:28	606
St.08	2009/11/16	10:42	156-00.23E	03-30.05N	10:58	670
St.09	2009/11/16	18:44	156-00.32E	03-00.51N	18:58	505
St.10	2009/11/16	22:22	156-00.24E	02-30.36N	22:36	505
St.11	2009/11/17	07:03	155-55.94E	02-00.48N	07:15	522
St.12	2009/11/18	03:03	156-00.27E	01-30.03N	03:19	581
St.13	2009/11/18	07:13	156-00.03E	01-00.00N	07:30	546
St.14	2009/11/18	10:35	156-00.22E	00-30.02N	10:48	521
St.15	2009/11/18	18:48	156-02.12E	00-01.76N	19:01	508
St.16	2009/11/20	07:03	155-59.67E	00-30.33S	07:16	523
St.17	2009/11/20	10:24	155-59.53E	00-59.87S	10:37	532
St.18	2009/11/20	21:39	155-59.54E	01-29.96S	21:52	535
St.19	2009/11/21	05:49	155-59.09E	01-59.10S	06:02	534
St.20	2009/11/22	07:09	155-59.55E	02-30.24S	07:23	606
St.21	2009/11/22	10:29	155-59.77E	03-00.17S	10:44	622
St.25	2009/11/23	02:14	156-01.98E	04-57.56S	02:27	512
St.24	2009/11/23	05:18	155-59.72E	04-29.61S	05:31	539
St.23	2009/11/23	08:32	156-00.15E	03-59.42S	08:44	508
St.22	2009/11/24	06:06	156-00.17E	03-29.81S	06:20	556
St.26	2009/11/26	08:25	147-01.84E	00-04.44N	08:40	575
St.27	2009/11/28	03:23	147-00.08E	00-29.60N	03:36	531
St.28	2009/11/28	06:44	146-59.88E	00-59.90N	06:58	563
St.29	2009/11/28	10:07	146-59.81E	01-29.68N	10:22	573
St.30	2009/11/28	20:00	147-01.77E	01-58.40N	20:13	554
St.31	2009/11/30	05:24	147-00.57E	02-29.66N	05:37	557

St.32	2009/11/30	20:17	147-01.65E	02-59.16N	20:29	508
St.33	2009/11/30	23:49	147-04.14E	04-57.91N	00:01	502
St.34	2009/12/1	03:23	147-00.96E	03-59.40N	03:35	509
St.35	2009/12/3	06:56	147-00.68E	04-29.30N	07:08	508
St.36-1	2009/12/3	03:53	147-04.14E	04-57.91N	04:07	563
St.36-2	2009/12/3	04:26	147-04.89E	04-57.79N	04:39	510
St.36-3	2009/12/3	04:59	147-05.70E	04-57.67N	05:11	520

(4) Operation and data processing

We operated the Turbo Map-L by a crane which is usually used for foods supply and installed in the middle of ship. We lowered it at the starboard of R/V Mirai (see below).

Figure 7-4-1. Observation using Turbo Map-L.

Measurement depth was 500m because our interest is ocean turbulence around thermocline. Decent rate of the Turbo Map-L was 0.6 – 0.8 m s^{-1}.

Data acquisition and processing were carried out using a PC in the Atmospheric Gas Observation Room of R/V Mirai. Data processing software was TM-Tool ver 3.04A provided by JFE Alec Co Ltd.

(5) Results

Vertical sections of logarithm of turbulent kinetic energy dissipation rate (epsilon) along 156E and 147E are plotted in Figure 7-5-2. Generally, epsilon at 147E was larger than that at 156E. Large epsilon was observed not only near surface but around 100-200m depth intermittently. It is interesting that large epsilon was also seen at the southern edge of 156E below 300m depth, where strong eastward undercurrent was observed.

To investigate the short time scale variations in epsilon, a series of 3 profiles was taken at 5S, 147E in quick succession (Figure 7-5-3). When the profiles are aligned with respect to potential density, peaks in epsilon in the individual profilers were found, in general, to occur at the same location. The depth averaged epsilon was found, however, to vary by as much as a factor of 3. Averaged over the 3 profiles, epsilon averaged between 50-250m depth was found to be 6.6×10^{-9} W kg^{-1}, with a standard error (based on the variation between profiles) of 2.5×10^{-9} W kg^{-1}.

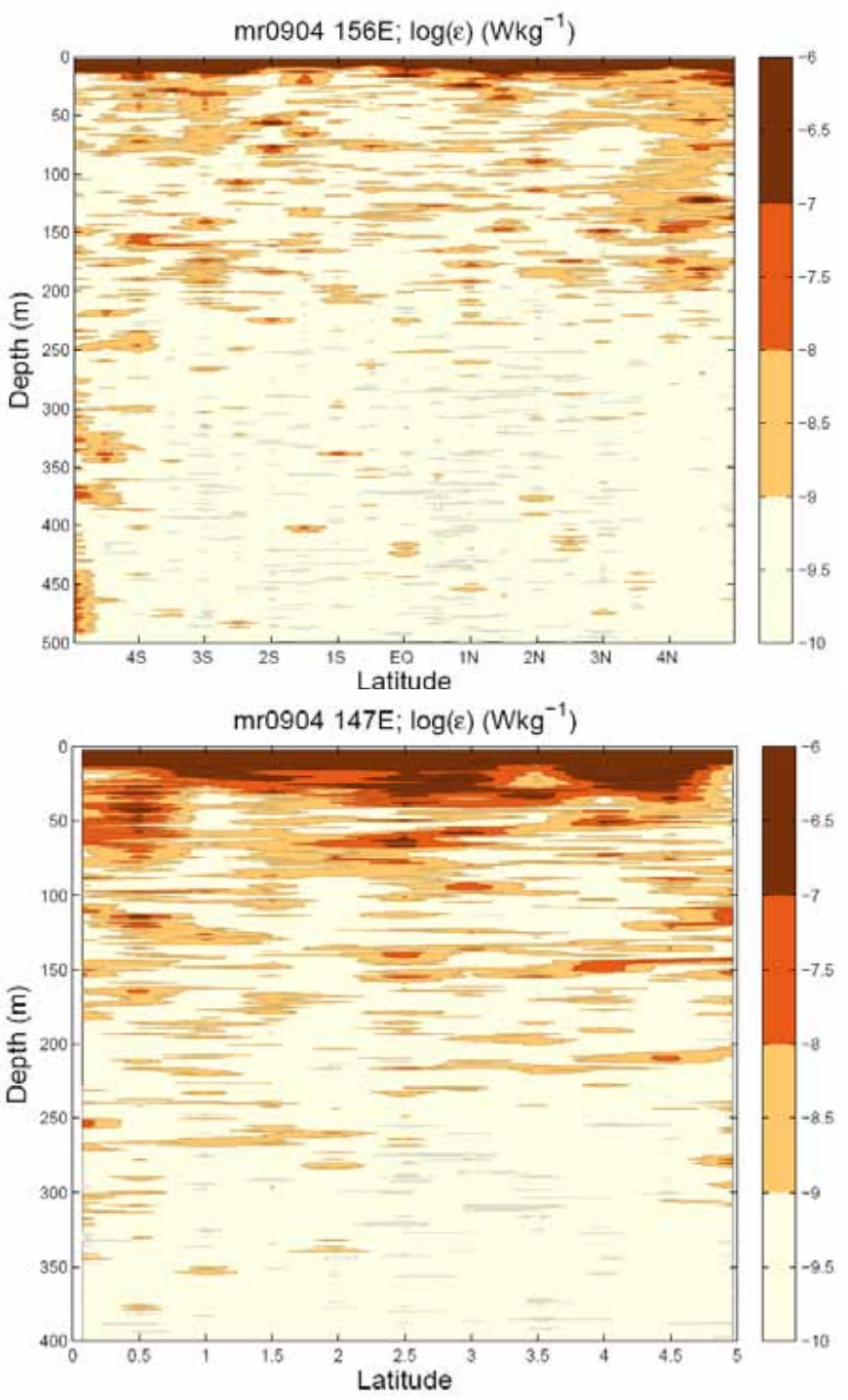

Figure 7-4-2. Vertical sections of logarithm of epsilon along 156E (upper panel) and 147E (lower panel).

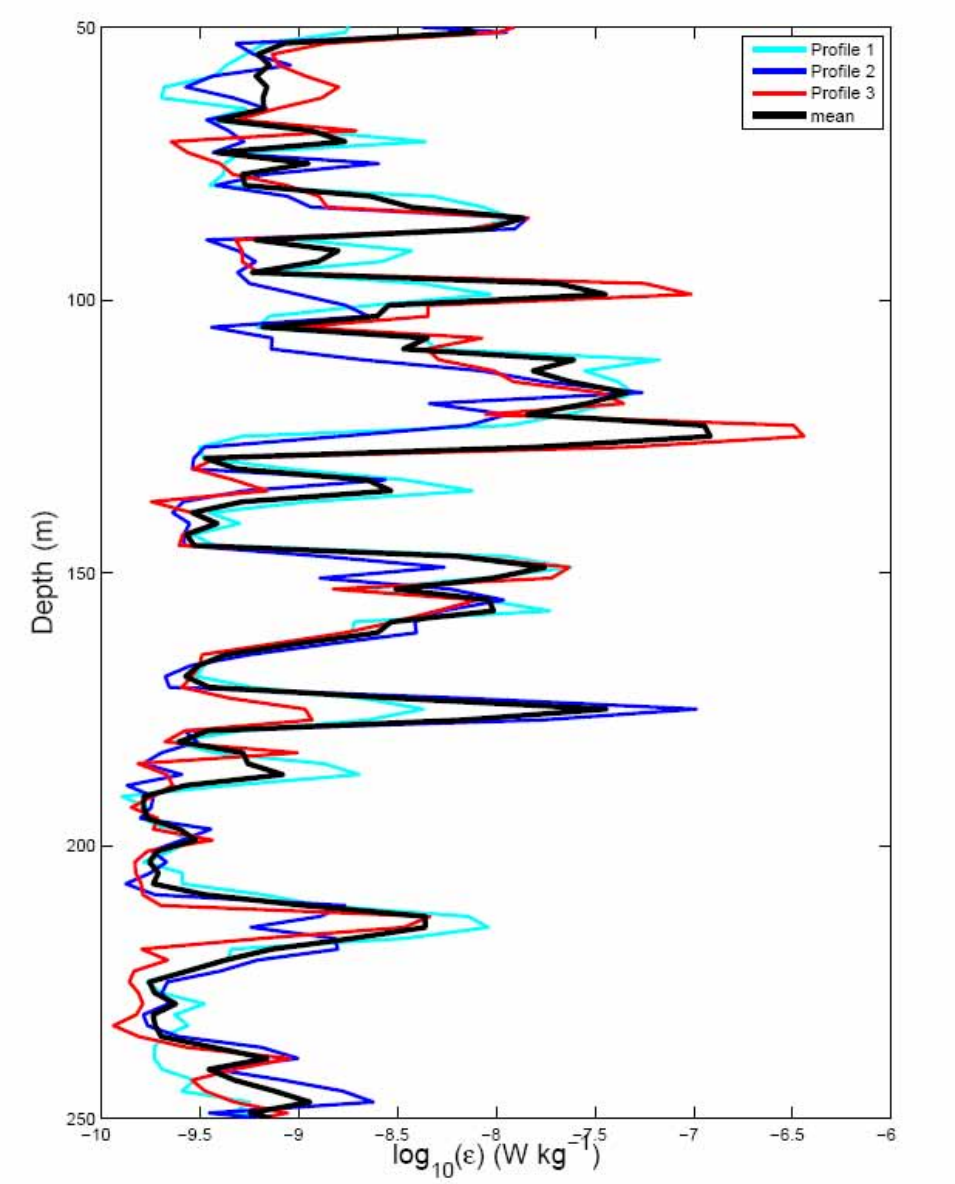

Figure 7-4-3. Vertical profiles of logarithm of epsilon at 5N, 147E.

Acknowledgement

We borrowed the Turbo Map-L used during MR09-04 cruise from Arctic Ocean Research Team of RIGC. We would like to thank Drs.Takashi Kikuchi and Motoyo Ito of this team. We also thank crew of R/V Mirai for their operation work.

7.5. Performance test of pCO_2 sensor

Shuichi Watanabe and Tetsuichi Fujiki (JAMSTEC)

(1) Objective

A lot of observations to obtain the fate of CO_2 in the atmosphere which is related with long term climate change have been carried in the world. However, the sea surface pCO_2 observations on ships of opportunity and research vessels concentrated in the North Atlantic and North Pacific. To obtain the spatial and temporal variation of surface pCO_2 in the whole ocean, new simplified automated pCO_2 measurement system is needed.

We have been developing newly small and simple *in situ* system for pCO_2 measurement using spectrophotometric technique. In this cruise, we aim at testing the new pCO_2 sensor and recovering prototype pCO_2 sensor deployed by MR08-03 cruse in the open sea. The new pCO_2 sensor is attached with TRITON buoy and start mooring (2^{O}N, 156^{O}E) for about one year.

(2) Method

The pCO_2 sensor for the measurement of pCO_2 is based on the optical absorbance of the pH indicator solution. The CO_2 in the surrounding seawater equilibrates with the pH indicator solution across gas permeable membranes, and the resulting change in optical absorbance, representing the change of pH, is detected by the photo multiplier detector. We calculated the pH in the pH indicator solution from the absorbance ratios. In this cruise I decided to use AF Teflon tube (amorphous fluoropolymer, AF Teflon, AF-2400) as an equilibrium membrane because this material is well suited to pCO_2 measurements due to its high gas permeability. This measuring system was constructed from LED light source, optical fiber, CCD detector, micro pump, and downsized PC. The new simple system is attached in aluminum drifting buoy with satellite communication system, which size is about 300 mm diameter and 500 mm length and weight is about 15 kg (Fig. 7.5-1). A Li-ion battery is occupied about one third of the drifting buoy. This system also has a lead-acid battery with two 5W solar panels. The solar panel unit is attached with the middle of TRITON buoy tower and connected with pCO_2 sensor by cable. In the laboratory experiment, we obtained high response time (less than 10 minutes) and precision within 3 μatm.

(3) Preliminary results

We succeeded in deploying the new pCO_2 sensor with TRITON buoy and recovering the prototype pCO_2 sensor at 2^{O}N, 156^{O}E. We obtained long term (about one year) pCO_2 data from the prototype pCO_2 sensor every three days via satellite system. These values are consistent with Mirai data and past data in this area (Fig. 7.5-2).

(4) Data Archive

All data will be submitted to JAMSTEC Data Management Office (DMO) and is currently under its control.

Reference
DOE (1994), Handbook of methods for the analysis of the various parameters of the carbon dioxide system in sea water; version 2, A. G. Dickson & C. Goyet, Eds., ORNS/CDIAC-74

Nakano, Y., H. Kimoto, S. Watanabe, K. Harada and Y. W. Watanabe (2006): Simultaneous Vertical Measurements of In situ pH and CO_2 in the Sea Using Spectrophotometric Profilers. J. Oceanogra., 62, 71-81.

Yao, W. and R. H. Byrne (2001): Spectrophotometric determination of freshwater pH using bromocresol purple and phenol red, Environ. Sci. Technol., 35, 1197-1201.

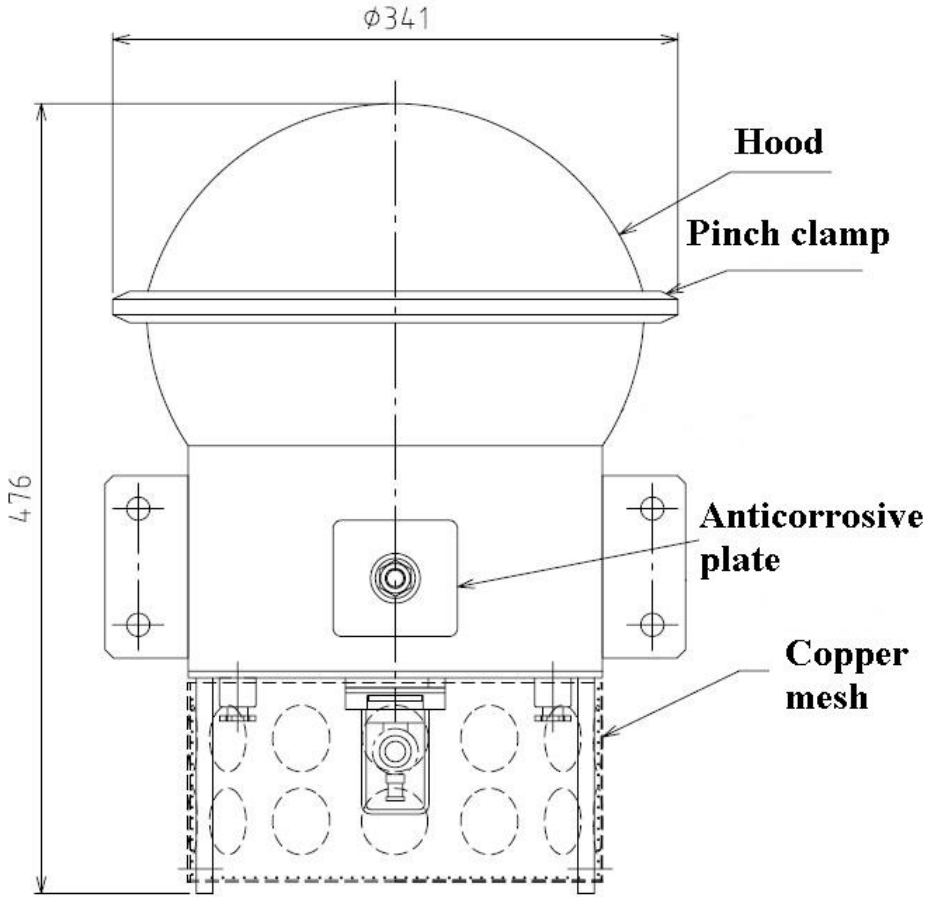

Fig. 7.5-1 Side view of pCO_2 sensor.

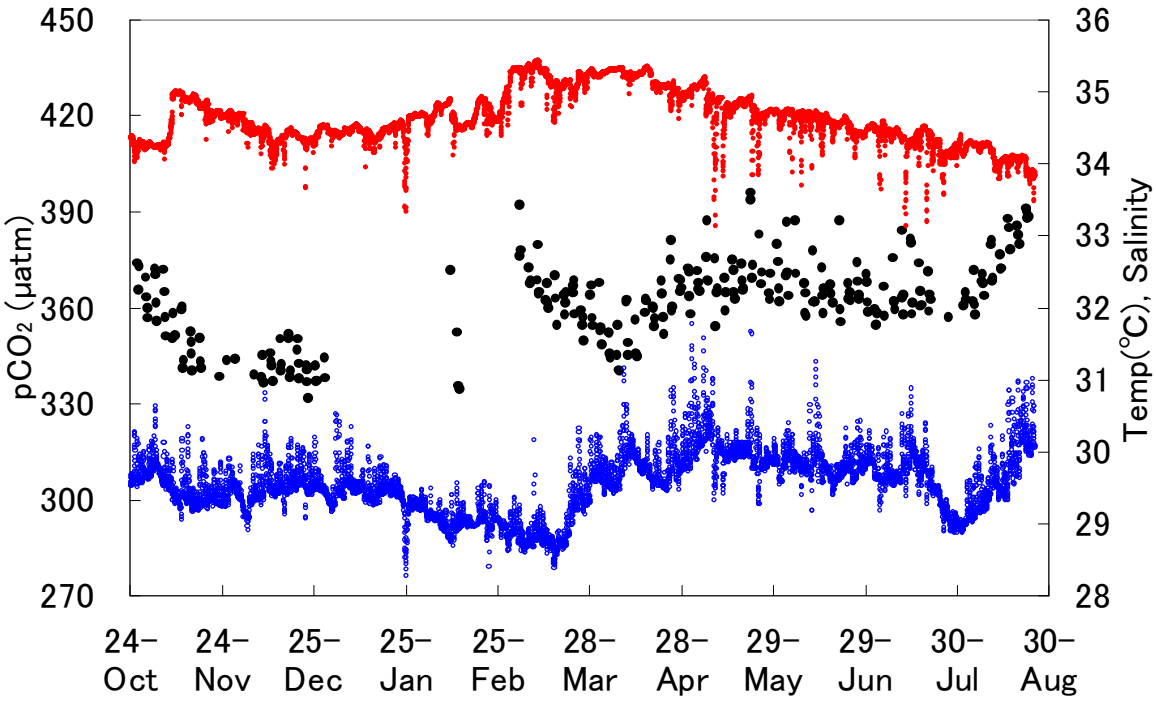

Fig. 7.5-2 Variations of sea surface temperature (SST, ●: right axis), sea surface salinity (SSS, ●: right axis) and pCO_2 （● : left axis） in the western equatorial Pacific. SST, SSS and pCO_2 sometimes had large daily variability because of squall and heavy insolation. This result is consistent with past observed value. We sometimes cannot obtain pCO_2 data over a period of time because our drifting system submerges with sinking of TRITON buoy water level.

7.6. Vertical and long-term measurements by in-situ pH/pCO_2 sensor and vertical measurements by in-situ radon

(1) Personnel

Kiminori Shitashima (CRIEPI)

(2) Objectives

The measurement of pH in the marine system is important because this parameter related to the chemical equilibrium conditions of the seawater and the biological and chemical processes occurring in the sea. In particular, the pH of seawater is reflected in the exchange of CO_2 between the atmosphere and the ocean, and oceanic carbon cycles. In order to characterize the oceanic CO_2 system, at least two of the parameters, pH, pCO_2, alkalinity and total CO_2 have to be measured. The measurement of pH and pCO_2 is comparatively easy in these four parameters. Furthermore, a change of pH and pCO_2 in seawater should preferably be observed continually in a long term and a wide area (vertically and horizontally) to monitor air-sea CO_2 exchange and oceanic carbon cycle concerning the global warming. Unfortunately, the onboard measurement of pH and pCO_2 in seawater is not convenient for the long term and continuous observations. In-situ measurement with a sensor is the most suitable for such observations, but a marketed in-situ pH sensor using a glass electrode cannot detect a detailed pH change because precision is extremely low and response time is too long. In addition, in the pCO_2 measurement, it is limited to only a measurement at the marine surface under the present conditions. The purpose of this study is to develop new type of high performance pH/pCO_2 sensor for in situ measurement in the deep sea, and apply it to chemical oceanography.

Underwater in-situ radon measurement is important scientific priority for oceanography, especially for survey and monitoring of submarine groundwater discharge (SDG), hydrothermal systems and terrestrial input from seasurface. The high sensitivity and lightweight underwater in-situ radon sensor using NaI(Tl) doped plastic scintillator was developed for oceanographic applications. A NaI(Tl) doped plastic scintillator can expect high sensitivity in comparison with a NaI(Tl) crystal sealed in a container because the plastic scintillator contacts seawater directly.

(3) Parameters

Vertical and long-term measurements data of in-situ pH and pCO_2
Vertical measurements data of in-situ radon

(4) Methods

The in-situ pH sensor employs an Ion Sensitive Field Effect Transistor (ISFET) as a pH electrode, and the Chloride ion selective electrode (Cl-ISE) as a reference electrode. The ISFET is a semiconductor made of p-type Si coated with SiO_2 and Si_3N_4 that can measure H^+ ion concentration in aqueous phase. New ISFET-pH electrode specialized for oceanographic use was developed by CRIEPI. The Cl-ISE is a pellet made of several chlorides having a response to the chloride ion, a major element in seawater. The electric potential of the Cl-ISE is stable in the seawater, since it has no inner electrolyte solution. Therefore, The in-situ pH sensor has a quick response (within a few second), high accuracy (±0.005pH) and pressure-resistant performance. The pCO_2 sensor was devised to incorporate the above-mentioned newly developed in-situ pH sensor to measure the in-situ pCO_2 in seawater. The principle of pCO_2 measurement is as follows. Both the ISFET-pH electrode and the Cl-ISE of the pH sensor are sealed in a unit with a gas permeable membrane whose inside is filled with inner electrolyte solution with 1.5 % of NaCl. The pH sensor can detect pCO_2 change as inner solution pH change caused by permeation of carbon dioxide gas species through the membrane. An amorphous Teflon membrane (Teflon AF™) manufactured by DuPont was used as the gas permeable membrane. The in-situ response time of the pCO_2 sensor was less than 60 seconds. The diode on ISFET can measure the temperature of seawater simultaneously and the in situ pH data can be calibrated using this temperature data. ISFET and Cl-ISE are connected to pH converter circuit in the pressure housing through the underwater cable connector. The pressure housing includes pH converter circuit, A/D converter, data logger RS-232C interface and Li ion battery. Before and after the observation, the pH sensor was calibrated using two different standard buffer

solutions, 2-aminopyridine (AMP; pH 6.7866) and 2-amino-2-hydroxymethil-1,3-propanediol (TRIS; pH 8.0893) described by Dickson and Goyet, for the correction of electrical drift of pH data. The measured pH and temperature data are stored in the data logger. After finish of the pH measurement, these data are transferred from the data logger into a personal computer (PC) connected with RS-232C cable, and the in situ pH is calculated using calibration data of AMP and TRIS in a PC. Since the calibration of in-situ pCO_2 measurements was not conducted in our field application reported here, only raw data (arbitrary unit) from the pCO_2 sensor output were obtained. Raw data showing small digit readings indicates pH depression of the inner solution, which reflects an increase in partial pressure of CO_2 in seawater. The in-situ pH/pCO_2 sensors were installed to the CTD-RMS, and in-situ data of pH and pCO_2 ware measured every 10 seconds during descent and ascent of the CTD-RMS. The in-situ pH sensor was also installed at 25m depth of the mooring wire of TRITON buoy in 2N-156E station and in-situ data will be measured every 60 minutes for 1year.

A plastic scintillator is made from polystyrene that doped scintillator such as NaI(Tl) and it absorbs radon like as liquid or crystal scintillator. Because NaI(Tl) doped plastic scintillator contacts seawater directly, the plastic scintillator can expect high sensitivity in comparison with NaI(Tl) crystal sealed in a container. In order to improve condensation efficiency of scintillation, the plastic scintillator was processed in funnel form. In the general scintillation measurement, a dark chamber is necessary to detect photon derived from only radon. However, in-situ scintillation measurement and downsizing of measurement unit are difficult because a dark chamber takes a lot of space. Therefore, the plastic scintilator was coated with a light-resistant paint instead of using a dark chamber. The radon sensor was installed to the CTD-RMS for performance test, and in-situ data of radon was measured every 1 second during descent and ascent of the CTD-RMS.

(5) Preliminary result

As an example, vertical profiles of in-situ pH and pCO_2 at casts of C15M02 and C30M02 are shown in Figure 1. The pH value obtained by the pH sensor agreed well with those obtained by onboard measurement of water samples collected by the Niskin bottles. The in-situ pH/pCO_2 sensors set up in MR08-03 cruise were recovered from 25m depth. Pressure housings oh the sensors were covered with biofouling (shells). There is few biofouling on pH electrode because an electric charge exists on the ISFET-pH electrode. Unfortunately, in-situ data of pH and pCO_2 were only measured every 10 minutes for 1.5 months because Li ion battery exhausted within 1.5 months. A change of daily periodicity was measured in in-situ pCO_2, but it was not measured in in-situ pH.

The radon sensor was detected some intensity in surface water, but I am not sure it is radon intensity. Although the radon sensor was coated with a light-resistant paint, it may be not enough.

(6) Data archive

All data will be archived at CRIEPI after checking of data quality and submitted to the DMO at JAMSTEC within 3 years.

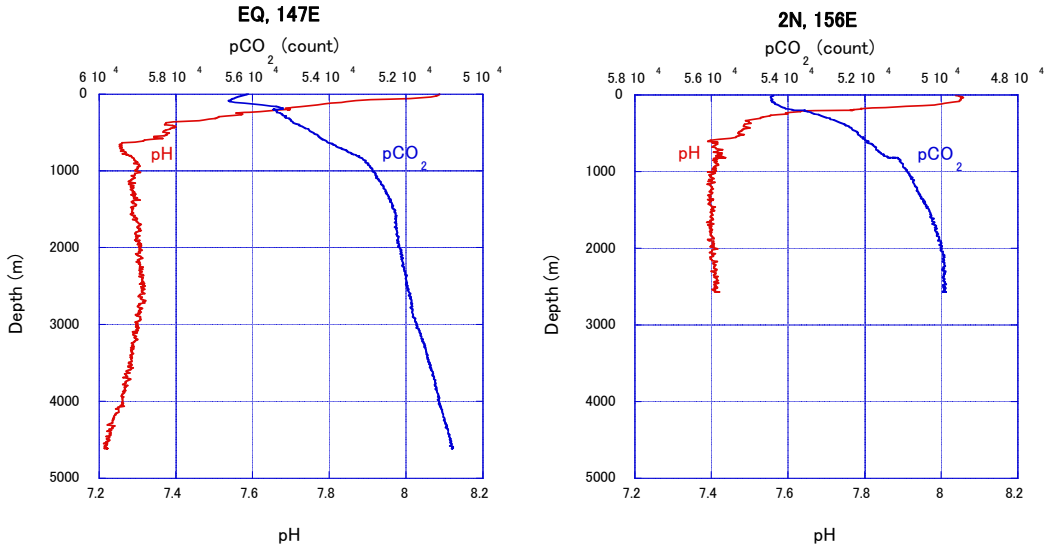

Figure 1 Vertical Profiles of in-situ pH and pCO2 by the in-situ pH/pCO_2 sensors

7.7 Influence of abnormal bases from bacteria in marine eco-system

(1) Personnel
Yasurou Kurusu (Ibaraki Univ)
Hiroe Hayashi (Ibaraki Univ)

(2) Objectives

Reactive oxygen species such as superoxide anion (O_2^-) and hydrogen peroxide (H_2O_2), and hydroxy radical (OH^*) are formed as a consequence of partial reduction of oxygen in the cellular component. The mechanism of the first step of oxidative mutagenesis is the reaction of bases in DNA or nucleotides in the pool with OH^*, a highly reactive oxygen species, which can be generated during the Harber-weiss/Fenton reaction that consists of an iron reduction step by O_2^- and OH^* generation step via the Fenton reaction. The genetic materials such as DNA, RNA, and their precursors in cellular nucleotide pools are important targets of reactive oxygen species that produces DNA lesion, such as 7,8-dihydro-8-oxoguanine (8-oxo-G), which cause mutation and replication block. On the other hands, organisms have potent system to reduce such mutagenic and cytotoxic effects caused by oxidative DNA lesions, and many bacteria (prokaryotes) have evolved DNA repair enzymes (MutM, DNA glycosyase; MutY, DNA glycosylase) and a clean-up enzyme (MutT, 8-oxo-dGTPase) to prevent G $\rightarrow$ T and A $\rightarrow$ C transversions in the chromosomal DNA.

In the view of the biological adaptation to marine environment, it is important to know the amount of 8-oxo-G in cells of marine bacteria. Our purpose of this cruise is to analysis of microflora at the equatorial area from surface to bottom.

(3) Parameters
Oceanic parameters for vertical profile: Temperature, salinity, dissolved oxygen, and microflora.

(4) Methods
Temperature, salinity and dissolved oxygen of various of seawater were performed by Marine Work Japan (see 6.3). Seawater samples for microflora analysis were collected in 10 L EVA cases from Niskin sampler. After the collection, samples of seawater for microflora analysis were filtered with 0.45 -μm and 0.22-μm filter (Diameter=47mm; MILLIPORE, DURAPORE® MEMBRANE FILTERS), and DNA (deoxyribonucleic acid) extraction from accumulated microorganisms was performed. On land laboratory, measurements of 8-oxo-G were performed using the above DNA samples.

(5) Data archive
All data will be archived at Ibaraki University after checking of data quality and submitted to the DMO at JAMSTEC within 3 years.

7.8 Distribution, heat-tolerance and super cooling point of the oceanic sea skaters of *Halobates*. (Heteroptera: Gerridae) inhabiting tropical area of western Pacific Ocean and oceanic dynamics

Tetsuo Harada[1,※], Kohki Iyota[1], Takashi Shiraki[1] & Chihiro Katagiri[2]

1: Laboratory of Environmental Physiology, Faculty of Education, Kochi University, Kochi 780-8520, Japan

2: Low Temperature Institute, Hokkaido University, Sapporo, Hokkaido Pref., Japan

※: Corresponding author: E-mail: haratets@kochi-u.ac.jp Tel. & Facsimile: +81-88-844-8410

INTRODUCTION

Many great voyages were launched to explore the oceans and what lies beyond, because they have always held a great fascination to us. A great variety of marine organisms were collected and describe during these voyages, but insects appear to have received little attention (Andersen & Chen, 2004). Although they are the most abundant animals on land, insects are relatively rare in marine environments (Cheng, 1985). However, a few thousand insect species belonging to more than 20 orders are considered to be marine (Cheng & Frank, 1993; Cheng, 2003). The majority of marine insects belong to the Coleoptera, Hemiptera, and Diptera, and they can be found in various marine habitats. However, the only insects to live in the open ocean are members of the genus *Halobates*, commonly known as sea-skaters. They belong to the family Gerridae (Heteroptera), which comprises the common pond-skaters or water-striders. Unlike most of its freshwater relatives, the genus *Halobates* is almost exclusively marine. Adults are small, measuring only about 0.5 cm in body length, but they have rather long legs and may have a leg span of 1.5 cm or more except for a new species, *Halobates megamoomario*. This new species which has very long boy length of 0.9 cm and large mid-leg span of 3.2 cm has been newly and recently collected in the tropical Pacific Ocean during the cruise, MR-06-05-Leg 3, and described (Harada et al., submitted). They are totally wingless at all stages of their life cycle and are confined to the air-sea interface, being an integral member of the pleuston community (Cheng, 1985). One may wonder how much tiny insects have managed to live in the open sea, battling waves and storms. In life, sea-skaters appear silvery. On calm days ocean-going scientists have probably seen them as shiny spiders skating over the sea surface. It is not known whether ancient mariners ever saw them, and no mention of their presence has been found in the logs of Christopher Columbus'S (1451-1506) ships or other ships that sailed to and from the New World (Andersen & Cheng, 2004).

Forty-seven species of *Halobates* are now known (Andersen & Cheng, 2004; Harada *et al.*, submitted). Six are oceanic and are widely distributed in the Pacific, Atlantic and the Indian Oceans. The remaining species occur in near-shore areas of the tropical seas associated with mangrove or other marine plants. Many are endemic to islands or island groups (Cheng, 1989).

The only insects that inhabit the open sea area are six species of sea skaters: *Halobates micans, H. sericeus, H.*

germanus, H. splendens, H. sobrinus (Cheng, 1985) and *H. megamoomario* newly described (Harada *et al.*, submitted). Three species, *Halobates sericeus, H. micans* and *H. germanus* inhabit tropical and temperate areas of the Pacific Ocean in the northern hemisphere, including The Kuroshio Current and the East China Sea (Andersen & Polhemus, 1976, Cheng, 1985). *Halobates sericeus, H. micans and H germanus* are reported from latitudes of 13ºN-40ºN, 0ºN-35ºNand 0ºN-37ºN, respectively, in the Pacific Ocean (Miyamoto & Senta,,1960; Andersen & Polhemus, 1976; Ikawa *et al.*, 2002). However, this information was collected on different cruises and in different times of the years. There have been several ecological studies based on samples collected in a specific area in a particular season during the six cruises of R/V HAKUHO-MARU: KH-02-01, KH-06-02, TANSEI-MARU: KT-07-19, KT-08-23 and R/V MIRAI: MR-06-05-Leg 3, MR-08-02.

During one cruise, KH-02-01, one sea skater species, *Halobates sericeus,* was collected at 18 locations in the East China Sea area (27°10' N- 33°24' N, 124º57' E - 129º30' E) (Harada, 2005), and *H. micans* and/or *H. germanus* at only 8 locations in the area south of 29° 47'N, where water temperatures were more than 25℃. At three locations, where the water temperature was less than 23℃, neither *H. micans* nor *H. germanus* were caught.

During another cruise, KH-06-02, in the latitude area of 12° N to 14° 30' N, *Halobates micans* were caught at 6 of 7 locations, while *H.germanus* and *H. sericeus* were caught at only 3 and 1 location(s), respectively (Harada *et al*, 2006). However, at 15° 00' N or northern area, *H. germanus* were caught at 14 of 19 locations, whereas *H. micans* and *H. cericeus* were caught at only 8 and 6 locations, respectively (Harada *et al*, 2006).

In the cruise, MR-06-05-Leg 3, larvae of both *H. micans* and *H. germanus* were very abundant at 6º N, whereas adults of *H. germanus* alone were completely dominant at 2º N on the longitudinal line of 130ºE. On the longitudinal line of 138ºE, larvae and adults of *H. micans* alone were dominant at points of 5 º and 8ºN, while adults of *H. germanus* were abundant between 0º and 2ºN. At the two stations of St. 37 (6º N, 130º E) and St. 52 (5º N, 138º E), relatively great number of larvae of *H. sericeus* were collected. This species has been known to be distributed in the northern area of the Pacific Ocean. At St. 52 (6º N, 138º E), it was heavily raining around the ship while trailed.

In the cruise, KT-07-19 on the northern edge of Kuroshio Current, *H. sericeus* was mainly collected in the northern-eastern area of 135º-140ºE, 34º-35ºN whereas *H. germanus and H. micans* were mainly collected in the relatively southern-western area of 131º-133ºE., 31º-33ºN. Only *H. sericeus* can be transferred by the Kuroshio Current onto the relatively northern-eastern area and to do reproduce at least in the summer season. In the cruise of KT-08-23, Most of "domestic" specimen collected in the area northern to Kuroshio current and near to Kyushu and Shikoku islands in September were *H. germanus* (Harada *et al.*, unpublished).

All samplings of *Halobates* have been performed at different geographical positions in any cruise in the Pacific Ocean so far. However, there has been no information on the dynamics in species and individual compositions in relatively eastern area of 145-160ºE, 0-10ºN of tropical Pacific Ocean. This study aims, first, to perform samplings in this area of the Western Pacific Ocean and examine dynamics of the species composition and reproductive and growth activity and compare these data to the data in the past which were got in more western area of 130-137ºE, 0-10ºN in the cruise, MR-06-05- Leg 3.

During the cruise, MR-08-02, on the longitudinal line of 130ºE, larvae of both *H. micans* and *H. germanus* were very abundant at 5-12º N, whereas adults of *H. sericeus* alone were dominant at 17º N. In the lower latitude area of 5-8 º N, all the three described species, *H. micans, H. germanus* and *H. sericeus* and un-described species, *Halobates moomario* (Harada *et al.*, unbublished) were collected. At a fixed point located at 12ºN, 135ºE, *H. micans* was dominant through the sampling period of 20 days, whereas *H. sericeus* was collected mainly in the latter half of the period. Higher number of *Halobates* (593) was collected in the first half of the sampling period (8^{th} – 17^{th} June, 2008) when the weather was very fine than that (427) in the second half (18^{th} – 27^{th} June, 2008) when the typhoon No 6 was born and developed near the fixed sampling point.

In this cruise of MR-09-04, the samplings are performed in relatively eastern area of 147° E-156° E with low latitude of 0-10° E of the tropical pacific ocean. Huge number of larva and adults more than 1000 were collected in the trailing by ORI-NET for 45 min. in three of seven sampling stations distributed in the area of 0-10ºN, 130-138ºE in the cruise, MR-06-05-Leg 3. This study aims, first, to examine whether sea skaters inhabit with extremely high population density also in relatively eastern tropical Pacific Ocean area like as in relatively western region of 130-138ºN.

Fresh water species in Gerridae seem to have temperature tolerance from -3℃ to 42℃ (Harada, 2003), because water temperature in fresh water in ponds and river highly changes daily and seasonally. However, water temperatures in the ocean are relatively stable and only range from 24℃ to 30 ℃ in the center of Kuroshio current in southern front of western Japan (Harada, 2005). Adults of *Halobates germanus* showed semi-heat-paralysis (SHP: static posture with no or low frequency to skate on water surface), when they were exposed to temp. higher than 32℃ (Harada unpublished, data in the TANSEIMARU cruise: KT-05-27).

In contrast to the temperate ocean, water temperature in the tropical ocean area, is more stable around 30℃. Therefore, the tropical species of *H. micans* is hypothesized to have lower tolerances to temperature changes than the tropical-temperate species, *H. cericeus*. This hypothesis was true in the laboratory experiment during the cruise of KH-06-02-Leg 5 (Harada *et al.*, submitted). When the water temperature increased stepwise 1℃ every 1 hour, heat-paralysis (ventral surface of thorax attaché to water surface and unable to skate) occurred at 29℃ to >35 ℃ (increase by 1 to >7 ℃). Three of four specimens in *Halobates sericeus* were not paralyzed even at 35 ℃ and highly resistant to temperature change, while only one of nine in *H. micans.* and only four of twelve in *H. germanus* were not paralyzed at 35 ℃. On average, *H. sericeus, H germanus and H. micans* were paralyzed at >35.6 ℃ (SD: 0.89), >32.9 ℃(SD: 2.17) and >31.6 ℃ (SD: 2.60) on average, respectively (Harada *et al.*, submitted).

As an index of cold hardiness, super cooling points (SCPs) have been used in many insects (Bale, 1987, 1993; Worland, 2005). The absence of ice-nucleating agents and/or the lack of an accumulation of cryo-protective elements can often promote higher super cooling points (Milonas & Savopoulou-Soultani, 1999). SCPs, however, might be estimated as only the lower limits of supercooling capacity and only a theoretical lower threshold for the survival of insects as freeze-non-tolerant organisms. Many insects show considerable non-freezing mortality at temperatures well above the SCPs, a “chill-injury” species (Carrillo *et al.*, 2005; Liu *et al.*, 2007). Liu *et al* (2009) recently showed that SCPs change in accordance with the process of winter diapauses, decreasing in Dec-Feb and

increasing rapidly in Feb-Apr (diapauses completing season) due to making glycogen from trehalose as a “blood suger” leading to lower osmotic pressure in haemolymph due to low “trehalose” level. This relation supports the possibility of SCPs available as an indirect indicator of cold hardiness of insects.

The 0-10ºN latitude-area in the Pacific Ocean has very complicated dynamic systems of ocean and atmosphere. Because of such complicated system, water/air temperatures and water conductivity (salinity) can be in dynamic change temporally and spatially. Sea skaters inhabiting this area of the Pacific Ocean show relatively high tolerance to temperature changes (heat tolerance)(Harada *et al.*, 2007: the cruise report of MR-06-05-Leg 3). However, there have been no data on the index on cold hardiness like as SCP on sea skaters yet. Recently, a cross-tolerance to high and low severe temperature has been reported by fresh water species of semi-aquatic bug, *Aquarius paludum* (Harada & Ishibashi, submitted). This study aims, second, to examine whether sea skaters living in very dynamic tropical sea area making “hot-water-pool” in tropical Pacific Ocean show high cross tolerance to high temperature and also lower super cooling points.

MATERIALS AND METHODS

Samplings

Samplings were performed in 1st – 27th June, 2008 with a Neuston NET (6 m long and with diameter of 1.3 m.)(Photos 1, 2). The Neuston NET was trailed for 45min.(15mm x 3 times) on the sea surface at 8 stations ranged 0 to 10 degrees North and 147 or 156 degree East in the western Pacific Ocean on the right side of R/V MIRAI (8687t) which is owned by JAMSTEC (Japan Agency for Marine-earth Science and TECHnology). The trailing was performed for 15min mostly at night (early in the morning at St 6) with the ship speed of 2.0 knot to the sea water (Table 1). It was repeated twice in each station. Surface area which was swept by Neuston NET was evaluated as a expression of [flow-meter value of ORI net trial at MR-06-05-Leg 3 x diameter of the ORI NET x (130 cm of width of the Neuston NET / 150cm of diameter of ORI NET) x 2.0knot /2.5 knot] based on the data obtained in the quite same samplings with ORI NET in MR-06-05-Leg 3. The area which was swept by the Neuston-NET during the trailing for 45 min can be estimated as the value of 2905.12 m^2 on average).

Laboratory experiment

Sea skaters trapped in the pants (grey plastic bottle)**(**Photo 2) located and fixed at the end of Neuston NET were paralyzed with the physical shock due to the trailing of the NET. Such paralyzed sea skaters were transferred on the surface of paper towel and to respire. Then, the paralysis of some ones was discontinued within 20min. When sea skaters were trapped in the jelly of jelly fishes, the jelly was removed from the body of sea skaters very carefully and quickly by hand for the recovering out of the paralysis.

All the adults and 5th instars which recovered out of the paralysis were moved on the sea water in the aquaria set in the laboratory for the Heat-Paralysis Experiments. Many white cube aquaria with 30cm X 30cm X 40cm) were used in the laboratory of the ship for the rearing of the adults and larvae which were recovered out of the paralysis

due to the trailing. Each aquarium contained ten to twenty adults or larvae of *Halobates*. Both the room temperature and sea water temperature in the aquaria were kept at 29±2℃. More than 12 hours after the collection, sea skaters were kept in the aquaria before the heat-paralysis experiment. Air was supplied to the sea water for the rearing and heat paralysis experiment in aquaria to prevent the increase of water surface viscosity due to bacterial activity. Without air supplying system, bodies of sea skaters would be caught by the water film several hours later and could not be kept long in the aquaria. All the individuals of *Halobates* kept in the aquaria were fed on mainly adult flies, *Lucillia illustris* before the heat-paralysis experiments. The transparent aquarium as the experimental arena has sea water with the same temperature (mostly 28 or 29℃) as that of the aquarium to keep sea skaters. 1 to 14 individuals at adult or larval stage were moved to the transparent aquarium. Temperature was stepwise increased by 1℃ every 1 hour till the high temperature paralysis occurring in all the experimental specimens.

Temperature was very precisely controlled by handy on-off-switching to keep in ±0.3 ℃ of the current water temperature. Handy-stirring with 10cm air tube with 5mm diameter and ball stone with 3cm diameter and supplying sea water of 26℃ with a syringe were effective to keep the precise controlling of the current temperature. Sea skaters on the water surface of the aquarium were recorded with Digital Handy Video Camera (GZ-MG840-S: VICTOR) from above position for the last fifteen of each 1hour under the current temperature(Photos 4, 5). Temperature at which Semi High Temperature Paralysis (SHTP: no or little movement on the water surface:
Photo 6) and High Temperature Paralysis (HTP: ventral surface of the body was caught by sea water film and no ability to skate any more) were recorded.

Determination of super cooling points (SCPs)

The determination of super cooling points was performed for the specimen (mainly adults) paralyzed by high temperature of the four species of oceanic *Halobates* (*H. micans, H. germanus, H. sericeus, H. moohario* as a new proposed species) at the end of heat paralysis experiment during this cruise (Photo 7). Surface of each adult was dried with filter paper, and thermocouples with consist of nickel and bronze were attached to the abdominal surface of the thorax and connected to automatic temperature recorders (Digital Thermometer, Yokogawa Co, LTD, Model 10, Made in Japan). The thermocouple was completely fixed to be attached to the ventral surface of abdomen by a kind of Sellotape. The specimen attached to thermocouples was placed into a compressed-styroform box (5×5×3 cm^3) whch was again set inside another insulating larger compressed Styrofoam to ensure that the cooling rate was about 1×℃/min for recording the SCP in the freezer in which temperature was -35℃. The lowest temperature which reached before an exothermic event occurred due to release of latent heat was regarded as the SCP (Zhao & Kang, 2000). All tested specimen were killed by the body-freezing when SCP was determined.

RESULTS

Distribution

On the longitudinal line of 155-156ºE *H. germanus* was very dominant, whereas three adults of *H. micans*, *H. germanus* and *H. sericeus* were dominant at 5º N on the longitudinal line of 147 ºE during this cruise held in Nov 4-Dec 12, 2009 (Tables 1, 5). Among several latitudes of 0-10 º N, peak of number of individuals collected was located at 8 º N, 5 º N and 0-2 º N for *H.m.*, *H.g.* and *H.s.*, respectively, on the longitudinal line of 155-156 º E (Table 1). From latitudinal point of view, *H. micans* and *H.germanus*. were abundant in 5-8 º N, whereas *H. sericeus* and *H. moomario* were in 0-5 º N (Table 3). Except for St. 6 at 3 º N, 147 º E, more than half of specimen collected were larvae at the remaining St. 1-5 and St.7,8. (Tables 1, 4). Un-described new species, *Halobates moomario* was mostly on the longitudinal line of 147ºE (Table 5). On the longitudinal line of 147 º E, more newly hatched larvae were collected than those on the line of 155-156E (Table 6).

Laboratory experiment (Table 2)

Temperature for semi heat paralysis (TSHP), temp. for heat paralysis (THP), gap temp. for heat paralysis (GTHP) and super cooling point (SCP) were ranged 29 ºC to 39 ºC, 29 ºC to 41 ºC, and 1 ºC to 12 ºC, respectively. Average and SD (n)(℃) of TSHP, THP, GTHP and SCP are 32.9±2.8(153), 35.5±3.2(153), 6.8±3.1(153) and -18.4±2.1(191).

On the latitudinal line of 155-156 º E, high heat tolerance and lower SCP were shown at St.4 (2 º N)(Table 7). The more northern the latitude, the higher the average SCP was on the 156 º E line (Table 7). Both heat tolerance and SCP were significantly higher on the 147 º E line rather than those on the 155-156 º E line (Tables 8, 9). Adults tended to show higher THP than 5th instar larvae (Table 10). There were no significant differences between sexes in all of TSHP, THP, GTHP and SCP (Table 11). In the order of *H. moo.*, *H.m.*, *H. g.*, *H.s.*, average GTHP tended to become higher (Table 12).

Correlation analysis

Significant negative correlation was shown between SCP and both of THP and GTHP especially in adults. In *H. germanus*, clear negative correlation was shown in higher range of THP more than 33℃ (Table 13, Figs 1, 2). In the other three species of *H. micans, H. sericeus and H. moomario*, very clear negative correlation appeared between SCP and THP with Pearson's correlation value of 0.45 (Table 13, Fig 2). Correlation between SCP and TSHP was also significant but relatively weak (Pearson's correlation value: 0.188, P=0.030, n=133).

Additional analysis

The data on field samplings in this study and environmental data on the oceanography during the cruise should be compared to the sampling data and related oceanography data in the area of 0-8 º N, 130-138 º E, in the Pacific Ocean at the cruise, MR-06-05-Leg 3 in the western tropical Pacific Ocean, as well as those in the area of 8 º N to 6 º S in the Indian Ocean at the cruise, KH-07-04-Leg1 (Harada *et al*., 2008), those in the area of 30-35 º N along the Kuroshio Current at the cruise, KT-07-19, KT-08-23, KT-09-20.

Cross tolerance between heat and cold hardiness was shown by *Halobates* inhabiting western tropical Pacific

Ocean with 0-8N, 147-156E during in this study. Similar analysis and comparative analysis will be done very soon with the data on SCP and heat paralysis experiment on *Halobates* inhabiting on and near the Kuroshio Current (Black Current). SCP measurement and heat paralysis experiment were done in the same manner during the cruise KT-09-20 in September, 2009. The relationship of the extent of the heat tolerance and SCP value to the ocean dynamics including several currents in the Pacific and Indian Ocean and also to the biological productivity by phyto-planktons and zoo-planktons should be analyzed in the near future.

The video camera data will be analyzed very soon after the cruise to examine the frequency and speed of skating and their responses to the temperature differences.

DISCUSSION

Distribution and ocean dynamics

Based on this study and another study during other three cruise, MR-06-05-Leg 3, MR-08-02 and KH-06-02, *Halobates micans* seems to, predominantly, inhabit the area of 12ºN and 135-138ºE in the Pacific Ocean, while higher number of *H. germanus* was collected than that of *H. micans* at 12ºN and 130ºE in MR-08-02. On the line of 12ºN, area of 130ºE is nearer to the current NEC than that of 135E. *H. germanus* is possible to be transferred from eastern area on the NEC. In the lower latitudinal area of 0-10ºN, huge amount of specimen more than 1000 (five or ten times of density in comparison with number of specimen collected in this cruise) were collected in the three of seven sampling station in the longitudinal area of 130-137ºE which was located at far western area during the cruise, MR-06-05-Leg 3. Probably, NECC might transfer individuals of *Halobates* from west to the east area of 147 or 156ºE. Three species of *H. micans, H.germanus and H.sericeus* could be transferred till the 147ºE, while only *H. germanus* might be further transferred and in survival to 156ºE where more than 300 individuals of *H. germanus* were collected at St. 3 in this cruise. Relatively low density of specimens of *Halobates* inhabiting the lines of 147ºE and 156ºE might be related to very low amount of biological productivity which could be speculated from very few amount of organisms collected during all trailing by Neuston NET in this cruise (Photo 3). *Halobates germanus* might be resistant to such low level of biological productivity in the tropical Pacific Ocean.

Many individuals of *Halobates sericeus* were collected in the area close to equator (0-2ºN) with 147-156ºE and also at 5ºN, 147ºE in this cruise. In the cruise, MR-06-05-Leg 3, very few individuals of *H. sericeus* were collected in the area of 0-2ºN, 130-137ºE. Andersen & Chen (2004) reported *H. sericeus* only northern area from 10ºN in the northern hemisphere in the Pacific Ocean. Many larvae of *H. sericeus* were collected St. 4(2ºN, 147ºE) and St.7(5ºN, 156ºE). Results of the samplings in this cruise showed that *H. sericeus* can inhabit and drive whole life cycles even in the low latitudinal area near to equator and added the new knowledge to the distribution of oceanic *Halobates.*

Individuals of *Halobates moomario* (un-described new species; Harada *et al.*, unpublished) were collected at St.3-6(5-8 ºN, 130ºE) in MR-08-02, MR-06-05-Leg 3 and also in this study. Size is between *H. micans* and *H. germanus* and has a specific morphometry with narrow and long body with relatively long intervals between abdominal segments lines. Another new species is *Halobates megamoomario* while is similar body shape and color

with *H. moomario,* but has much larger body (9mm long and span of mid-legs: 35mm: Harada et al., submitted). Only three species of *H..micans, H. germanus and H. sericeus* have been known in the western Pacific Ocean (Chen, 1985). However, the two new species of *H. megamoomario* and *H.moomario* should be described in very near future. In such case, the number of species of oceanic *Halobates* becomes "7".

Heat paralysis and SCP

Heat-paralysis and super cooling points (SCPS) can be used as the indices to show a resistance to high and low temperatures, respectively. In comparison with average THP measured on *Halobates* species collected in the area of 12-15ºN, 140-145ºE in the tropical Pacific Ocean during KH-06-02-Leg 5, THP measured in this study was higher [0-10N, 147-156ºE versus 12-15ºN, 140-145ºE, *H. micans*: 34.5±3.2 (17) versus 31.6±2.6 (9); *H.germanus*: 35.7± 3.3 (85) versus 32.9±2.17 (11); *H.sericeus*: 36.2±2.8 (32) versus 35.6±0.89 (4)]. Dynamism of weather and currents in this "hot water pool" in lower latitudinal area of the western Pacific Ocean might be related to relatively high resistance to temperature change. Both SCP and THP were significantly lower and higher, respectively, on the longitudinal line of 147ºE than the line of 156ºE. During the cruise, MR-06-05-Leg 3, very high resistance to high temperature was shown by *H.micans* and *H. germanus* in the latitudinal area of 0-8N on the longitudinal line of 138ºE. In the 138-147ºE area, oceanic dynamism might be higher than western or eastern area of 0-8ºN in the western Pacific Ocean. Further analysis on the relationship between physiological properties and oceanographic data remain to be done in near future.

Cross tolerance

Many works have been done on the tolerance to severe conditions like as extreme low, extreme high temperatures, desiccation, high osmotic pressure and so on. Cross tolerance in which tolerance to one environmental stressor results in increased tolerance to another is thought to be widespread in insects, particularly with regards to low temperature and drought, longevity and starvation tolerance, and high temperatures and desiccation (Bayley *et al*., 2001; Harshman & Hoffman, 2000; Ramløv & Lee, 2000; Ring & Danks, 1994; Vermeuleu & Loeshcke, 2007; Wu *et al.,* 2000). Because of ease of rearing and artificial selection, *Drosophila* has been good model for selection experiments on the cross-tolerance (Harshman & Hoffmann, 2000). Selection of cold hardy strain can be followed by higher tolerance to desiccation (Bubliy and Loeschcke, 2005), whereas it was not vise-versa (Ring & Danks, 1994; Sinclair *et al.*, 2007). Such discordance in the results could suggest independence of the profiles in the mechanism of cold tolerance and desiccation tolerance. How would be about the cross tolerance between cold and heat hardiness? There have been few such reports on such cross tolerance (Ohtsu *et al.*, 1998), but trade-off relationship has been reported in Drosophila (Kellett *et al.*, 2005; MacMillan *et al.*, 2009) and other ectotherms (Stillman, 2003).

Recently, an example of cross tolerance between cold and heat tolerances was shown in larvae of a water strider, *Aquarius paludum paludum* and *Aquarius paludum amamiensis* (Harada and Ishibashi, submitted). This study also very clearly showed the cross tolerance between heat tolerance and SCP value as an index of cold hardiness

In oceanic sea skaters, *Halobates* at the first time. Such cross tolerances between heat and cold hardiness are hypothesized to be common physiological characteristics in the semi-aquatic bugs. However, more fundamental data should be needed for clarifying whether this hypothesis is true or not.

ACKNOWLEDGEMENT

We would like to thank Dr. Yuji KASHINO (Head Scientist of the cruise: MR-09-04) for the permission to do this study during the cruise on the R/V MIRAI, for his warm suggestion on ocean dynamics, and encouragement and help throughout this cruise. The samplings and the experimental study were also possible due to supports from all of the crew (Captain: Mr. Yasushi ISHIOKA) and all the scientists and the engineers from GODI and MWJ in this cruise. We would like to give special thanks to them.

REFERENCES

Andersen NM, Chen L 2004: The marine insect Halobates (Heteroptera: Gerridae): Biology, adaptations distribution, and phylogeny. *Oceanography and Marine Biology: An Annual Review* **42**: 119-180.

Andersen NM, Polhemus JT 1976: Water-striders (Hemiptera: Gerridae, Vellidae, etc). In L. Cheng L. (ed): *Marine Insects.* North-Holland Publishing Company, Amsterdam, pp 187-224.

Bale JS 1987: Insect cold hardiness: freezing and supercooling- an ecophysiological perspective. *J. Insect Physiol.*, **33**: 899-908.

Bale JS 1993: Classes of Insect Cold Hardiness. *Functional Ecol.* **7**: 751–753.

Baley M, Petersen SO, Knigge T, Kohler HR, Holmstrup M 2001: Drought acclimation confers cold tolerance in the soil collembolan Folsomia candida. *J. Insect Physiol.*, **47**:1197-1204.

Bubliy OA, Loeschcke V 2005: Correlated responses to selection for stress resistance and longevity in a laboratory population of *Drosophila melanogaster*. *J. Evolutionary Biol.*, **18**: 789–803.

Carrillo MA, Heimpel GE, Moon RD, Cannon CA, Hutchison WD 2005: Cold hardiness of *Habrobracon hebetor* (Say) (Hymnoptera: Braconidae), a parasitoid of pyralid moths. *J. Insect Physiol.* **51**: 759-768.

Cheng L 1985: Biology of Halobates (Heteroptera: Gerridae) *Ann. Rev. Entomol.* **30**: 111-135.

Cheng L 1989: Factors limiting the distribution of Halobates species. In Reproduction, Genetics and Distribution of Marine Orgaminisms, J.S. Ryland & P.A. Tyler (eds), Fredensbor, Denmark: Olsen & Olsen, 23rd European Marine Biology Symposium, pp. 357-362.

Cheng L 2003: Marine insects. In Resh VH & Carde RT (eds), *Encyclopedia of Insects*, pp. 679-682, Academic Press, San Diego.

Cheng L, Frank JH 1993: Marine insects and their reproduction. *Oceanography and Marine Biology: An Annual Review* **31**: 479-506.

Harada T 2005: Geographical distribution of three oceanic Halobates spp. and an account of the behaviour of *H.*

sericeus (Heteroptera: Gerridae). *Eur. J. Entomol.* **102**: 299-302.

Harada T, Ishibashi T, Inoue T 2006: Geographical distribution and heat-tolerance in three oceanic *Halobates* species (Heteroptera: Gerridae). *The Cruise Report of Kh-06-02-Leg 5.*

Harada T, Nakajyo M, Inoue T 2007: Geographical distribution in the western tropical Pacific Ocean and heat-tolerance in the oceanic sea skaters of *Halobates*. (Heteroptera: Gerridae) and oceanic dynamics. *The Cruise Report of MR-06-05-Leg3.*

Harada T, Sekimoto T, Osumi Y, Ishigaki H 2008. Geographical distribution in the Indian Ocean and heat-tolerance in the oceanic sea skaters of Halobates. (Heteroptera: Gerridae) and oceanic dynamics.. *The Cruise Report of KH-07-04-Leg 1*.

Harshman LG, Hoffmann AA 2000: Laboratory selection experiments using Drosophila: what do they really tell us? *Trends Ecol. Ecolution*, **15**: 32-36.

Ikawa T, Okabe H, Hoshizaki S, Suzuki Y, Fuchi T, Cheng L 2002: Species composition and distribution of ocean skaters Halobates (Hemiptera: Gerridae) in the western pacific ocean. *Entomol. Sci.* **5**: 1-6.

Kellentt M, Hoffmann AA, Mckechnie SW 2005: Hardening capacity in the *Drosophila melanogaster* species group is constrained by basal thermotolerance. *Functional Ecol.*, **19**: 853–858.

Liu ZD, Gong PY, Wu KJ, Wei W, Sun JH, Li DM 2007: Effects of larval host plants on over-wintering preparedness and survival of the cotton ballwarm, *Helicoverpa armigera* (Hübner) (Lepidoptera: Noctuidae). *J. Insect Physiol.* **53**: 1016-1026.

Liu ZD, Gong PY, Heckel DG, Wei W, Sun JH, Li DM 2009: Effects of larval host plants on over-wintering physiological dynamics and survival of the cotton bollwarm, *Helicoverpa armigera* (Hübner)(Lepidoptera: Noctuidae). *J. Insect Physiol.* **55**: 1-9.

Macmillan HA, Walsh JP, Sinclair BJ 2009: The effects of selection for cold tolerance on cross-tolerance to other environmental stressors in *Drosophila melanogaster Insect Sci.*, **16**: 263-276

Milonas P, Savopoulou-Soultani M 1999: Cold hardiness in diapause and non-diapause larvae of the summer fruit tortorix, *Adoxophes orana* (Lepidoptera: Tortricidae). *Eur. J. Entomol.* **96**: 183-187.

Miyamoto S, Senta T 1960: Distribution, marine condition and other biological notes of marine water-striders, *Halobates* spp., in the south-western sea area of Kyushu and western area of Japan Sea. *Sieboldia* (In Japanese with English summary). **2**:171-186.

Ohtsu T, Kimura M, Katagiri C 1998: How *Drosophila* species acquire cold tolerance Quantitative changes of phospholipids. *Eur. J. Biochem.* **252**: 608-611.

Vermeulen CJ, Loeschcke V 2007: Longevity and the stress response in *Drosophila*. *Exp. Gerontology*, **42**: 153–159.

Worland M. R. 2005: Factors that influence freezing in the sub-antarctic springtail *Tullbergia antarctica*. *J. Insect Physiol.* **51**: 881-894.

Wu BS, Lee JK, Thompson KM., Walker VK, Moyes CD, Robertson RM 2002: Anoxia induces thermotolerance in the locust flight system. *J.Exp. Biol.*, **205**: 815–827.

Ramløv H, Lee JR RE 2000: Extreme resistance to desiccation in overwintering larvae of the gall fly *Eurosta solidaginis* (Diptera, Tephritidae). *J. Exp. Biol.*, **203**: 783–789.

Ring RA, Danks HV 1994: Desiccation and cryoprotection: Overlapping adaptations. *CryoLetters*, **15**: 181–190.

Sinclair BJ, Nelson S, Nilson TL, Roberts SP, Gibbs AG 2007: The effect of selection for dessication resistance on cold tolerance of *Drosophila melanogaster*. *Physiol. Entomol.*, **32**: 322–327.

Stillman JH 2003: Acclimation capacity underlies susceptibility to climate change. *Science*, **301**: 65–65.

Zhao YX, Kang L. 2000: Cold tolerance of the leafminer *Liriomyza sativae* (Dipt., Agromyzidae). *J. Appl. Entomol.* **124**: 185-189.

Table 1. Number of *Halobates* collected at 8 locations in the western region of the pacific ocean in Nov 12, 2009 to Dec 04, 2009. (N:Total number of individuals collected; *H.m.: Halobates micans; H.g.: Halobates germanus; H.s.: Halobates sericeus*; *H.moo*.:undescribed *Halobates moomario (new species)*; Stat: Station number; WT: Water temperature (℃); AT: Air temp.; L: N of larvae; A: N of adults, E: N of exuviae; Date: sampling date; Sampling was performed for 45min. EG: eggs on some substrates like as polystyrene form thousands of eggs laid on the substrate. Surface area which was swept by Neuston NET was expressed as value of flow-meter x diameter of the ORI NET x (130 cm of width of Neuston NET / 150cm of diameter of ORI NET) based on the data obtained in the quite same samplings with ORI NET in MR-06-05-Leg 3 (estimated value: 3631.4 m^2 on average for Nesston NET trailing for 45 min); WS: wind velocity (m/s); W: weather; TD: Time of day.

Latitude	Longitude	N	L	A	*H.m.*	*H.g.*	*H.s.*	*H.moo.*	EG	E	Stat	WT	AT	WV	W	TD	Date		
09˚56'N	154˚56'E	3	2	1	3	0	0	0	0	0	0	St. 1	29.6	28.6	11.1	Fine	19:06 ~	Nov 12
08˚00'N	155˚58'E	140	123	17	53	86	1	0	10	5	St. 2	29.7	29.5	9.9	Cloudy	18:53~	Nov 13
04˚58'N	156˚20'E	320	110	210	8	310	1	1	0	4	St. 3	29.8	28.7	2.6	Fine	18:40~	Nov 15
01˚59'N	155˚55'E	52	19	33	4	4	40	4	0	1	St. 4	29.8	26.3	4.7	Rainy	18:41~	Nov 17
00˚04'N	156˚07'E	64	25	39	1	24	39	0	0	0	St. 5	29.3	30.2	1.3	Cloudy	18:48~	Nov 19
02˚59'N	147˚09'E	119	12	107	3	74	25	17	0	0	St. 6	28.9	27.5	8.9	Cloudy	04:33~	Dec 01
05˚11'N	147˚18'E	188	140	48	66	57	61	4	0	20	St. 7	29.3	29.9	5.5	Fine	18:33~	Dec 02
09˚59'N	146˚59'E	21	12	9	12	6	2	1	0	0	St. 8	28.8	28.2	4.5	Fine	18:23~	Dec 04
Total		907	443	464	150	561	169	27	10	30								

Table 2-Sheet 1. Results of "heat-paralysis" experiments and SCP (Super Cooling Point) measurement performed on larvae and adults of *Halobates micans* (H.m.), *H.germanus*(H.g.), *H. sericeus*(H.s.) and un-described new species *H. moomario* (proposed name: H. moo.) TA: temp. at which specimen adapted, TSHP: temp. at which semi-heat-paralysis occurred; THP: temp. at which heat-paralysis occurred ; GTHP: gap temp. for heat paralysis (from base temp.); "Date and Time of day" when experiments were performed. (MR-09-04: Nov. 4-Dec 12, 2009) TD: Time of day; Increase in temp. at SCP shown in the parenthesis after SCP.

St.No.	Latitude(N)	Longitude(E)	Exp.No.	TA	TSHP	THP	GTHP	SCP	Species	Stage (sex)	Date	TD
St. 1	10°N	155°E	1	27	31	32	5	-11.6	H.g.	Adult (female)	Nov 13	06:45~
St. 2	8°N	156°E	2	27	30	31	4	-15.5	H.m.	Adult (female)	Nov 14	06:55~
St.2	8°N	156°E	2	27	30	32	5	-13.4	H.g.	5th instar	Nov 14	06:55~
St.2	8°N	156°E	2	27	30	32	5	-17.4	H.s.	Adult (female)	Nov 14	06:55~
St.2	8°N	156°E	2	27	31	32	5	-19.4	H.g.	4th instar	Nov 14	06:55~
St.2	8°N	156°E	2	27	34	34	7	-17.1	H.m.	5th instar	Nov 14	06:55~
St.2	8°N	156°E	2	27	34	34	7	-15.7	H.s.	Adult (female)	Nov 14	06:55~
St.2	8°N	156°E	2	27	33	37	10	-18.8	H.g.	Adult (male)	Nov 14	06:55~
St.2	8°N	156°E	3	28.5	29	30	1.5	-16.6	H.m.	Adult (female)	Nov 15	06:45~
St.2	8°N	156°E	3	28.5	29	31	2.5	-17.9	H.m.	Adult (female)	Nov 15	06:45~
St.2	8°N	156°E	3	28.5	29	31	2.5	-20.8	H.g.	5th instar	Nov 15	06:45~
St.2	8°N	156°E	3	28.5	29	32	3.5	-18.6	H.m.	Adult (male)	Nov 15	06:45~
St.2	8°N	156°E	3	28.5	29	33	4.5	-18.1	H.m.	Adult(female)	Nov 15	06:45~
St.2	8°N	156°E	3	28.5	31	34	5.5	-18.2	H.m.	Adult(female)	Nov 15	06:45~
St.2	8°N	156°E	3	28.5	31	34	5.5	-17.7	H.g.	Adult(female)	Nov 15	06:45~
St.2	8°N	156°E	3	28.5	31	36	7.5	-16.4	H.m.	5th instar	Nov 15	06:45~
St.2	8°N	156°E	3	28.5	31	36	7.5	-17.4	H.g.	Adult (female)	Nov 15	06:45~
St.2	8°N	156°E	3	28.5	32	37	8.5	-18.1	H.m.	5th instar	Nov 15	06:45~
St.2	8°N	156°E	3	28.5	32	37	8.5	-20.6	H.m.	5th instar	Nov 15	06: 45~
St.2	8°N	156°E	3	28.5	37	37	8.5	-17.0	H.m.	5th instar	Nov 15	06: 45~
St.2	8°N	156°E	3	28.5	39	39	10.5	No data	H.g.	Adult (female)	Nov 15	06:45~
St.2	8°N	156°E	3	28.5	34	39	10.5	-18.1	H.g.	5th instar	Nov 15	06:45~

Table 2-Sheet 2. Results of "heat-paralysis" experiments and SCP (Super Cooling Point) measurement performed on larvae and adults of *Halobates micans* (H.m.), *H.germanus*(H.g.), *H. sericeus*(H.s.) and un-described new species *H. moomario* (proposed name: H. moo.) TA: temp. at which specimen adapted, TSHP: temp. at which semi-heat-paralysis occurred; THP: temp. at which heat-paralysis occurred ; GTHP: gap temp. for heat paralysis (from base temp.); "Date and Time of day" when experiments were performed. (MR-09-04: Nov. 4-Dec 12, 2009) TD: Time of day; Increase in temp. at SCP shown in the parenthesis after SCP.

St.No.	Latitude(N)	Longitude(E)	Exp.No.	TA	TSHP	THP	GTHP	SCP	Species	Stage (sex)	Date	TD
St.3	5°N	156°E	4	29	30	31	2	-17.5	H.g.	Adult (female)	Nov 16	06:50~
St.3	5°N	156°E	4	29	30	31	2	-17.5	H.g.	Adult (female)	Nov 16	06:50~
St.3	5°N	156°E	4	29	30	32	3	-17.9	H.g.	Adult (female)	Nov 16	06:50~
St.3	5°N	156°E	4	29	33	34	5	-18.2	H.g.	Adult (male)	Nov 16	06:50~
St.3	5°N	156°E	4	29	33	35	6	-18.3	H.g.	Adult (male)	Nov 16	06:50~
St.3	5°N	156°E	4	29	33	36	7	-19.6	H.g.	Adult (male)	Nov 16	06:50~
St.3	5°N	156°E	4	29	33	36	7	-15.5	H.g.	Adult (male)	Nov 16	06:50~
St.3	5°N	156°E	4	29	33	36	7	-17.1	H.g.	Adult (female)	Nov 16	06:50~
St.3	5°N	156°E	4	29	33	36	7	-16.2	H.g.	Adult (female)	Nov 16	06:50~
St.3	5°N	156°E	4	29	34	36	7	-14.8	H.g.	Adult (female)	Nov 16	06:50~
St.3	5°N	156°E	5	28		No data		-14.6	H.g.	Adult (female)	Nov 17	06:55~
St.3	5°N	156°E	5	28		No data		-18.4	H.g.	Adult (female)	Nov 17	06:55~
St.3	5°N	156°E	5	28		No data		-17.4	H.g.	Adult(female)	Nov 17	06:55~
St.3	5°N	156°E	5	28		No data		-18.6	H.g.	Adult(male)	Nov 17	06:55~
St.3	5°N	156°E	5	28		No data		-19.6	H.g.	Adult(male)	Nov 17	06:55~
St.3	5°N	156°E	5	28		No data		-14.6	H.g.	Adult (male)	Nov 17	06:55~
St.3	5°N	156°E	5	28		No data		-14.6	H.g.	Adult (female)	Nov 17	06:55~
St.3	5°N	156°E	5	28		No data		-18.8	H.g.	Adult (male)	Nov 17	06:55
St.3	5°N	156°E	5	28		No data		-20.0	H.g.	Adult (female)	Nov 17	06: 55~
St.3	5°N	156°E	5	28		No data		-14.3	H.g.	Adult (male)	Nov 17	06: 55~

Table 2-Sheet 3. Results of "heat-paralysis" experiments and SCP (Super Cooling Point) measurement performed on larvae and adults of *Halobates micans* (H.m.), *H.germanus*(H.g.), *H. sericeus*(H.s.) and un-described new species *H. moomario* (proposed name: H. moo.) TA: temp. at which specimen adapted, TSHP: temp. at which semi-heat-paralysis occurred; THP: temp. at which heat-paralysis occurred ; GTHP: gap temp. for heat paralysis (from base temp.); "Date and Time of day" when experiments were performed. (MR-09-04: Nov. 4-Dec 12, 2009) TD: Time of day; Increase in temp. at SCP shown in the parenthesis after SCP

St.No.	Latitude(N)	Longitude(E)	Exp.No.	TA	TSHP	THP	GTHP	SCP	Species	Stage (sex)	Date	TD
St.3	5°N	156°E	5'	29	30	35	6	-20.3(7.3)	H.moo.	Adult (female)	Nov 17	12:45~
St.3	5°N	156°E	5'	29	30	36	7	-18.6(4.0)	H.g.	Adult (female)	Nov 17	12:45~
St.3	5°N	156°E	5'	29	30	36	7	-20.6(6.5)	H.g.	Adult (female)	Nov 17	12:45~
St.3	5°N	156°E	5'	29	31	36	7	-18.9(4.0)	H.g.	Adult (male)	Nov 17	12:45~
St.3	5°N	156°E	5'	29	31	37	8	-18.9(2.7)	H.g.	Adult (male)	Nov 17	12:45~
St.3	5°N	156°E	5'	29	31	37	8	-21.0(9.1)	H.g.	Adult (female)	Nov 17	12:45~
St.3	5°N	156°E	5'	29	33	38	9	-18.3(5.0)	H.g.	Adult (male)	Nov 17	12:45~
St.3	5°N	156°E	5'	29	33	39	10	-19.5(5.4)	H.g.	Adult (female)	Nov 17	12:45~
St.3	5°N	156°E	5'	29	33	39	10	-14.2(5.7)	H.g.	Adult (female)	Nov 17	12:45~
St.3	5°N	156°E	5'	29	33	39	10	-18.3(6.3)	H.g.	Adult (male)	Nov 17	12:45~
St.3	5°N	156°E	6	29	30	30	1	-20.7(1.8)	H.g.	Adult (female)	Nov 18	06:50~
St.3	5°N	156°E	6	29	30	32	3	-18.3(0.8)	H.g.	Adult (male)	Nov 18	06:50~
St.3	5°N	156°E	6	29	31	33	4	-17.3(2.5)	H.g.	Adult(male)	Nov 18	06:50~
St.3	5°N	156°E	6	29	35	35	6	-16.8(5.0)	H.g.	Adult(male)	Nov 18	06:50~
St.3	5°N	156°E	6	29	32	38	9	-17.5(5.0)	H.g.	Adult(female)	Nov 18	06:50~
St.3	5°N	156°E	6	29	35	38	9	-18.0(8.5)	H.g.	Adult (male)	Nov 18	06:50~
St.3	5°N	156°E	6	29	36	40	11	-20.8(7.3)	H.g.	Adult (female)	Nov 18	06:50~
St.3	5°N	156°E	6	29	38	40	11	-20.2(8.6)	H.g.	Adult (female)	Nov 18	06:50~
St.3	5°N	156°E	6	29	38	40	11	-16.5(6.1)	H.g.	Adult (female)	Nov 18	06: 50~
St.3	5°N	156°E	6	29	36	40	11	-19.7(4.3)	H.g.	Adult (male)	Nov 18	06: 50~

Table 2-Sheet 4. Results of "heat-paralysis" experiments and SCP (Super Cooling Point) measurement performed on larvae and adults of *Halobates micans* (H.m.), *H.germanus*(H.g.), *H. sericeus*(H.s.) and un-described new species, *H. moomario* (proposed name: H. moo.) TA: temp. at which specimen adapted, TSHP: temp. at which semi-heat-paralysis occurred; THP: temp. at which heat-paralysis occurred ; GTHP: gap temp. for heat paralysis (from base temp.); "Date and Time of day" when experiments were performed. (MR-09-04: Nov. 4-Dec 12, 2009) TD: Time of day; Increase in temp. at SCP shown in the parenthesis after SCP.

St.No.	Latitude(N)	Longitude(E)	Exp.No.	TA	TSHP	THP	GTHP	SCP	Species	Stage (sex)	Date	TD
St.4	2°N	156°E	7	28	31	34	6	-18.9(5.1)	H.s.	Adult (female)	Nov 19	06:45~
St.4	2°N	156°E	7	28	31	35	7	-18.4(0.9)	H.s.	Adult (male)	Nov 19	06:45~
St.4	2°N	156°E	7	28	31	35	7	-19.8(3.3)	H.s.	Adult (male)	Nov 19	06:45~
St.4	2°N	156°E	7	28	33	35	7	-16.4(1.2)	H.s.	Adult (male)	Nov 19	06:45~
St.4	2°N	156°E	7	28	33	37	9	-19.1(1.8)	H.s.	Adult (female)	Nov 19	06:45~
St.4	2°N	156°E	7	28	35	37	9	-18.0(0.8)	H.s.	Adult (male)	Nov 19	06:45~
St.4	2°N	156°E	7	28	35	37	9	-20.2(4.3)	H.s.	Adult (male)	Nov 19	06:45~
St.4	2°N	156°E	7	28	35	38	10	-19.8(5.3)	H.s.	Adult (female)	Nov 19	06:45~
St.4	2°N	156°E	7	28	37	39	11	-19.7(5.8)	H.s.	Adult (male)	Nov 19	06:45~
St.4	2°N	156°E	7	28	37	39	11	-16.5(9.5)	H.s.	Adult (male)	Nov 19	06:45~
St.5	0°N	156°E	8	28	30	30	2	-19.2(8.5)	H.g.	Adult (female)	Nov 20	06:45~
St.5	0°N	156°E	8	28	31	31	3	-20.5(9.3)	H.s.	5^{th} instar	Nov 20	06:45~
St.5	0°N	156°E	8	28	31	31	3	-15.6(1.0)	H.s.	3^{rd} instar	Nov 20	06:45~
St.5	0°N	156°E	8	28	33	33	5	-20.0(5.2)	H.s.	5^{th} instar	Nov 20	06:45~
St.5	0°N	156°E	8	28	30	34	6	-16.9(5.0)	H.g.	5^{th} instar	Nov 20	06:45~
St.5	0°N	156°E	8	28	34	35	7	-19.4(6.1)	H.s.	Adult (female)	Nov 20	06:45~
St.5	0°N	156°E	8	28	30	37	9	-21.7(7.9)	H.g.	Adult (female)	Nov 20	06:45~
St.5	0°N	156°E	8	28	30	37	9	-19.6(5.6)	H.s.	Adult (male)	Nov 20	06:45~
St.5	0°N	156°E	8	28	31	37	9	-20.3(4.2)	H.g.	Adult (female)	Nov 20	06: 45~
St.5	0°N	156°E	8	28	36	37	9	-16.3(9.2)	H.g.	Adult (female)	Nov 20	06: 45~

Table 2-Sheet 5. Results of "heat-paralysis" experiments and SCP (Super Cooling Point) measurement performed on larvae and adults of *Halobates micans* (H.m.), *H.germanus*(H.g.), *H. sericeus*(H.s.) and un-described new species, *H. moomario* (proposed name: H. moo.) TA: temp. at which specimen adapted, TSHP: temp. at which semi-heat-paralysis occurred; THP: temp. at which heat-paralysis occurred ; GTHP: gap temp. for heat paralysis (from base temp.); "Date and Time of day" when experiments were performed. (MR-09-04: Nov. 4-Dec 12, 2009) TD: Time of day; Increase in temp. at SCP shown in the parenthesis after SCP.

St.No.	Latitude(N)	Longitude(E)	Exp.No.	TA	TSHP	THP	GTHP	SCP	Species	Stage (sex)	Date	TD
St.3	5°N	156°E	9	29	31	31	2	-15.4(5.3)	H.g.	Adult (male)	Nov 21	06:40~
St.3	5°N	156°E	9	29	31	32	3	-19.0(7,1)	H.g.	Adult (male)	Nov 21	06:40~
St.3	5°N	156°E	9	29	31	33	4	-13.7(7.6)	H.g.	Adult (male)	Nov 21	06:40~
St.3	5°N	156°E	9	29	33	34	5	-16.3(2.2)	H.g.	Adult (male)	Nov 21	06:40~
St.3	5°N	156°E	9	29	31	36	7	-17.3(2.1)	H.g.	Adult (female)	Nov 21	06:40~
St.3	5°N	156°E	9	29	35	36	7	-17.2(5.8)	H.g.	Adult (female)	Nov 21	06:40~
St.3	5°N	156°E	9	29	36	37	9	-18.3(5.0)	H.g.	Adult (female)	Nov 21	06:40~
St.3	5°N	156°E	9	29	36	37	9	-17.8(4.3)	H.g.	Adult (female)	Nov 21	06:40~
St.3	5°N	156°E	9	29	37	37	9	-19.5(7.0)	H.g.	Adult (female)	Nov 21	06:40~

Table 2-Sheet 6. Results of "heat-paralysis" experiments and SCP (Super Cooling Point) measurement performed on larvae and adults of *Halobates micans* (H.m.), *H.germanus*(H.g.), *H. sericeus*(H.s.) and un-described new species, *H. moomario* (proposed name: H. moo.) TA: temp. at which specimen adapted, TSHP: temp. at which semi-heat-paralysis occurred; THP: temp. at which heat-paralysis occurred ; GTHP: gap temp. for heat paralysis (from base temp.); "Date and Time of day" when experiments were performed. (MR-09-04: Nov. 4-Dec 12, 2009) TD: Time of day; Increase in temp. at SCP shown in the parenthesis after SCP.

St.No.	Latitude(N)	Longitude(E)	Exp.No.	TA	TSHP	THP	GTHP	SCP	Species	Stage (sex)	Date	TD
St.3	5°N	156°E	10	29	30	30	1	-15.0(9.0)	H.moo.	Adult (female)	Nov 22	06:45~
St.3	5°N	156°E	10	29	30	31	2	-18.1(7.4)	H.g.	Adult (female)	Nov 22	06:45~
St.3	5°N	156°E	10	29	32	32	3	-18.4(2.7)	H.g.	Adult (female)	Nov 22	06:45~
St.3	5°N	156°E	10	29	30	34	5	-18.8(7.7)	H.moo.	Adult (female)	Nov 22	06:45~
St.3	5°N	156°E	10	29	30	36	7	-17.3(2.0)	H.g.	5th instar	Nov 22	06:45~
St.3	5°N	156°E	10	29	36	37	8	-19.3(4.6)	H.moo.	Adult (female)	Nov 22	06:45~
St.3	5°N	156°E	10	29	33	37	8	-18.8(6.2)	H.g.	Adult (male)	Nov 22	06:45~
St.3	5°N	156°E	10	29	33	37	8	-16.4(4.1)	H.g.	Adult (male)	Nov22	06:45~
St.3	5°N	156°E	10	29	32	37	8	-17.9(5.0)	H.g.	Adult (female)	Nov 22	06:45~
St.3	5°N	156°E	10	29	33	38	9	-18.1(4.2)	H.g.	Adult (female)	Nov 22	06:45~
St.3	5°N	156°E	11	28	29	30	2	-19.7(2.8)	H.g.	5th instar	Nov 23	06:55~
St.3	5°N	156°E	11	28	30	31	3	-20.3(3.4)	H.g.	5th instar	Nov 23	06:55~
St.3	5°N	156°E	11	28	29	32	4	-20.4(5.7)	H.moo.	Adult (female)	Nov 23	06:55~
St.4	2°N	156°E	12	28	29	30	2	-16.6(8.8)	H.g.	Adult (male)	Nov 24	06:35~
St.5	0°N	156°E	12	28.5	31	32	3.5	-21.7(1.7)	H.g.	3rd instar	Nov 24	06:35~

Table 2-Sheet 7. Results of "heat-paralysis" experiments and SCP (Super Cooling Point) measurement performed on larvae and adults of *Halobates micans* (H.m.), *H.germanus*(H.g.), *H. sericeus*(H.s.) and un-described new species, *H. moomario* (proposed name: H. moo.) TA: temp. at which specimen adapted, TSHP: temp. at which semi-heat-paralysis occurred; THP: temp. at which heat-paralysis occurred ; GTHP: gap temp. for heat paralysis (from base temp.); "Date and Time of day" when experiments were performed. (MR-09-04: Nov. 4-Dec 12, 2009) TD: Time of day; Increase in temp. at SCP shown in the parenthesis after SCP.

St.No.	Latitude(N)	Longitude(E)	Exp.No.	TA	TSHP	THP	GTHP	SCP	Species	Stage (sex)	Date	TD
St.6	3°N	147°E	13	29	30	30	1	-18.7(2.0)	H.moo.	Adult (male)	Dec 2	06:50~
St.6	3°N	147°E	13	29	31	31	2	-19.3(1.4)	H.moo.	Adult (male)	Dec 2	06:50~
St.6	3°N	147°E	13	29	31	36	7	-20.2(0.6)	H.moo.	Adult (female)	Dec 2	06:50~
St.6	3°N	147°E	13	29	34	36	7	-19.6(2.7)	H.moo.	Adult (female)	Dec 2	06:50~
St.6	3°N	147°E	13	29	34	37	8	-20.7(5.1)	H.g.	Adult (male)	Dec 2	06:50~
St.6	3°N	147°E	13	29	34	40	11	-21.9(2.4)	H.moo.	Adult (female)	Dec 2	06:50~
St.6	3°N	147°E	13	29	34	40	11	-22.5(1.7)	H.g.	Adult (female)	Dec 2	06:50~
St.6	3°N	147°E	13	29	34	40	11	-19.7(4.1)	H.moo.	Adult (female)	Dec 2	06:50~
St.6	3°N	147°E	13	29	34	40	11	-21.7(7.1)	H.g.	Adult (male)	Dec 2	06:50~
St.6	3°N	147°E	13	29	34	41	12	-17.8(1.1)	H.g.	Adult (female)	Dec 2	06:50~
St.6	3°N	147°E	13	29	34	41	12	-17.9(0.4)	H.moo.	Adult (female)	Dec 2	06:50~
St.6	3°N	147°E	14	29	30	30	1	-16.3(1.3)	H.g.	Ault (male)	Dec 3	06:50~
St.6	3°N	147°E	14	29	31	31	2	-20.2(2.5)	H.g.	Adult (female)	Dec 3	06:50~
St.6	3°N	147°E	14	29	31	35	6	-18.9(0.6)	H.moo	Adult (female)	Dec 3	06:50~
St.6	3°N	147°E	14	29	31	36	7	-19.2(1.4)	H.s.	Adult (male)	Dec 3	06:50~
St.6	3°N	147°E	14	29	38	38	9	-18.0(6.3)	H.moo.	Adult (male)	Dec 3	06:50~
St.6	3°N	147°E	14	29	38	38	9	-18.6(5.9)	H.moo.	Adult (female)	Dec 3	06:50~
St.6	3°N	147°E	14	29	34	38	9	-17.9(6.0)	H.g.	Adult (female)	Dec 3	06:50~
St.6	3°N	147°E	14	29	36	39	10	-17.2(2.1)	H.s.	Adult (male)	Dec 3	06:50~
St.6	3°N	147°E	14	29	39	39	10	-21.5(2.5)	H.g.	Adult (female)	Dec 3	06:50~
St.6	3°N	147°E	14	29	36	39	10	-18.8(5.7)	H.g.	Adult (male)	Dec 3	06:50~

Table 2-Sheet 8. Results of "heat-paralysis" experiments and SCP (Super Cooling Point) measurement performed on larvae and adults of *Halobates micans* (H.m.), *H.germanus*(H.g.), *H. sericeus*(H.s.) and un-described new species, *H. moomario* (proposed name: H. moo.) TA: temp. at which specimen adapted, TSHP: temp. at which semi-heat-paralysis occurred; THP: temp. at which heat-paralysis occurred ; GTHP: gap temp. for heat paralysis (from base temp.); "Date and Time of day" when experiments were performed. (MR-09-04: Nov. 4-Dec 12, 2009) TD: Time of day; Increase in temp. at SCP shown in the parenthesis after SCP.

St.No.	Latitude(N)	Longitude(E)	Exp.No.	TA	TSHP	THP	GTHP	SCP	Species	Stage (sex)	Date	TD
St.6	3°N	147°E	15	29.5	32	32	2.5	-21.4(0.6)	H.g.	Adult (female)	Dec 4	07:05~
St.6	3°N	147°E	15	29.5	35	37	7.5	-19.6(5.4)	H.g.	Adult (female)	Dec 4	07:05~
St.6	3°N	147°E	15	29.5	35	37	7.5	-20.1(4.5)	H.g.	Adult (male)	Dec 4	07:05~
St.6	3°N	147°E	15	29.5	35	37	7.5	-18.3(5.0)	H.g.	Adult (female)	Dec 4	07:05~
St.6	3°N	147°E	15	29.5	35	37	7.5	-18.3(6.2)	H.g.	Adult (female)	Dec 4	07:05~
St.6	3°N	147°E	15	29.5	37	38	8.5	-16.2(4.1)	H.g.	Adult (female)	Dec 4	07:05~
St.6	3°N	147°E	15	29.5	39	40	10.5	-21.6 (4.7)	H.g.	Adult (female)	Dec 4	07:05~
St.6	3°N	147°E	15	29.5	35	40	10.5	-19.4(3.1)	H.g.	Adult (male)	Dec 4	07:05~
St.6	3°N	147°E	15	29.5	38	41	11.5	-20.7(3.7)	H.g.	Adult (female)	Dec 4	07:05~
St.6	3°N	147°E	15	29.5	37	41	11.5	-19.0(5.5)	H.g.	Adult (male)	Dec 4	07:05~
St.7	5°N	147°E	16	29	30	30	1	-16.1(7.2)	H.g.	Adult (female)	Dec 5	06:55~
St.7	5°N	147°E	16	29	30	30	1	-18.0(1.6)	H.s.	Adult (female)	Dec 5	06:55~
St.7	5°N	147°E	16	29	30	35	6	-16.3(1.2)	H.s.	Ault (male)	Dec 5	06:55~
St.7	5°N	147°E	16	29	30	37	8	-19.6(4.6)	H.s.	Adult (female)	Dec 5	06:55~
St.7	5°N	147°E	16	29	37	37	8	-18.6(0.7)	H.s.	Adult (female)	Dec 5	06:55~
St.7	5°N	147°E	16	29	30	38	9	-21.6(7.3)	H.s.	Adult (male)	Dec 5	06:55~
St.7	5°N	147°E	16	29	38	39	10	-18.0(4.6)	H.s.	Adult (female)	Dec 5	06:55~
St.7	5°N	147°E	16	29	38	39	10	-20.3(6.5)	H.s.	Adult (female)	Dec 5	06:55~
St.7	5°N	147°E	16	29	36	39	10	-19.4(5.5)	H.g.	Adult (female)	Dec 5	06:55~
St.7	5°N	147°E	16	29	37	39	10	-21.5(1.4)	H.s.	Adult (male)	Dec 5	06:55~
St.7	5°N	147°E	16	29	38	39	10	-20.9(4.2)	H.s.	Adult (male)	Dec 5	06:55~

Table 2-Sheet 9. Results of "heat-paralysis" experiments and SCP (Super Cooling Point) measurement performed on larvae and adults of *Halobates micans* (H.m.), *H.germanus*(H.g.), *H. sericeus*(H.s.) and un-described new species, *H. moomario* (proposed name: H. moo.) TA: temp. at which specimen adapted, TSHP: temp. at which semi-heat-paralysis occurred; THP: temp. at which heat-paralysis occurred ; GTHP: gap temp. for heat paralysis (from base temp.); "Date and Time of day" when experiments were performed. (MR-09-04: Nov. 4-Dec 12, 2009) TD: Time of day; Increase in temp. at SCP shown in the parenthesis after SCP.

St.No.	Latitude(N)	Longitude(E)	Exp.No.	TA	TSHP	THP	GTHP	SCP	Species	Stage (sex)	Date	TD
St.8	10°N	147°E	17	29	30	30	1	-16.7(4.1)	H.m.	Adult (male)	Dec 6	06:55~
St.8	10°N	147°E	17	29	34	36	7	-16.7(0.6)	H.s.	Adult (female)	Dec 6	06:55~
St.8	10°N	147°E	17	29	36	36	7	-17.8(4.8)	H.m.	Adult (female)	Dec 6	06:55~
St.8	10°N	147°E	17	29	35	37	8	-21.2(3.9)	H.m.	5th instar	Dec 6	06:55~
St.8	10°N	147°E	17	29	36	39	10	-17.6(6.5)	H.m.	Adult (male:'*Kai*')	Dec 6	06:55~
St.8	10°N	147°E	17	29	36	39	10	-22.5(1.3)	H.g.	Adult (male)	Dec 6	06:55~
St.8	10°N	147°E	17	29	39	40	11	-20.4 (5.2)	H.m.	Adult (female)	Dec 6	06:55~
St.8	10°N	147°E	17	29	36	41	12	-22.0(5.4)	H.s.	Adult (female)	Dec 6	06:55~
St.6	3°N	147°E	18	29	30	30	1	-17.5(2.0)	H.moo.	Adult (female)	Dec 7	05:50~
St.6	3°N	147°E	18	29	30	30	1	-20.4(6.5)	H.g.	Adult (female)	Dec 7	05:50~
St.6	3°N	147°E	18	29	30	31	2	-20.4(0.8)	H.moo.	Adult (female)	Dec 7	05:50~
St.6	3°N	147°E	18	29	30	35	6	-21.1(4.6)	H.g.	Adult (female)	Dec 7	05:50~
St.7	5°N	147°E	19	28	29	32	4	-19.4(9.3)	H.m.	Adult (female)	Dec 8	06:45~
St.7	5°N	147°E	19	28	32	32	4	-11.4 (4.1)	H.moo.	5th instar	Dec 8	06:45~
St.7	5°N	147°E	19	28	31	33	5	-15.7 (4.7)	H.moo.	Adult (female)	Dec 8	06:45~

Table 3: Species component of sea skaters, Halobates collected with Neuston-NET during the cruise, MR-09-04 due to latitude at which sampling was performed. *H. m.=Halobatges micans; H.g.=Halobates germanus; H.s.=Halobates sericeus; H.moo.=Halobates moomario* (un-described new species: Harada et al., submitted)

	Latitude						
	0° N	**2° N**	**3° N**	**5° N**	**8° N**	**10° N**	**Total**
H.m	1	4	3	74	53	15	150
H.g.	24	4	74	367	86	6	561
H.s	39	40	25	62	1	2	169
H.moo	0	4	17	5	0	1	24
	χ^2-test: χ^2-value=348.97, df=15, P<0.001						

Table 4: Stage component of sea skaters, *Halobates* collected with Neuston-NET during the cruise, MR-09-04 due to latitude at which sampling was performed. 0^{th}: 0^{th} instar larva, 1^{st} : 1^{st} instar larva; 2^{nd}: 2^{nd} instar larva; 3^{rd}: 3^{rd} instar larva; 4^{th}: 4^{th} instar larva; 5^{th} 5^{th} instar larva

	Stage							
Latitude	**0^{th}**	**1^{st}**	**2^{nd}**	**3^{rd}**	**4^{th}**	**5^{th}**	**Adult**	**Total**
0° N	2	0	2	5	2	14	39	64
2° N	0	0	2	5	5	7	33	52
3° N	2	0	0	2	0	8	107	119
5° N	16	34	52	34	54	60	258	508
8° N	1	36	32	27	10	17	17	140
10° N	0	1	3	4	0	6	10	24
	χ^2-test: χ^2-value=287.65, df=30, P<0.001							

Table 5: Species component of sea skaters, *Halobates* collected with Neuston-NET during the cruise, MR-09-04 due to longitude at which sampling was performed. *H. m.=Halobatges micans; H.g.=Halobates germanus; H.s.=Halobates sericeus; H.moo.=Halobates moomario* (un-described new species: Harada et al., submitted)

	Species				
Longitude	**H.m.**	**H.g.**	**H.s.**	**H.moo.**	**Total**
147° E	81	137	88	22	328
155° E	3	0	0	0	3
156° E	66	424	81	5	576
	χ^2-test: χ^2-value=109,323, df=6, P<0.001				

Table 6: Stage component of sea skaters, *Halobates* collected with Neuston-NET during the cruise, MR-09-04 due to longitude at which sampling was performed. 0^{th}: 0^{th} instar larva, 1^{st} : 1^{st} instar larva; 2^{nd}: 2^{nd} instar larva; 3^{rd}: 3^{rd} instar larva; 4^{th}: 4^{th} instar larva; 5^{th} 5^{th} instar larva

	Stage							
Longitude	**0^{th}**	**1^{st}**	**2^{nd}**	**3^{rd}**	**4^{th}**	**5^{th}**	**Adult**	**Total**
147° E	18	26	30	31	23	36	164	328
155° E	0	0	0	0	0	2	1	3
156° E	3	45	61	46	48	74	299	576
	χ^2-test: χ^2-value=30.087, df=12, P=0.003							

Table 7. Comparison among stations in the results of "heat-paralysis" experiments and SCP (Super Cooling Point) measurement performed on larvae and adults of *Halobates micans* (H.m.), *H.germanus*(H.g.), *H. sericeus*(H.s.) and un-described new species *H. moomario* (proposed name: H. moo.) TSHP: temp. at which semi-heat-paralysis occurred; THP: temp. at which heat-paralysis occurred ; GTHP: gap temp. for heat paralysis (from base temp.) [Mean±SD(n)]

St.No.	**Latitude(N)**	**Longitude(E)**	**TSHP**	**THP**	**GTHP**	**SCP**
St. 1	09˚56'N	154˚56'E	31.0(1)	32.0(1)	5(1)	-11.6 (2)
St. 2	08˚00'N	155˚58'E	31.7±2.7(21)	34.2±2.8(21)	6.2 ±2.7(21)	-17.6±1.7(20)
St. 3	04˚58'N	156˚20'E	32.4±2.4(52)	35.3±2.9(52)	6.4±2.9(52)	-18.1±1.9 (75)
St. 4	01˚59'N	155˚55'E	33.4±2.7(11)	36.0±2.6(11)	8.0±2.6(11)	-18.5±1.4 (11)
St. 5	00˚04'N	156˚07'E	31.5±2.0(11)	34.0±2.8(11)	6.0±2.8(11)	-18.9±2.0 (22)
St. 6	02˚59'N	147˚09'E	33.9±2.8(35)	36.6±3.7(35)	7.5±3.7(35)	-19.4±1.6(36)
St. 7	05˚11'N	147˚18'E	33.3±3.7(14)	35.6±3.5(14)	6.9±3.3(14)	-18.5±2.6(17)
St. 8	09˚59'N	146˚59'E	35.3±2.5 (8)	37.3±3.5 (8)	8.3±3.5 (8)	-19.4±2.4 (8)
Kruskal-Wallis-test among Stations1-8						
χ^2-value	-	-	***18.148***	***14.510***	***9.322***	***21.655***
df	-	-	***7***	***7***	***7***	***7***
P	-	-	*0.011*	*0.043*	*0.230*	*0.003*

Table 8. Comparison among latitudes at which specimens were collected, in the results of "heat-paralysis" experiments and SCP (Super Cooling Point) measurement performed on larvae and adults of *Halobates micans* (H.m.), *H.germanus*(H.g.), *H. sericeus*(H.s.) and un-described new species *H. moomario* (proposed name: H. moo.) TSHP: temp. at which semi-heat-paralysis occurred; THP: temp. at which heat-paralysis occurred ; GTHP: gap temp. for heat paralysis (from base temp.) [Mean±SD(n)]

Latitude(N)	**TSHP**	**THP**	**GTHP**	**SCP**
0° N	31.5±2.0(11)	34.0±2.8(11)	6.0±2.8(11)	-18.9±2.0(22)
2° N	33.4±2.7(11)	36.0±2.6(11)	8.0±2.6(11)	-18.5±1.4(11)
3° N	33.9±2.8(35)	36.6±3.7(35)	7.5±3.7(35)	-19.4±1.6(36)
5° N	32.6±2.7(66)	35.4±3.0(66)	6.5±3.0(66)	-18.2±2.0(92)
8° N	31.7±2.7(21)	34.2±2.8(21)	6.2±2.7(21)	-17.6±1.7(20)
10° N	34.8±2.8(9)	36.7±3.7(9)	7.9± 3.4(9)	-17.8±3.9(10)
Kruskal-Wallis among latitude 0-10° N				
χ^2-value	***16.297***	***12.089***	***7.599***	***13.950***
df	***5***	***5***	***5***	***5***
P	*0.006*	*0.034*	*0.180*	*0.016*

Table 9. Comparison among longitues at which specimens were collected, in the results of "heat-paralysis" experiments and SCP (Super Cooling Point) measurement performed on larvae and adults of *Halobates micans* (H.m.), *H.germanus*(H.g.), *H. sericeus*(H.s.) and un-described new species *H. moomario* (proposed name: H. moo.) TSHP: temp. at which semi-heat-paralysis occurred; THP: temp. at which heat-paralysis occurred ; GTHP: gap temp. for heat paralysis (from base temp.) [Mean±SD(n)]

Longitude(N)	**TSHP**	**THP**	**GTHP**	**SCP**
147° E	33.9±3.0(57)	36.5±3.6(57)	7.4±3.5(57)	-19.1±2.0(61)
155° E	31.0(1)	32.0(1)	5.0(1)	-11.6(2)
156° E	32.3±2.5(95)	35.0±2.9(95)	6.5±2.8(95)	-18.2±1.9(128)
Kruskal-Wallis-test among longitudes 147-156° E				
χ^2-value	***10.811***	***9.985***	***5.170***	***15.133***
df	***2***	***2***	***2***	***2***
P	*0.004*	*0.007*	*0.075*	*0.001*
Mann-Whitney U-test between longitudes 147° E and 156° E				
Z	***-3.254***	***-3.018***	***-2.151***	***-3.094***
P	*0.001*	*0.003*	*0.032*	*0.002*

Table 10. Comparison among stages in the results of "heat-paralysis" experiments and SCP (Super Cooling Point) measurement performed on larvae and adults of *Halobates micans* (H.m.), *H.germanus*(H.g.), *H. sericeus*(H.s.) and un-described new species *H. moomario* (proposed name: H. moo.) TSHP: temp. at which semi-heat-paralysis occurred; THP: temp. at which heat-paralysis occurred ; GTHP: gap temp. for heat paralysis (from base temp.) [Mean±SD(n)]

Stage	**TSHP**	**THP**	**GTHP**	**SCP**
3rd instar	31.0(2)	31.5(2)	3.3(2)	-18.7±4.3(2)
4th instar	31.0(1)	32.0(1)	5.0(1)	-19.4(1)
5th instar	31.8±2.3(16)	34.2±2.8(16)	6.0±2.6(16)	-18.1±2.8(24)
Adult	33.0±2.9(134)	35.8±3.2(134)	7.0±3.2(134)	-18.5±1.9(164)
Kruskal-Wallis-test among stages of 3rd to 5th instars and adult				
χ^2-value	***3.272***	***7.081***	***4.873***	***0.365***
df	***3***	***3***	***3***	***3***
P	*0.352*	*0.069*	*0.181*	*0.947*
Mann-Whitney U-test between 5th instar and adult stages				
Z	***-1.588***	***-1.866***	***-1.396***	***-0.269***
P	*0.112*	*0.062*	*0.163*	*0.788*

Table 11. Comparison between females and males of adult *Halobates* in the results of "heat-paralysis" experiments and SCP (Super Cooling Point) measurement performed on larvae and adults of *Halobates micans* (H.m.), *H.germanus*(H.g.), *H. sericeus*(H.s.) and un-described new species *H. moomario* (proposed name: H. moo.) TSHP: temp. at which semi-heat-paralysis occurred; THP: temp. at which heat-paralysis occurred ; GTHP: gap temp. for heat paralysis (from base temp.) [Mean±SD(n)]

.	**TSHP**	**THP**	**GTHP**	**SCP**
Females	32.9±3.0(83)	35.5±3.3(83)	6.8±3.2(83)	-18.5±2.0(99)
Males	33.1±2.6(50)	36.1±3.1(50)	7.3±3.1(50)	-18.5±1.9(65)
Mann-Whitney U-test between females and males				
Z	***-0.725***	***-0.883***	***-0,887***	***-0.197***
P	*0.469*	*0.377*	*0.375*	*0.844*

Table 12. Comparison among species in the results of "heat-paralysis" experiments and SCP (Super Cooling Point) measurement performed on larvae and adults of *Halobates micans* (*H.m.*), *H.germanus*(*H.g.*), *H. sericeus*(*H.s.*) and un-described new species *H. moomario* (proposed name: *H. moo*.) TSHP: temp. at which semi-heat-paralysis occurred; THP: temp. at which heat-paralysis occurred ; GTHP: gap temp. for heat paralysis (from base temp.) [Mean±SD(n)]

Species	**TSHP**	**THP**	**GTHP**	**SCP**
H.m	32.2±3.3(17)	34.5±3.2(17)	6.0±3.0(17)	-17.9±2.1(21)
H.g.	32.9±2.7(85)	35.7±3.3(85)	6.9±3.2(85)	-18.4±2.1(117)
H.s.	33.5±2.9(32)	36.2±2.8(32)	7.8±2.5(32)	-18.9±1.9(34)
H.moo.	32.3±2.8(19)	34.7±3.6(19)	5.8±3.5(19)	-18.5±2.4(19)
Kruskal-Wallis-test among stages of 3rd to 5th instars and adult				
χ^2-value	***4.121***	***4.252***	***5.481***	***3.236***
df	***3***	***3***	***3***	***3***
P	*0.249*	*0.236*	*0.140*	*0.357*

Table 13: Correlation analysis (Pearson's-test) between SCP and indices of heat tolerance [TSHP: temp. at which semi-heat-paralysis occurred; THP: temp. at which heat-paralysis occurred ; GTHP: gap temp. for heat paralysis (from base temp.)] *Halobates micans* (*H.m.*), *H.germanus*(*H.g.*), *H. sericeus*(*H.s.*) and un-described new species *H. moomario* (proposed name: *H. moo*.)

	Correlation value (r)		***P***		***N***	
	SCP vs THP	SCP vs GTHP	SCP vs THP	SCP vs GTHP	SCP vs THP	SCP vs GTHP
All the data	*-0.295*	*-0.261*	*<0.001*	*0.001*	*152*	*152*
Adults only	*-0.345*	*-0.315*	*<0.001*	*<0.001*	*133*	*133*
Adult H.g.	*-0.293*	*-0.264*	*0.011*	*0.023*	*74*	*74*
Adult H.m.,H.s.and H.moo.	*-0.450*	*-0.404*	*<0.001*	*0.002*	*58*	*58*

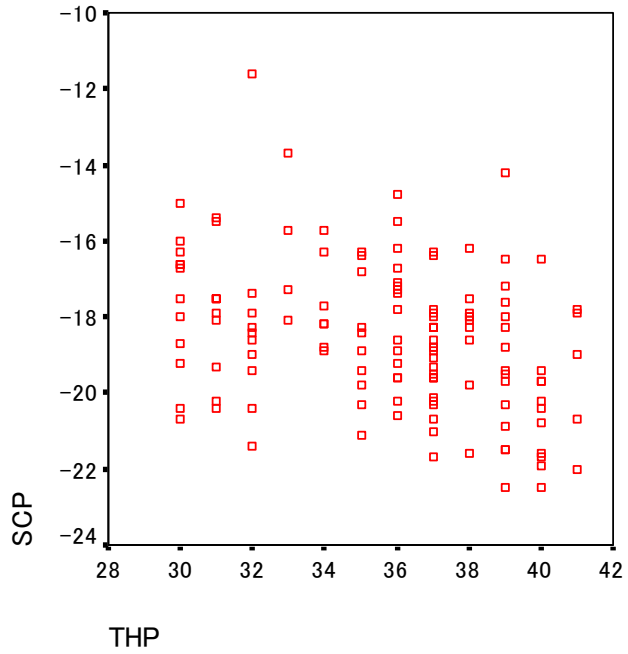

Fig.1 : Clear exhibition of “cross tolerance” between super cooling points (SCP:℃) and temperatures for heat paralysis (THP:℃) shown by adults of all four species of *Halobates micans*, *H. germanus*, *H. sericeus* and *H. moomario*.

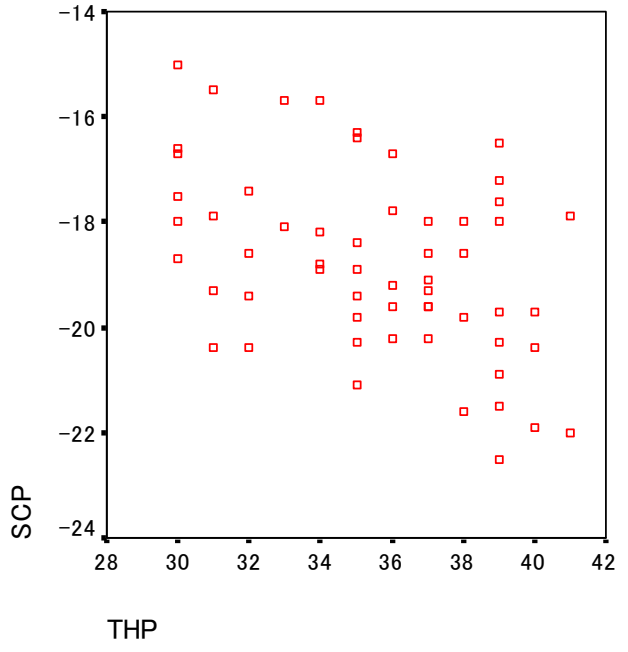

Fig. 2: Very clear exhibition of “cross tolerance” between super cooling points (SCP:℃) and temperatures for heat paralysis (THP:℃) shown by adults of three species of *Halobates micans*, *H. sericeus* and *H. moomario*.

Photo 1: The trailing of Neuston-NET

Photo 2: Washing the “pants” of the Neuston net just after the trailing to collect all the *Halobates* individuals into the round-shaped transparent aquarium.

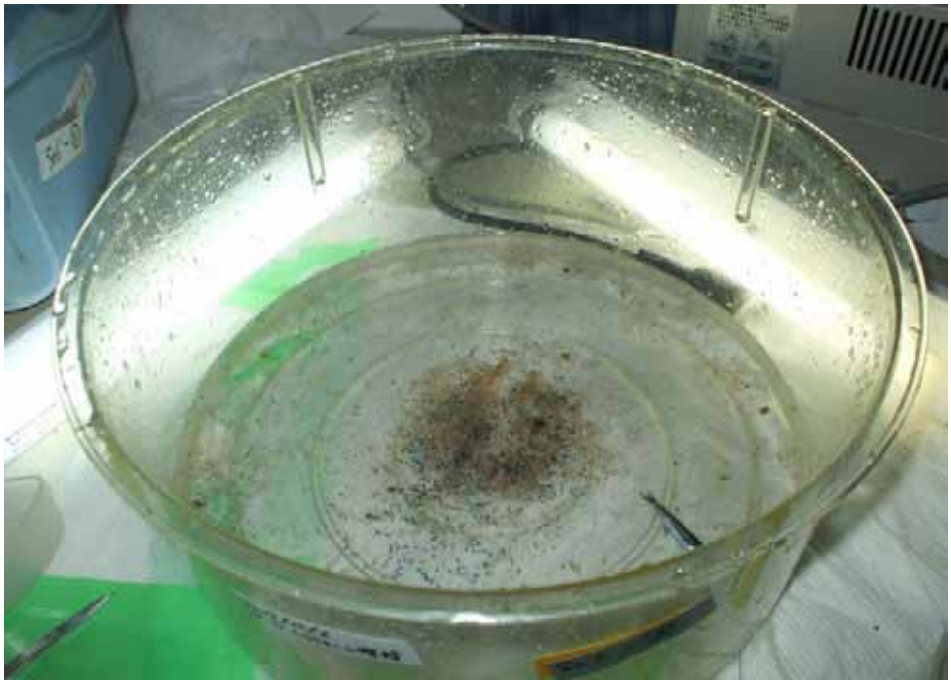

Photo 3: Sample of Neuston-NET trailing at Station 6 (3° N, 147E) on the 1st December, 2009

Photo 4: Laboratory showing the heat paralysis experiment arena (on the left) and incubating aquaria filled with sea water into which air was supplied from pomp and air tubes for keeping freshmen of

the sea water. Air temperature was kept within 29±2℃ with air-conditioners.

Photo 5: Scene in which heat paralysis experiment is starting early in the morning. In most cases, this experiment starts at the same time of the day (6:30-7:00).

Photo 6: A female of *Halobates moomario* (un-described new species) under semi-paralysis

in which she is in completely static posture without no movement at all due to increased temperature. Low of hairs like “oar” can be seen in the tibia and tarsus of the left hind leg.

Photo 7: Scene in which super cooling point (SCP) was measured with automatic temperature recorders With a thermo-sensor consisting of nickel-bronze coupling and freezer in which temperature was kept at -35℃. When heat paralysis occurred in a specimen, he (or she) is attached with the thermo-coupling at ventral surface of abdomen and transferred inside a box made of high-dense-type-polystyrene-form (another box can be seen on the freezer) and then put into the freezer to measure SCP.

Photo 8: “Oar” hairs on the tibia of mid-leg of adult *Halobates germanus*, which was enlarged by binocular.

7.9 Argo floats

(1) Personnel

Toshio Suga	*(JAMSTEC/RIGC): Principal Investigator (not on board)*
Shigeki Hosoda	*(JAMSTEC/RIGC): not on board*
Kanako Sato	*(JAMSTEC/RIGC): not on board*
Mizue Hirano	*(JAMSTEC/RIGC): not on board*
Shungo Oshitani	*(MWJ): Technical Staff (Operation Leader)*
Tomohide Noguchi	*(MWJ): Technical Staff*

(2) Objectives

The objective of deployment is to clarify the structure and temporal/spatial variability of water masses in the North Pacific such as North Pacific Tropical Water in the subtropical North Pacific.

The profiling floats launched in this cruise measure vertical profiles of temperature and salinity automatically every ten days. The data from the floats will enable us to understand the phenomenon mentioned above with time/spatial scales much smaller than in previous studies.

(3) Parameters

・water temperature, salinity, and pressure

(4) Methods

i. Profiling float deployment

We launched an APEX float manufactured by Webb Research Ltd. These floats equip an SBE41 CTD sensor manufactured by Sea-Bird Electronics Inc.

The floats usually drift at a depth of 1000 dbar (called the parking depth), diving to a depth of 1500 dbar and rising up to the sea surface by decreasing and increasing their volume and thus changing the buoyancy in ten-day cycles. During the ascent, they measure temperature, salinity, and pressure. They stay at the sea surface for approximately nine hours, transmitting the CTD data to the land via the ARGOS system, and then return to the parking depth by decreasing volume. The status of floats and their launches are shown in Table 4.1.1.

Table 4.1.1 Status of floats and their launches
Float(1500dbar)

Float Type	**APEX floats manufactured by Webb Research Ltd.**
CTD sensor	**SBE41 manufactured by Sea-Bird Electronics Inc.**
Cycle	**10 days (approximately 9 hours at the sea surface)**
ARGOS transmit interval	**30 sec**
Target Parking Pressure	**1000 dbar**
Sampling layers	**105 (1500, 1450, 1400, 1350, 1300, 1250, 1200, 1150, 1100, 1050, 1000, 980, 960, 940, 920, 900, 880, 860, 840, 820, 800, 780, 760, 740, 720, 700, 680, 660, 640, 620, 600, 580, 560, 540, 520, 500, 490, 480, 470, 460, 450, 440, 430, 420, 410, 400, 390, 380, 370, 360, 350, 340, 330, 320, 310, 300, 290, 280, 270, 260, 250, 240, 230, 220,210, 200, 195, 190, 185, 180, 175, 170, 165, 160, 155, 150, 145, 140, 135, 130, 125, 120, 115, 110, 105, 100, 95, 90, 85, 80, 75, 70, 65, 60, 55, 50, 45, 40, 35, 30, 25, 20, 15, 10, 4 or surface dbar)**

Launches

Float S/N	ARGOS ID	Date and Time of Reset (UTC)	Date and Time of Launch(UTC)	Location of Launch	CTD St. No.
3867	**80644**	**2009/11/12 02:32**	**2009/11/12 03:48**	**10-00.69N 154-50.84E**	**C03M-01**
3868	**80645**	**2009/11/13 04:39**	**2009/11/13 05:31**	**08-03.99N 155-51.81E**	**C04M-02**
4145	**86546**	**2009/11/15 03:42**	**2009/11/15 04:48**	**04-56.63N 156-06.80E**	**C05M-02**

(5) Data archive

The real-time data are provided to meteorological organizations, research institutes, and universities via Global Data Assembly Center (GDAC: http://www.usgodae.org/argo/argo.html, http://www.coriolis.eu.org/) and Global Telecommunication System (GTS), and utilized for analysis and forecasts of sea conditions.

7.10 Air-sea surface eddy flux measurement

(1) Personnel

Osamu Tsukamoto	(Okayama University) Principal Investigator	* not on board
Fumiyoshi Kondo	(The University of Tokyo)	* not on board
Hiroshi Ishida	(Kobe University)	* not on board
Souichiro Sueyoshi	(Global Ocean Development Inc. (GODI))	
Ryo Kimura	(GODI)	
Ryo Ohyama	(MIRAI Crew)	

(2) Objective

To better understand the air-sea interaction, accurate measurements of surface heat and fresh water budgets are necessary as well as momentum exchange through the sea surface. In addition, the evaluation of surface flux of carbon dioxide is also indispensable for the study of global warming. Sea surface turbulent fluxes of momentum, sensible heat, latent heat, and carbon dioxide were measured by using the eddy correlation method that is thought to be most accurate and free from assumptions. These surface heat flux data are combined with radiation fluxes and water temperature profiles to derive the surface energy budget.

(3) Instruments and Methods

The surface turbulent flux measurement system (Fig. 7.10-1) consists of turbulence instruments (Kaijo Co., Ltd.) and ship motion sensors (Kanto Aircraft Instrument Co., Ltd.). The turbulence sensors include a three-dimensional sonic anemometer-thermometer (Kaijo, DA-600) and an infrared hygrometer (LICOR, LI-7500). The sonic anemometer measures three-dimensional wind components relative to the ship. The ship motion sensors include a two-axis inclinometer (Applied Geomechanics, MD-900-T), a three-axis accelerometer (Applied Signal Inc., QA-700-020), and a three-axis rate gyro (Systron Donner, QRS-0050-100). LI7500 is a CO_2/H_2O turbulence sensor that measures turbulent signals of carbon dioxide and water vapor simultaneously. These signals are sampled at 10 Hz by a PC-based data logging system (Labview, National Instruments Co., Ltd.). By obtaining the ship speed and heading information through the Mirai network system it yields the absolute wind components relative to the ground. Combining wind data with the turbulence data, turbulent fluxes and statistics are calculated in a real-time basis. These data are also saved in digital files every 0.1 second for raw data and every 1 minute for statistic data.

(4) Observation log

The observation was carried out throughout this cruise.

(5) Data Policy and citation

All data are archived at Okayama University, and will be open to public after quality checks and corrections. Corrected data will be submitted to JAMSTEC Data Integration and Analysis Group (DIAG).

Fig. 7.10-1 Turbulent flux measurement system on the top deck of the foremast.

7.11 Lidar observations of clouds and aerosols

(1) Personnel

Nobuo Sugimoto, Ichiro Matsui, and Atsushi Shimizu (National Institute for Environmental Studies, not on board), lidar operation was supported by GODI.

(2) Objectives

Objectives of the observations in this cruise is to study distribution and optical characteristics of ice/water clouds and marine aerosols using a two-wavelength lidar.

(3) Measured parameters

- Vertical profiles of backscattering coefficient at 532 nm
- Vertical profiles of backscattering coefficient at 1064 nm
- Depolarization ratio at 532 nm

(4) Method

Vertical profiles of aerosols and clouds were measured with a two-wavelength lidar. The lidar employs a Nd:YAG laser as a light source which generates the fundamental output at 1064 nm and the second harmonic at 532 nm. Transmitted laser energy is typically 100 mJ per pulse at 1064 nm and 50 mJ per pulse at 532 nm. The pulse repetition rate is 10 Hz. The receiver telescope has a diameter of 20 cm. The receiver has three detection channels to receive the lidar signals at 1064 nm and the parallel and perpendicular polarization components at 532 nm. An analog-mode avalanche photo diode (APD) is used as a detector for 1064 nm, and photomultiplier tubes (PMTs) are used for 532 nm. The detected signals are recorded with a digital oscilloscope and stored on a hard disk with a computer. The lidar system was installed in the radiosonde container on the compass deck. The container has a glass window on the roof, and the lidar was operated continuously regardless of weather.

(5) Results

Data obtained in this cruise has not been analyzed.

(6) Data archive

- raw data

lidar signal at 532 nm

lidar signal at 1064 nm

depolarization ratio at 532 nm

temporal resolution 15 min.

vertical resolution 6 m.

data period (utc) : 21:45 Nov. 3, 2009 – 00:00 Dec. 12, 2009,

- processed data

cloud base height, apparent cloud top height

phase of clouds (ice/water)

cloud fraction

boundary layer height (aerosol layer upper boundary height)

backscatter coefficient of aerosols

particle depolarization ratio of aerosols

7.12 Water isotopes in atmospheric vapor, precipitation, and sea surface water

(1) Personnel

Naoyuki Kurita	(JAMSTEC)	Principal Investigator
Ryu Uemura	(LSCE/CEA)	
Kimpei Ichiyanagi	(Kumamoto Univ.)	
Hironori Fudeyasu	(Hawaii Univ.)	

(2) Objective

It is well known that the variability of stable water isotopes (HDO and $H_2{}^{18}O$) is closely related with the moisture origin and hydrological processes during the transportation from the source region to deposition site. Thus, water isotope tracer is recognized as the powerful tool to study of the hydrological cycles in the atmosphere. However, oceanic region is one of sparse region of the isotope data, it is necessary to fill the data to identify the moisture sources by using the isotope tracer. In this study, to fill this sparse observation area, intense water isotopes observation was conducted along the cruise track of MR-09-04.

(3) Method

Following observation was carried out throughout this cruise.

- Atmospheric moisture sampling:

  Water vapor was sampled from the height about 20m above the sea level. The air was drawn at rate of 1.6-4.5L/min through a plastic tube attached to top of the compass deck. The flow rate is regulated according to the water vapor content to collect the sample amount 10-30ml. The water vapor was trapped in a glass trap submerged into an ethanol cooled to 100 degree C by radiator, and then they are collected every 12 hour during the cruise. After collection, water in the trap was subsequently thawed and poured into the 6ml glass bottle.

- Rainwater sampling

  Rainwater samples gathered in rain collector were collected just after precipitation events have ended. The collected sample was then transferred into glass bottle (6ml) immediately after the measurement of precipitation amount.

- Surface seawater sampling

  Seawater sample taken by the pump from 4m depth were collected in glass bottle (6ml) around the noon at the local time.

(4) Results

Sampling of water vapor for isotope analysis is summarized in Table 7.12-1 (76 samples). The detail of rainfall sampling (31 samples) is summarized in Table 7.12-2. Described rainfall amount is calculated from the collected amount of precipitation. Sampling of surface seawater taken by pump from 4m depths is summarized in Table 7.12-3 (37 samples).

(5) Data archive

Isotopes (HDO, $H_2{}^{18}O$) analysis will be done at RIGC/JAMSTEC, and then analyzed isotopes data will be submitted to JAMSTEC Data Integration and Analysis Group (DIAG).

Table 7.12-1 Summary of water vapor sampling for isotope analysis.

Sample	Date	Time (UT)	Date	Time (UT)	Lon	Lat	Total (m^3)	MASS (ml)
V-01	11/3	21:50	11/4	12:19	144-21.30E	40-14.43N	2.58	20.2
V-02	11/4	12:22	11/5	00:00	147-05.19E	39-02.20N	2.07	19.8
V-03	11/5	00:03	11/5	12:02	146-28.13E	37-25.44N	2.12	21.2
V-04	11/5	12:06	11/6	00:00	145-35.80E	35-14.44N	2.10	23.8
V-05	11/6	00:03	11/6	12:00	144-44.99E	33-07.27N	1.78	17.8
V-06	11/6	12:02	11/7	00:00	144-12.53E	31-47.59N	1.79	20.5
V-07	11/7	00:04	11/7	12:00	143-44.69E	29-34.37N	1.78	23.0
V-08	11/7	12:02	11/8	00:00	144-58.18E	27-25.00N	1.77	28.2
V-09	11/8	00:02	11/8	12:00	146-09.20E	25-21.52N	1.43	24.0
V-10	11/8	12:02	11/9	00:00	147-14.23E	23-25.55N	1.41	26.0
V-11	11/9	00:03	11/9	12:00	148-28.03E	21-16.10N	1.36	26.2
V-12	11/9	12:02	11/10	00:00	149-40.61E	19-10.20N	1.35	26.2
V-13	11/10	00:02	11/10	12:00	150-52.09E	17-01.93N	1.36	26.0
V-14	11/10	12:02	11/10	23:37	152-00.77E	15-01.50N	1.28	26.0
V-15	11/10	23:41	11/11	12:00	153-21.24E	12-39.64N	1.25	24.2
V-16	11/11	12:02	11/12	00:00	154-38.19E	10-23.70N	1.21	26.0
V-17	11/12	00:02	11/12	12:00	155-16.31E	09-23.99N	1.22	26.2
V-18	11/12	12:02	11/13	00:00	155-55.17E	08-02.10N	1.22	26.0
V-19	11/13	00:03	11/13	12:00	155-56.50E	08-01.36N	1.22	26.2
V-20	11/13	12:02	11/14	00:00	155-56.69E	08-00.80N	1.22	25.8
V-21	11/14	00:02	11/14	12:00	155-59.97E	05-57.94N	1.22	26.0
V-22	11/14	12:04	11/15	00:00	156-04.81E	04-56.46N	1.21	26.2
V-23	11/15	00:02	11/15	12:00	156-02.95E	04-58.42N	1.22	26.0
V-24	11/15	12:02	11/16	00:00	156-01.64E	04-58.43N	1.21	26.0
V-25	11/16	00:03	11/16	12:00	156-00.31E	03-26.20N	1.22	26.0
V-26	11/16	12:02	11/17	00:00	156-00.75E	02-15.80N	1.22	25.8
V-27	11/17	00:01	11/17	12:00	156-02.08E	01-59.05N	1.22	24.8
V-28	11/17	12:02	11/18	00:16	156-03.44E	01-58.61N	1.23	26.0
V-29	11/18	00:18	11/18	12:00	156-01.29E	00-22.42N	1.19	25.0
V-30	11/18	12:03	11/19	00:00	156-04.71E	00-00.74S	1.21	26.0
V-31	11/19	00:02	11/19	12:00	156-00.73E	00-01.77S	1.21	25.8
V-32	11/19	12:02	11/19	22:40	155-57.74E	00-00.40S	1.02	21.0
V-33	11/19	22:43	11/20	11:35	155-59.35E	01-03.77S	1.27	26.2
V-34	11/20	11:36	11/21	00:00	155-56.90E	01-57.49S	1.22	26.0
V-35	11/21	00:01	11/21	12:00	155-57.37E	01-57.82S	1.18	25.4
V-36	11/21	12:01	11/21	23:54	155-58.48E	01-57.02S	1.13	24.0
V-37	11/21	23:57	11/22	12:00	155-59.71E	03-14.35S	1.16	24.8
V-38	11/22	12:02	11/23	00:00	156-01.50E	05-01.93S	1.16	25.0

V-39	11/23	00:02	11/23	12:00	156-00.39E	04-18.50S	1.16	23.6
V-40	11/23	12:02	11/24	00:00	155-58.85E	04-52.26S	1.16	24.8
V-41	11/24	00:02	11/24	12:00	154-46.57E	02-55.73S	1.16	25.0
V-42	11/24	12:02	11/25	00:00	151-52.34E	01-50.54S	1.16	24.6
V-43	11/25	00:03	11/25	12:00	148-54.00E	00-41.45S	1.15	24.6
V-44	11/25	12:02	11/26	00:00	147-01.64E	00-01.30S	1.15	24.2
V-45	11/26	00:02	11/26	12:00	147-03.62E	00-00.72S	1.15	24.8
V-46	11/26	12:02	11/27	00:00	146-58.58E	00-00.31S	1.15	24.2
V-47	11/27	00:03	11/27	12:00	147-03.41E	00-00.61S	1.15	24.8
V-48	11/27	12:02	11/28	00:00	147-04.80E	00-00.15S	1.15	24.2
V-49	11/28	00:02	11/28	12:00	146-59.89E	01-36.37N	1.15	24.0
V-50	11/28	12:02	11/29	00:00	147-03.57E	01-58.30N	1.15	23.8
V-51	11/29	00:01	11/29	12:00	147-01.39E	01-58.54N	1.15	24.2
V-52	11/29	12:01	11/30	00:00	147-02.14E	01-58.82N	1.15	24.0
V-53	11/30	00:02	11/30	12:00	147-00.37E	02-59.77N	1.15	24.2
V-54	11/30	12:01	12/1	00:00	147-01.42E	03-29.21N	1.15	24.2
V-55	12/1	00:01	12/1	12:00	147-01.42E	03-29.21N	1.15	24.2
V-56	12/1	12:03	12/2	00:00	147-02.71E	04-57.41N	1.15	24.0
V-57	12/2	00:01	12/2	12:00	147-01.40E	05-01.73N	1.15	24.6
V-58	12/2	12:02	12/3	00:00	146-59.34E	05-03.72N	1.15	24.6
V-59	12/3	00:02	12/3	12:00	146-55.32E	06-13.48N	1.15	24.0
V-60	12/3	12:02	12/4	00:00	146-32.49E	08-32.78N	1.15	24.0
V-61	12/4	00:02	12/4	12:00	147-03.68E	10-34.27N	1.15	24.0
V-62	12/4	12:02	12･5	00:00	147-26.41E	13-25.80N	1.15	23.8
V-63	12/5	00:02	12/5	12:00	147-48.54E	16-14.54N	1.15	24.0
V-64	12/5	12:02	12/6	00:00	148-10.33E	18-58.83N	1.15	24.0
V-65	12/6	00:02	12/6	12:00	147-15.78E	21-17.06N	1.15	23.6
V-66	12/6	12:02	12/7	00:00	146-20.96E	23-33.11N	1.22	24.2
V-67	12/7	00:02	12/7	12:00	145-10.09E	25-47.43N	1.22	21.8
V-68	12/7	12:02	12/8	00:00	144-36.71E	28-22.36N	1.23	12.2
V-69	12/8	00:02	12/8	12:00	144-06.81E	30-55.64N	1.36	12.0
V-70	12/8	12:03	12/9	00:00	143-37.05E	33-22.25N	1.50	10.4
V-71	12/9	00:02	12/9	12:00	143-13.32E	35-46.82N	1.65	13.6
V-72	12/9	12:01	12/10	00:00	142-45.05E	38-05.05N	1.78	10.2
V-73	12/10	00:02	12/10	12:00	142-20.62E	39-57.18N	2.16	7.8
V-74	12/10	12:02	12/11	00:00	141-32.57E	40-31.80N	2.87	8.8
V-75	12/11	00:02	12/11	12:00	141-31.40E	41-30.54N	3.23	16.0
V-76	12/11	12:02	12/12	00:03	141-14.37E	41-21.97N	3.24	23.6

Table 7.12-2 Summary of precipitation sampling for isotope analysis.

Sample	Date	Time (UT)	Lon	Lat	Date	Time (UT)	Lon	Lat	Rain (mm)
R-01	11/03	21:44	141-14.4E	41-21.9N	11/04	03:57	142-49.1E	40-56.9N	23.0
R-02	11/04	03:57	142-49.1E	40-56.9N	11/05	02:38	146-53.5E	38-28.7N	24.0
R-03	11/05	02:38	146-53.5E	38-28.7N	11/05	20:36	145-50.5E	35-51.5N	134.0
R-04	11/05	20:36	145-50.5E	35-51.5N	11/06	05:10	145-13.8E	34-19.4N	9.0
R-05	11/06	05:10	145-13.8E	34-19.4N	11/08	23:52	147-13.5E	23-26.7N	166.0
R-06	11/08	23:52	147-13.5E	23-26.7N	11/12	13:39	155-27.8E	09-02.8N	3.6
R-07	11/12	13:39	155-27.8E	09-02.8N	11/13	05:39	155-52.2E	08-03.8N	34.0
R-08	11/13	05:39	155-52.2E	08-03.8N	11/14	03:45	155-58.4E	07-49.5N	25.0
R-09	11/14	03:45	155-58.4E	07-49.5N	11/15	11:06	156-02.3E	04-58.2N	12.0
R-10	11/15	11:06	156-02.3E	04-58.2N	11/15	13:10	156-03.6E	04-58.5N	3.7
R-11	11/15	13:10	156-03.6E	04-58.5N	11/16	08:01	156-00.5E	03-56.8N	39.0
R-12	11/16	08:01	156-00.5E	03-56.8N	11/17	03:20	156-00.8E	02-03.6N	300.0
R-13	11/17	03:20	156-00.8E	02-03.6N	11/17	11:29	156-03.0E	01-59.2N	91.5
R-14	11/17	11:29	156-03.0E	01-59.2N	11/18	23:04	156-02.6E	00-01.1N	37.8
R-15	11/18	23:04	156-02.6E	00-01.1N	11/20	02:55	156-08.3E	00-02.9S	142.0
R-16	11/20	02:55	156-08.3E	00-02.9S	11/20	11:07	155-59.3E	01-01.0S	263.0
R-17	11/20	11:07	155-59.3E	01-01.0S	11/22	08:39	155-59.6E	02-43.8S	6.0
R-18	11/22	08:39	155-59.6E	02-43.8S	11/23	22:15	156-00.9E	04-57.3S	7.7
R-19	11/23	22:15	156-00.9E	04-57.3S	11/25	02:16	151-18.7E	01-37.4S	61.0
R-20	11/25	02:16	151-18.7E	01-37.4S	11/28	05:11	146-59.9E	00-48.2N	4.2
R-21	11/28	05:11	146-59.9E	00-48.2N	11/28	23:38	147-03.0E	01-58.8N	33.0
R-22	11/28	23:38	147-03.0E	01-58.8N	11/29	08:14	147-01.8E	01-58.7N	27.0
R-23	11/29	08:14	147-01.8E	01-58.7N	11/29	14:11	147-01.5E	01-58.9N	12.4
R-24	11/29	14:11	147-01.5E	01-58.9N	11/30	03:37	147-01.0E	02-14.7N	15.4
R-25	11/30	03:37	147-01.0E	02-14.7N	12/01	05:39	147-00.0E	04-22.8N	132.5
R-26	12/01	05:39	147-00.0E	04-22.8N	12/05	22:25	148-07.4E	18-42.4N	16.1
R-27	12/05	22:25	148-07.4E	18-42.4N	12/06	12:36	147-13.1E	21-23.7N	77.0
R-28	12/06	12:36	147-13.1E	21-23.7N	12/07	04:50	145-55.8E	24-22.6N	202.0
R-29	12/07	04:50	145-55.8E	24-22.6N	12/07	08:15	145-28.1E	24-59.8N	5.3
R-30	12/07	08:15	145-28.1E	24-59.8N	12/09	14:00	143-09.1E	36-09.9N	86.0
R-31	12/09	14:00	143-09.1E	36-09.9N	12/12	00:10	141-14.3E	41-21.9N	71.5

* Rainfall shows collected amount (ml).

Table 7.12-3 Summary of surface seawater sample taken from 4m depths

Sampling No.	Date	Time	Position	
		(UTC)	LON	LAT
O-1	11/04	03:00	142-32.62E	41-04.15N
O-2	11/05	03:01	146-51.89E	38-24.60N
O-3	11/06	03:00	145-23.17E	34-42.92N
O-4	11/07	02:00	144-03.61E	31-24.86N
O-5	11/08	02:00	145-10.59E	27-03.52N
O-6	11/09	02:00	147-26.56E	23-04.52N
O-7	11/10	02:00	149-52.53E	18-48.79N
O-8	11/11	02:00	152-16.44E	14-33.38N
O-9	11/12	01:00	154-44.31E	10-12.72N
O-10	11/13	01:00	155-54.20E	08-02.13N
O-11	11/14	01:07	155-56.64E	08-00.42N
O-12	11/15	01:00	156-06.04E	04-56.48N
O-13	11/16	01:00	156-02.45E	04-52.45N
O-14	11/17	01:00	156-01.19E	02-04.55N
O-15	11/18	01:00	156-02.41E	01-48.84N
O-16	11/19	01:00	156-06.88E	00-02.34S
O-17	11/20	01:00	156-04.34E	00-02.97S
O-18	11/21	01:00	155-55.47E	02-01.33S
O-19	11/22	01:00	155-57.54E	02-01.54S
O-20	11/23	01:00	156-02.24E	04-57.90S
O-21	11/24	01:00	155-58.72E	04-36.73S
O-22	11/25	01:02	151-37.09E	01-44.69S
O-23	11/26	02:00	147-02.39E	00-00.54N
O-24	11/27	02:00	147-01.38E	00-00.38S
O-25	11/28	02:00	147-01.23E	00-20.90N
O-26	11/29	02:00	147-05.81E	01-56.94N
O-27	11/30	02:00	147-01.47E	01-59.79N
O-28	12/01	02:00	147-00.86E	03-50.82N
O-29	12/02	02:00	147-01.95E	04-58.67N
O-30	12/03	02:00	147-02.88E	05-04.34N
O-31	12/04	02:00	146-39.87E	08-56.49N
O-32	12/05	02:00	147-30.12E	13-54.16N
O-33	12/06	02:00	148-01.43E	19-22.22N
O-34	12/07	02:00	146-11.68E	23-56.12N
O-35	12/08	03:00	144-30.00E	29-00.88N
O-36	12/09	03:00	143-31.21E	33-58.56N
O-37	12/10	03:00	142-40.22E	38-29.40N